Summer 8-2023

Design and Implementation of a Launching Method for Free to Oscillate Dynamic Stability Testing

Kristen M. Carey
Old Dominion University, kmcarey99@gmail.com

DESIGN AND IMPLEMENTATION OF A LAUNCHING METHOD FOR FREE TO OSCILLATE DYNAMIC STABILITY TESTING

by

Kristen M. Carey
B.S. December 2020, Old Dominion University

A Thesis Submitted to the Faculty of Old
Dominion University in Partial Fulfillment
of the Requirements for the Degree of

MASTER OF SCIENCE

AEROSPACE ENGINEERING

OLD DOMINION UNIVERSITY

AUGUST 2023

Approved by:

Dr. Colin Britcher (Director)

Dr. Drew Landman

Dr. Krishnanand Kaipa

ABSTRACT

DESIGN AND IMPLEMENTATION OF A LAUNCHING METHOD FOR FREE TO OSCILLATE DYNAMIC STABILITY TESTING

Kristen M. Carey
Old Dominion University, 2023
Director: Dr. Colin Britcher

Magnetic Suspension and Balance Systems (MSBS) allow for static, forced oscillation and free to oscillate dynamic stability testing in a wind tunnel without the need for a physical support. The objectives of study are to assist in the application of the free to oscillate testing method in an MSBS to determine dynamic stability characteristics for various re-entry capsule designs.

This thesis discusses the development and testing of a launching method called the grabber for use in the MSBS Subsonic Wind Tunnel at NASA Langley Research Center. Aerodynamic tests were run to support the use of this method and compare the data gathered to data taken from previous runs with other supports.

Aerodynamic testing showed that the implementation of the designed launching method yielded less axial and vertical interference overall by the newly designed launcher as opposed to previous launching approaches, with the designed launching method having a maximum axial movement of 4.11 mm and a maximum vertical movement of 5.075 mm, and the other supports having displacements of more than twice that. While the outcome was successful, possible improvements and streamlined designs were identified and preliminarily developed for use in a future supersonic MSBS facility. A simulation was created to visualize the behavior of a model released into the windstream unsuspended for both subsonic and supersonic conditions. This data

was mapped against the results from the launcher's retraction to show the estimated path the model would follow. These results indicate the feasibility of this launching method in the proposed supersonic facility.

ACKNOWLEDGEMENTS

The completion of this research could not have been possible without the expertise of my advisor, Dr. Colin Britcher. This work would not have been possible without the support of the Virginia Space Grant Consortium and NASA. I would like to thank the rest of my thesis committee: Dr. Drew Landman and Dr. Krishnanand Kaipa for their support. My sincere thanks also goes to Mark Schoenenberger, David Cox, Tim Schott, and Tony Ramirez for their guidance and support in this work.

Lastly, I would like to thank my family for their support in everything I do. Without them, I would not be where I am today.

NOMENCLATURE

α	Angle of attack
β	Roll angle.
C_m	Pitching moment coefficient.
C_{m_α}	Slope of pitching moment coefficient
C_{m_q}	Pitch damping coefficient
$C_{m_{\dot{\alpha}}} + C_{m_q}$	Pitch damping sum
C_{m_1}	Initial pitching moment coefficient value
C_N	Normal force coefficient
C_{N_1}	Initial normal force coefficient value
C_{N_α}	Slope of normal force coefficient
C_{MAG}	Input from MSBS controller for amplitude damping
C_A	Axial force coefficient
C_{A_1}	Initial axial force coefficient value
C_{A_α}	Slope of axial force coefficient
CP	Center of pressure of model
CG	Center of gravity of model
F_x	Axial force
F_z	Normal force
M_y	Pitching moment
g	The standard acceleration due to gravity; 9.80665 m/s^2
m	Mass of the model, 0.057 kg.
ρ	Air density, kg/m^3.
I	Moment of inertia of model
V	Velocity of airstream, m/s.
S	Reference span of the model.
A	Reference area of the model

TABLE OF CONTENTS

LIST OF TABLES viii
LIST OF FIGURES viii
1. INTRODUCTION 1
1.1. Background 1
1.2. Technology Review 1
2. SUBSONIC MSBS DESIGN AND TESTING 7
2.1. Experimental Methodology 7
2.1.1. Subsonic Wind Tunnel 7
2.1.2. Magnetic Suspension and Balance System 11
2.2. Launching Methods 13
2.2.1. Mark 1 grabber 13
2.1.2. Sting attachments 19
2.1.3. Magnetically suspended models 21
2.2. Aerodynamic Tests 22
2.3. Overall results of Stardust testing in MSBS and discussion 41
3. SUBSONIC AND SUPERSONIC MSBS LAUNCH SIMULATION 44
3.1. Simulation Overview 44
3.2. Simulation Setup 44
3.3. Results for Subsonic Simulation 53
3.4. Subsonic simulation discussion 56
3.5. Results for unsuspended supersonic simulation 57
3.6. Unsuspended supersonic simulation discussion 60
4. SUPERSONIC DESIGN FOR FUTURE WORK 65
4.1. Mark 2 grabber 65
5. FUTURE WORK 73
6. CONCLUSIONS 74
REFERENCES 76
APPENDIX A. MSBS TESTING DESIGNS 79
APPENDIX B. MAGNETICALLY SUSPENDED MODEL DRAWING 86
APPENDIX C. STING TIPS AND EDGE HOLDERS FOR STARDUST TESTING 87
APPENDIX D. MATLAB CODES FOR LAUNCHING METHOD CALCULATIONS 88
APPENDIX E: UNCERTAINTY ANALYSIS 92

APPENDIX F: FREQUENCY OF OSCILLATIONS BLOCK 93
APPENDIX G: SUBSONIC AND SUPERSONIC SIMULATIONS 94
APPENDIX H: MARK 2 GRABBER SCHEMATICS 143
VITA 149

LIST OF TABLES

Table 1: Axial and vertical movements from trial 1 30
Table 2: Axial and vertical movements from trial 2. 33
Table 3: Axial and vertical movements from trial 3 35
Table 4: Axial and vertical movements from standard sting test 37
Table 5: Axial and vertical movements from edge holder test 40
Table 6: Adjusted Mark 1 grabber trials. 41
Table 7: Comparison of launching methods. 42
Table 8: Frequency comparison between launchers 42
Table 9: Initial coefficient values for subsonic MSBS simulation. 48
Table 10: Initial coefficient values for supersonic MSBS simulation. 50
Table 11: Starting values for subsonic simulation. 51
Table 12: Starting values for supersonic simulation. 52
Table 13: Data from subsonic simulation 103
Table 14: Data from supersonic simulation with no preload 112
Table 15: Data from supersonic simulation with -10% preload 123
Table 16: Data from supersonic simulation with +10% preload 134

LIST OF FIGURES

Figure 1: 3D rendering of Stardust capsule. 5
Figure 2: Overall dimensions of Stardust used for testing. Dimensions in inches. 6
Figure 3: Diagram of MSBS subsonic wind tunnel at NASA Langley. 7
Figure 4: Inlet section of MSBS subsonic tunnel. 8
Figure 5: 6-inch octagonal test section. 8
Figure 6: Removeable section of diffuser. 9
Figure 7: Diffuser with pneumatic retractor and vertical support struts. 10
Figure 8: Fixed diffuser section and fan assembly. 10
Figure 9: Upstream section of MSBS. 11
Figure 10: Coil configuration for MSBS. 12
Figure 11: 3D rendering of Mark 1 grabber. 14
Figure 12: Mark 1 3D printed long gripper and short grippers for MSBS testing. 15
Figure 13: Solenoid for Mark 1 MSBS testing. 16
Figure 14: Mark 1 cap for solenoid housing for MSBS testing. Dimensions in inches. 17

Figure 15: Mark 1 solenoid housing with solenoid base inside for MSBS testing. 17
Figure 16: 3D printed Mark 1 grabber base for MSBS testing. 18
Figure 17: Mark 1 grabber attached to pneumatic retractor in MSBS subsonic tunnel. 19
Figure 18: Conceptual drawing of sting. 19
Figure 19: 20-degree standard sting for Stardust MSBS testing. 20
Figure 20: 20-degree edge holder for Stardust MSBS testing. 21
Figure 21: 3D printed Stardust model. [Heatshield (front) side up] 21
Figure 22: Calibration image for pixel to meter conversion. 23
Figure 23: Experimental setup for uncertainty analysis with traverse 24
Figure 24: Dot labels for "track2dot" code 24
Figure 25: Dot 1 time history for traverse data 25
Figure 26: Dot 2 time history for traverse data 25
Figure 27: Linear fit with ± 2 sigma for Dot 1 26
Figure 28: Linear fit with ± 2 sigma from Dot 2 27
Figure 29: Mark 1 grabber holding Stardust capsule for free to oscillate testing. 28
Figure 30: Mark 1 grabber and Stardust configuration for trial 1. 29
Figure 31: Pitch, axial movements, and vertical movements vs. time for trial 1 30
Figure 32: Mark 1 grabber and Stardust configuration for trial 2. 32
Figure 33: Pitch, axial movements and vertical movements vs. time for trial 2. 32
Figure 34: Pitch, axial movements and vertical movements vs. time for trial 3. 34
Figure 35: Standard sting holding Stardust capsule for free to oscillate testing. 36
Figure 36: Pitch, axial movements and vertical movements vs. time for standard sting 37
Figure 37: Edge holder holding Stardust capsule for free to oscillate testing. 39
Figure 38: Pitch, axial movements and vertical movements vs. time for edge holder 40
Figure 39: Top level block diagram of the simulation. 44
Figure 40: Subsonic axial force coefficient measurements from Mitcheltree et al.[20] 45
Figure 41: Subsonic normal force coefficient measurements from Mitcheltree et al.[20] 46
Figure 42: Subsonic Pitching Moment Coefficient measurements from Mitcheltree et al.[20] ... 46
Figure 43: C_{mq} values as functions of location of CG. 48
Figure 44: Supersonic axial force coefficient measurements from Mitcheltree et al.[20] 49
Figure 45: Supersonic normal force coefficient measurements from Mitcheltree et al.[20] 49
Figure 46: Supersonic pitching moment coefficient measurements from Mitcheltree et al.[20] . 50
Figure 47: Body attitude for subsonic MSBS. 53
Figure 48: Body velocity for subsonic MSBS. 53
Figure 49: Body accelerations for subsonic MSBS. 54
Figure 50: Displacement of model for subsonic MSBS. 54
Figure 51: Model Dynamic pressure for subsonic MSBS. 55
Figure 52: Model Mach number for subsonic MSBS. 55
Figure 53: Model movement unsuspended vs. Grabber retraction. 56
Figure 54: Body attitude for unsuspended supersonic MSBS. 57
Figure 55: Body velocity for unsuspended supersonic MSBS. 58
Figure 56: Body accelerations for unsuspended supersonic MSBS. 58
Figure 57: Displacement of model for unsuspended supersonic MSBS. 59

Figure 58: Model dynamic pressure for unsuspended supersonic MSBS. 59
Figure 59: Model Mach number for unsuspended supersonic MSBS. 60
Figure 60: Velocity of model for -10% preload case 61
Figure 61: Displacement of model for -10% preload case 62
Figure 62: Velocity of model for +10 preload case 62
Figure 63: Displacement of model for +10 preload case 63
Figure 64: Comparison of supersonic cases. 64
Figure 65: Representation of one-motion retraction. 66
Figure 66: Schematic of Mark 2 grabber 67
Figure 67: Mark 2 outer rod with flanges. 68
Figure 68: Mark 2 inner rod with 3D printed parts attached with epoxy. 68
Figure 69: Mark 2 connector rod from inner rod to retractor. 69
Figure 70: Mark 2 aero fairing cap. 70
Figure 71: Mark 2 stop cap. 70
Figure 72: Mark 2 3D printed long gripper and short grippers for MSBS testing. 71
Figure 73: Mark 2 grabber prototype Assembly. 72
Figure 74: Vertical support strut top. Dimensions in inches. 79
Figure 75: Vertical support strut bottom. Dimensions in inches. 80
Figure 76: Vertical support strut assembly. 81
Figure 77: Solenoid for Mark 1 grabber. Dimensions in inches. 81
Figure 78: Solenoid housing for Mark 1 grabber. Dimensions in inches. 82
Figure 79: Grabber base for Mark 1 grabber. Dimensions in inches. 82
Figure 80: Connector for solenoid housing for Mark 1 grabber. Dimensions in inches. 83
Figure 81: Connector rod for Mark 1 grabber. Dimensions in inches. 83
Figure 82: Long gripper for Mark 1 grabber. Dimensions in inches. 84
Figure 83: Short gripper for Mark 1 grabber. Dimensions in inches. 84
Figure 84: Schematic of assembly of Mark 1 grabber. Dimensions in inches. 85
Figure 85: Stardust model with cavity for cylindrical ¾ inch magnet. Dimensions in inches. 86
Figure 86: Sting attachment for Stardust testing. Dimensions in inches. 87
Figure 87: Edge holder for Stardust testing. Dimensions in inches. 87
Figure 88: Sine wave block parameters. 93
Figure 89: Simulink model for Subsonic and Supersonic Simulations. 94
Figure 90: Aerodynamic coefficient subsystem 95
Figure 91: Pitch rate nondimensionalizing subsystem 96
Figure 92: C_{mq} slope subsystem 96
Figure 93: Aerodynamic Forces and Moments Subsystem. 97
Figure 94: Three Degree of Freedom Body Axes Subsystem. 97
Figure 95: Attitude of model for -10% preload case 121
Figure 96: Accelerations of model for -10% preload case 121
Figure 97: Mach for -10% preload case 122
Figure 98: Dynamic pressure for -10% preload case 122
Figure 99: Attitude of model for +10 preload case 132
Figure 100: Accelerations of model for +10 preload case 132

Figure 101: Mach for +10% preload case 133
Figure 102: Dynamic pressure for +10% preload case 133
Figure 103: Long gripper for Mark 2 grabber. Dimensions in inches. 143
Figure 104: Short gripper for Mark 2 grabber. Dimensions in inches. 143
Figure 105: Aero fairing cap for Mark 2 grabber. Dimensions in inches. 144
Figure 106: End cap for Mark 2 grabber. Dimensions in inches. 144
Figure 107: Outer rod for Mark 2 grabber. Dimensions in inches 145
Figure 108: Inner rod for Mark 2 grabber. Dimensions in inches. 146
Figure 109: Connector rod for Mark 2 grabber. Dimensions in inches. 147
Figure 110: 3D rendering of Mark 2 grabber 148

1. INTRODUCTION

1.1. Background

The 6-inch MIT/NASA/ODU Magnetic Suspension and Balance System (MSBS) at NASA Langley is currently being used to study dynamic stability of atmospheric entry vehicles. It was originally built in 1957 and used for dynamic stability testing at the Massachusetts Institute of Technology, before it was sent to NASA Langley to be utilized and subsequently retired in the 1990s. The MSBS was reactivated in 2016 and has supported dynamic stability research for atmospheric entry vehicles, moving towards the future goal of a supersonic MSBS development [1]. The MSBS uses electromagnetic coils and an electromagnetic position sensor system (EPS) with a feedback controller to suspend a model. Previously tested models included a range of existing capsule geometries for NASA missions [2]. The models were scaled for the MSBS and modified to house the magnetic core, usually either a 0.75-inch cylindrical Neodymium-Iron-Boron (NdFeBo) core or a 0.75-inch spherical NdFeBo core. The models previously used for testing were often created with 3D printing for simplicity. The previous launching methods for the MSBS have consisted of small attachments that attach to a nylon rod mounted to a pneumatic retractor in the wind tunnel. These launching methods were designed to push up against the testing model to deflect it a at predetermined angle. Issues with these methods were the lack of repeatability and the inability to effectively generate extreme angles as initial conditions. To remedy this, a new launching method needed to be designed to hold the model at a predetermined angle with as little surface area touching the model as possible followed by a rapid retraction. By introducing less interference with the testing model, more accurate data collection of an entry vehicle's dynamic stability could be achieved.

1.2. Technology Review

Dynamic stability is defined as the ability of a flight vehicle to return to a state of aerodynamic equilibrium after being disturbed [3]. For atmospheric entry vehicles, dynamic stability is important as it prevents tumbling which would create an unsafe and possible detrimental landing. Most instabilities in re-entry occur at high dynamic pressures, low supersonic or high subsonic speeds, which is just before counter measures such as drogue chutes and parachutes are deployed [4]. Drogue chutes are used to stabilize an unstable flight before the parachute deploys to slow the vehicle's descent, but if a vehicle is too unstable, then the deployment will not be successful [6]. According to Kazemba et al., oscillations must be within 10 degrees to ensure proper deployment [5]. At low supersonic and high subsonic speeds, aerodynamic characteristics such as dynamic stability, drag, and lift are more sensitive to geometry and dynamic pressure. According to a paper by M. Baillion on blunt body aerodynamics, blunted capsules may be dynamically unstable in the high subsonic and low supersonic Mach range [7]. While being unstable in these regimes, capsules tend to have a larger drag force to decelerate than other entry vehicles such as large angle nose cones which is why they are desirable for planetary entry [7]. At this range of speeds, the dynamic instability increases if the shape of the backshell of the entry vehicle is a truncated cone and lessens or stays the same if the backshell of the entry vehicle is a spherical surface. This is due to the way the flow separates and reattaches around the vehicle, becoming unsteady when combined with the wake [8]. Upon re-entry, an entry vehicle will encounter high dynamic pressures and flow separation. When a flow reattaches at the aft end of a blunt or flat forebody, large amounts of dynamic instability are caused. To remedy this, the noses of entry vehicles were designed to have rounded edges and be less blunt. This increases dynamic stability but will also increase the need for more durable aeroshells [9].

MSBS

Magnetic suspension was first developed in 1937 by Professor B. A. Holmes at the University of Virginia with the goal of reducing frictional losses in a centrifuge. A Magnetic Suspension and Balance System (MSBS) was first used for aerodynamic testing in 1954 to suspend a tested model freely without the need for a mechanical support [10]. Mechanical supports, such as stings, limit the available range of motion for a test model and disrupt the wake flow, thus yielding inaccurate data. By using an MSBS for dynamic stability testing, a more complete range of motion is available [11]. A MSBS uses electromagnetic coils to suspend a model, a position sensing system (an EPS here) to track the model. The EPS gives position feedback that is linked to a feedback controller [12]. The electromagnetic coils suspend the model in the X, Y, and Z directions, thus providing support for the model without limiting the range of motion. A MSBS provides up to six degrees of freedom for a tested model, thus giving a more accurate simulation of the motion a vehicle would have upon re-entry [13]. Throughout the years, many universities and research establishments both in the USA and abroad have developed and tested aerodynamic models in their own MSBS. The speeds in which this technology is viable ranges from subsonic to hypersonic, but the usable test section size is an issue. Currently the MSBSs in use have a test section ranging from six inches in diameter to 1 meter (Tohoku University) in diameter [14]. This means only scaled down models can be used. In the 1990s, there was a push to develop a large-scale transonic wind tunnel that was outfitted with an MSBS, but the expense of such a facility was very high and therefore development was not continued. Since then, smaller MSBS wind tunnels have been used and improved upon to continue dynamic stability testing of various re-entry capsules such as the Mars sample return capsule and the Dragonfly capsule.

Free-to-oscillate dynamic stability testing occurs when a model is held, by either a testing rig or sting, and released at a predetermined angle to freely oscillate with the air flow. By removing the mechanical support, the wake flow remains unperturbed by its influence [15]. This type of testing provides valuable insight into the characteristics of entry vehicles, both stable and unstable. It also provides a useful tool for redesigning of reentry vehicles based on flight characteristics. By testing using MSBS, reliable data can be collected to improve upon previous flight vehicle designs.

The purpose of this thesis is to design and test a launching method for free to oscillate dynamic stability testing in a MSBS and to examine the quality of the data gathered . A secondary goal of this thesis was to project the design of the launching methods for future use in the NASA Glenn Supersonic Tunnel. A tertiary goal of this thesis was to create a simulation in Simulink that would model a blunt body in a subsonic and supersonic testing environment to determine the downstream path the model would follow if suddenly released or launched in the MSBS.

Three experiments were designed for comparison between the launching mechanisms. The first experiment involved launching the test model with the standard sting attachment that has been used previously in the MSBS subsonic tunnel. The second experiment involved launching the test model with the edge holder attachment that has been used previously in the MSBS subsonic tunnel. The last experiment involved launching the test model with a newly designed grabber that would actuate opened and closed to grab and release the model when testing began.

Model Geometry

The model geometry used in this thesis was that of the Stardust sample return capsule. Stardust, the fourth Discovery class mission, was launched in 1999 to collect interstellar dust [16]. This model was chosen based on the availability of previous dynamic stability and MSBS test data and the simplicity of design. All experiments utilize a 3D printed model, in this case the existing Stardust geometry, that holds a magnetic core. The chosen deflection angle for the tests was 20 degrees whereas the standard testing angle was previously 5 degrees, so with a larger deflection angle, oscillation can be seen more clearly to determine the interference that may be created from the various launching methods. For future testing in a supersonic setting, the grabber was redesigned to take a more mechanically-sequenced approach that would reduce the time between release and retraction. Figure 1 is a 3D rendering of the Stardust geometry with the nose of the models facing upwards.

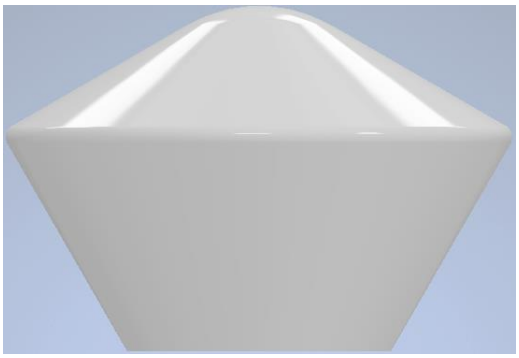

Figure 1: 3D rendering of Stardust capsule.

The test model for the MSBS testing had a nominal diameter of 1.75 inches. This is 5% scale of the Stardust return capsule. Figure 2 below shows a simplified schematic of the Stardust model with a cavity for the magnetic core. A detailed overview of the model dimensions for Stardust is shown in Appendix B.1.

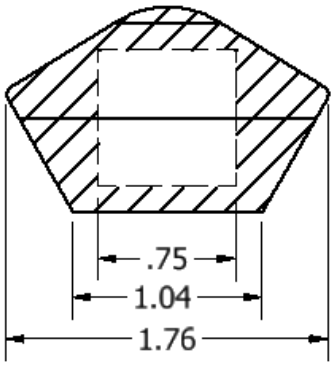

Figure 2: Overall dimensions of Stardust used for testing. Dimensions in inches.

2. SUBSONIC MSBS DESIGN AND TESTING

2.1. Experimental Methodology

2.1.1. Subsonic Wind Tunnel

The wind tunnel used for this research was the 6-inch subsonic MSBS wind tunnel at NASA Langley. This tunnel is a total 8.8 meters long with a 1.22-meter width [17]. The subsonic wind tunnel is suitable for testing due to similar dynamic pressures compared to low supersonic speeds. This wind tunnel can reach speeds of Mach 0.5 and produce dynamic pressures as high as 17.5 kPa [18]. As previously discussed, atmospheric entry vehicles become the most dynamically unstable at low supersonic and high subsonic speeds, with a large dynamic pressure. Therefore, data gathered at subsonic speeds with high dynamic pressure can be used to represent results from a supersonic environment. Figure 3 below is a diagram of the wind tunnel used in this research.

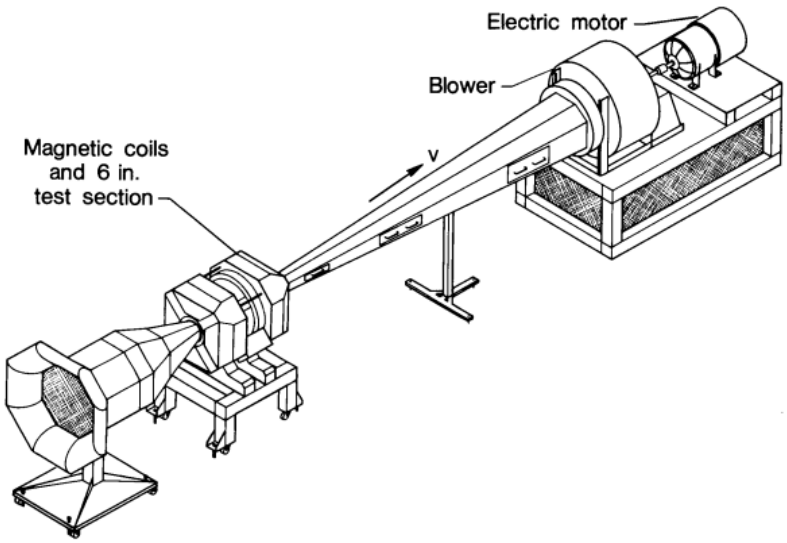

Figure 3: Diagram of MSBS subsonic wind tunnel at NASA Langley.

Inlet section

The inlet section of the MSBS subsonic wind tunnel is composed of two parts: the settling chamber and contraction cone. The settling chamber contains three screens to reduce the turbulence of the flow. The contraction cone has a contraction ratio of 20:1 [2]. The inlet moves on slides to open the test section for model insertion and is then closed and clamped into place for testing. The inlet section is shown below in Figure 4.

Figure 4: Inlet section of MSBS subsonic tunnel.

The test section is a 6-inch (across flats) octagonal duct fabricated from clear acrylic plastic. The test section is shown below in Figure 5.

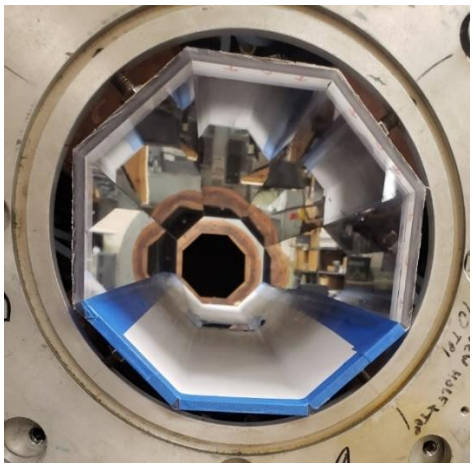

Figure 5: 6-inch octagonal test section.

The aft end of the MSBS is connected to the removable section of the diffuser via a diffuser flange plate which bolts into the MSBS to ensure no relative movement.

Diffuser

The diffuser of the subsonic tunnel is comprised of a removable section and a fixed section connected to the fan assembly of the tunnel. The diffuser is 3.785 meters long with three access panels for lighting, cable access, and model retrieval [2]. Figure 6 below shows the removeable diffuser section.

Figure 6: Removeable section of diffuser.

The removable section was previously outfitted with a short extension which included an aluminum strut, which in turn supported a sting. A later version included a pneumatic retractor that is secured by two vertical support struts. The current strut design was 3D printed with nylon filament and was based on the previous struts that existed in the tunnel. The previous struts were 3D printed with ABS filament and were designed to have a track that the pneumatic retractor slid into. For a design that produced less blockage than the previous one, the struts were redesigned to have small tabs on the side that would utilize small screws to hold the pneumatic retractor in place via threaded holes tapped into the outer shell of the retractor. Dimensional drawings for the struts and assembly are shown in Appendix A.1 – A.3. Below, as shown in Figure 7, is the diffuser section outfitted with the vertical support struts and pneumatic retractor.

Figure 7: Diffuser with pneumatic retractor and vertical support struts.

Once the retractor was successfully installed, the removable section of the diffuser was reconnected to the MSBS test section and the fixed diffuser section. Figure 8 shows the fixed diffuser section that is connected to the fan assembly of the wind tunnel.

Figure 8: Fixed diffuser section and fan assembly.

Fan and Motor

A squirrel-cage fan with an inlet diameter of 20 inches is used to give a required pressure differential. The fan is powered by a Century E-plus 3 14.9 kW AC motor. A Cerus Industrial Titan S Series motor drive powers the AC motor.

2.1.2. Magnetic Suspension and Balance System

The MSBS consists of multiple systems of magnetic coils. Each system of coils controls a separate aerodynamic axis. A view of the MSBS is shown below in Figure 9.

Figure 9: Upstream section of MSBS.

The magnetic coils position the testing model to be at the origin in the X, Y, and Z plane. The MSBS is currently configured for vertical magnetization, which means that the rotation observed in the model is technically yawing but is regarded as aerodynamic pitch. Figure 10 below shows the coil configuration of the 6-inch MSBS [18].

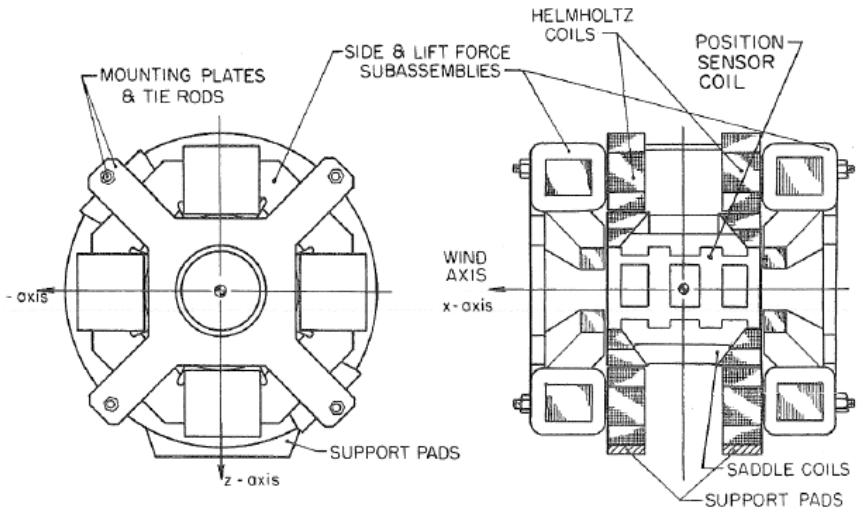

Figure 10: Coil configuration for MSBS.

The MSBS is powered by two 15 kW DC power supplies feed the magnetizing coil and five 60A PWM amplifiers are used to double the current capacity of the power supplies. The coils that control the drag and alignment functions are powered by a maximum current of 60A. The coils that control the side and vertical forces are powered by maximum currents of 60A and 120A, respectively [19]. Speed is controlled by a LabVIEW VI on a local PC. The MSBS controller used is a Speedgoat, which is a real time controller that gathers data from the LabVIEW VI, EPS, and other components [2].

Camera

For testing, model movement is observed and recorded using a camera. The camera used for testing was the Edgertronic SCI high speed camera that was mounted to the bottom of the MSBS, pointing upwards to capture video of testing through the clear circular bottom window [2]. The camera has been configured to only take video upon an event trigger such as a sting retracting. As was stated before, due to the MSBS suspending the model with vertical

magnetization, the observed movement is yawing, however, since the camera is on the bottom of the MSBS, the movement of model observed through the camera is interpreted as pitching.

Data Processing

The video data from tests is gathered using MATLAB motion tracking to determine angle of attack and position. The values for pitch damping are then derived in further research from the mass of the object, moment of inertia, dynamic pressure, angle of attack, and the static aerodynamic coefficients of the model using Equation (1) below.

$$\alpha = Ae^{\frac{\rho VS}{2m}\left(C_{N_\alpha}+C_{MAG}+\frac{md^2}{2I}C_{m_q}\right)^t} cos\left(\sqrt{\frac{\rho VS^2}{2I}}C_{m_\alpha}t+\beta\right) \qquad (1)$$

In this equation, the initial values for model geometry and flow conditions are input. The variables linked to the model geometry are the reference area (A), reference span (S), mass (m), moment of inertia (I), and diameter of the model (d). The variables linked to the flow are the velocity (V) and density (ρ). The final variables for input are the aerodynamic derivatives, normal force slope coefficient (C_{N_α}), pitching moment slope coefficient (C_{m_α}), and input from the MSBS (C_{MAG}), as well as the pitching attitude (α) and the sideslip (β). Through this equation, the resultant pitch damping coefficient (C_{m_q}) is calculated to determine the dynamic stability of the model.

2.2. Launching Methods

2.2.1. Mark 1 grabber

The design of the grabber was the main goal of this research. The objective of the grabber was to launch a selected re-entry capsule model in the NASA Langley MSBS wind tunnel in a manner that interfered less with the model than previous launching methods. Various concepts were considered for the grabber design, the design chosen for the grabber resembled a claw that

would extend and then grip around a testing model. The grabber had a slender body to prevent high levels of blockage, and an opened “base” that would accommodate most entry vehicles being tested in the subsonic MSBS wind tunnel at NASA Langley. For this project, the design for the subsonic tunnel was named the “Mark 1 grabber”. This design included a solenoid for actuation of cables that closed the grippers and small elastic bands that pulled the grippers open when the solenoid was turned off. The design for the future supersonic tunnel was named the “Mark 2 grabber” and was purely mechanical and relied on internal cam action without the need for cables. More information on the Mark 2 grabber will be presented later. Figure 11 below shows a 3D rendering of the Mark 1 grabber.

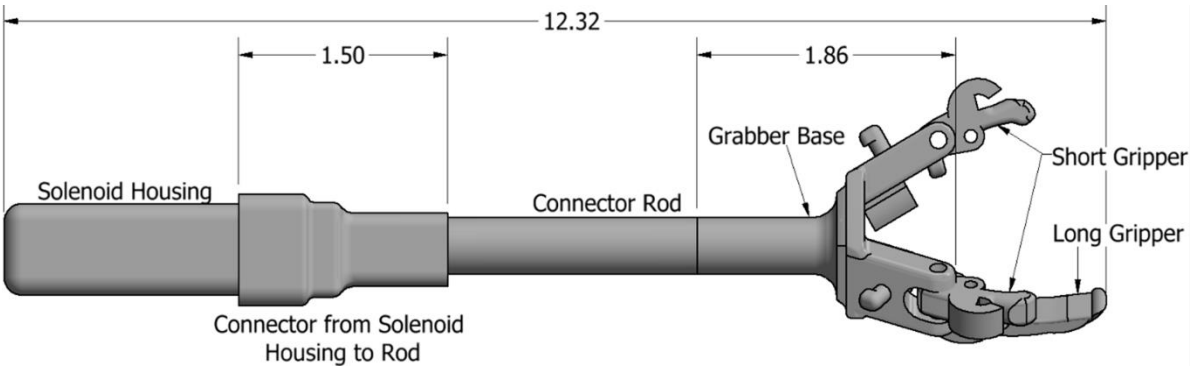

Figure 11: 3D rendering of Mark 1 grabber.

The Mark 1 grabber was designed to hold the magnetically suspended model at a predetermined angle, in this case 20 degrees. The Mark 1 grabber assembly is composed of five main parts: the solenoid, solenoid housing, connector rod, base, and grippers. All dimensional drawings for the Mark 1 grabber parts are shown in Appendix A.4.

Mark 1 grabber grippers

The Mark 1 grabber grippers were designed to hold a test model at a fixed angle of 20 degrees. For this to be achieved, the grippers had to be two different sizes. By modeling the

Stardust model in Autodesk Inventor, the gripper lengths were designed to be 1.33 inches for the long gripper, and 0.87 inches for the short grippers. Each gripper features a mounting hole that is held to the grabber base by a small pin. There is also a small hole in the middle of the grippers that the retraction cables are passed through. For the release motion of the grabber, there are small hooks on the back of the grippers that hold small elastic bands that connect to the grabber base. The long and short grippers are shown below in Figure 12.

Figure 12: Mark 1 3D printed long gripper and short grippers for MSBS testing.

Solenoid

The solenoid is the driving actuator for the opening of the grippers, The solenoid for the Mark 1 grabber needed to be small enough to fit into the assembly without protruding out in the airstream to incur blockage. To fulfill these requirements, a solenoid with a nominal diameter of 0.5 inches was chosen. The length of the solenoid was not as important as the connector rod could be lengthened or shortened if needed. The solenoid chosen for MSBS testing was model number 69905K112 from McMaster Carr and is shown below in Figure 13.

Figure 13: Solenoid for Mark 1 MSBS testing.

The solenoid had a 2-ounce retraction force and a 0.25-inch throw with a power draw of 2.5 watts. A power system was created and integrated into the tunnel control software at the subsonic MSBS wind tunnel. A 12-volt regulator was used, powered by a 15-volt power supply and was controlled by the LabVIEW software. Since the solenoid would only be activated for launch, without it being powered on for a prolonged amount of time, a 15-volt power supply was deemed acceptable to use. From there, a trigger was created in the LabVIEW software that allowed the tunnel controller to retract and redeploy the solenoid.

Solenoid housing

The solenoid housing was designed to screw onto the pneumatic retractor rod and have the solenoid slide into place inside. Then a small cap, as seen in Figure 14, snapped on securing the solenoid in place and space for the solenoid arm to actuate. The cap and solenoid housing are shown below in Figure 14 and Figure 15 respectfully.

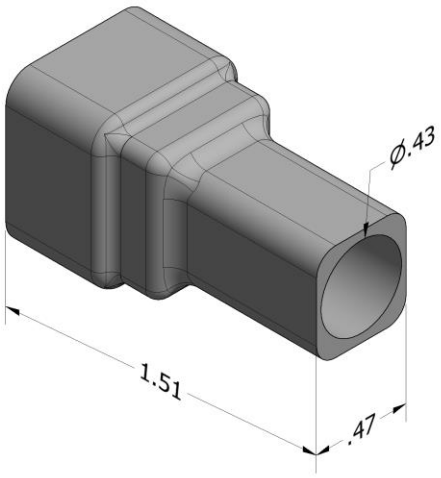

Figure 14: Mark 1 cap for solenoid housing for MSBS testing. Dimensions in inches.

Figure 15: Mark 1 solenoid housing with solenoid base inside for MSBS testing.

Connector rod

The connector rod is a hollow rod 7.159 inches in length that screwed into the top of the solenoid housing as well as the Mark 1 grabber base. The cables that cause the actuation of the grabber fingers are housed in this section.

Mark 1 grabber base

The Mark 1 grabber base has a hollow cylindrical section that is screwed on to the connector rod. The base spreads outward to form three arms for the grippers to connect via small pins. There are small loops at the center of the base that act as cable guides to keep the cables

from interfering with the model. There are also small hooks attached to the backside of the Mark 1 grabber base that hold the elastic bands that connect from the base to the grippers. The Mark 1 grabber base is shown below in Figure 16.

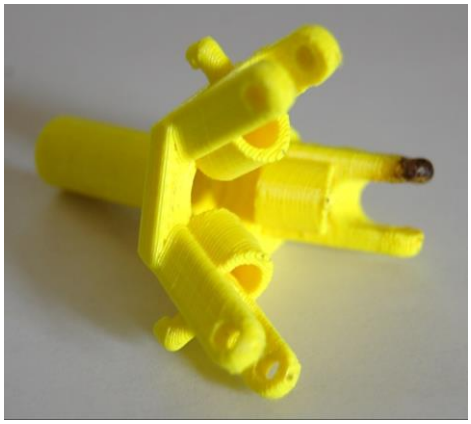

Figure 16: 3D printed Mark 1 grabber base for MSBS testing.

Mark 1 grabber assembly

For the Mark 1 assembly, the solenoid fits into the solenoid housing with the cap fitting on top. The cables are connected to the solenoid via the small holes in the solenoid rod. The cables were then fed through the connector rod and the rod was screwed into the solenoid housing cap. The connector rod then screwed into the grabber base and the cables were pulled through. From there, the grippers were mounted to the grabber base by means of small pins and the cables were fed through the grabber base and into the grippers. The small elastic bands were then hooked on to the grabber base hooks and the cutouts on the grippers. Manual adjustment was needed to set the grippers at the correct position so that the grabbing motion of the assembly would hold the model sufficiently without the hold being too tight or too loose. The grabber is shown installed in the tunnel section in Figure 17.

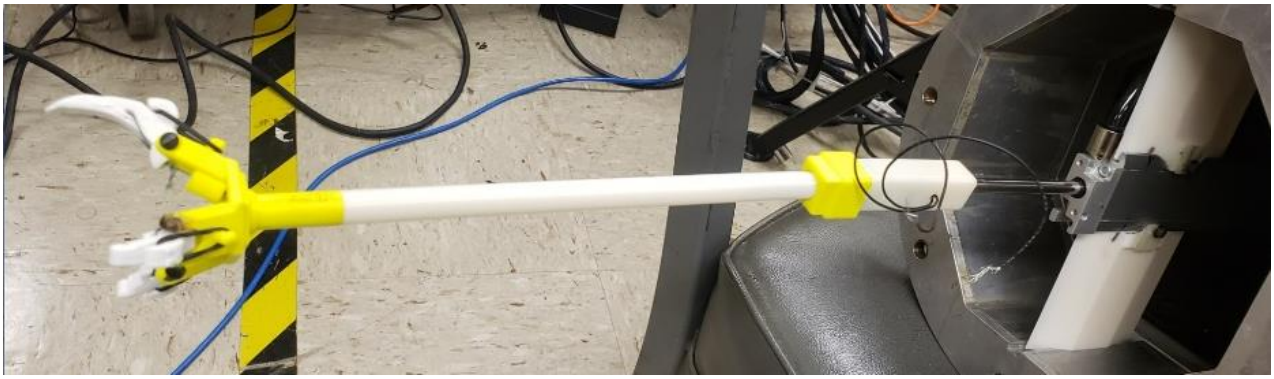

Figure 17: Mark 1 grabber attached to pneumatic retractor in MSBS subsonic tunnel.

Mark 1 grabber setup

To setup the Mark 1 grabber in the Subsonic MSBS tunnel at NASA Langley, the LabVIEW software used to control the tunnel was augmented to include a controller for the actuation of the grippers. This is included as a separate action for ease of operation as the grabber can open and close without retraction to reset the position of the model if the first grab is not at the correct position.

2.1.2. Sting attachments

All the sting attachments previously used for MSBS testing were designed to have a deflection angle of 20 degrees. Exact model dimensions are shown in Appendix C. A conceptual drawing of the sting and attachments is shown below in Figure 18.

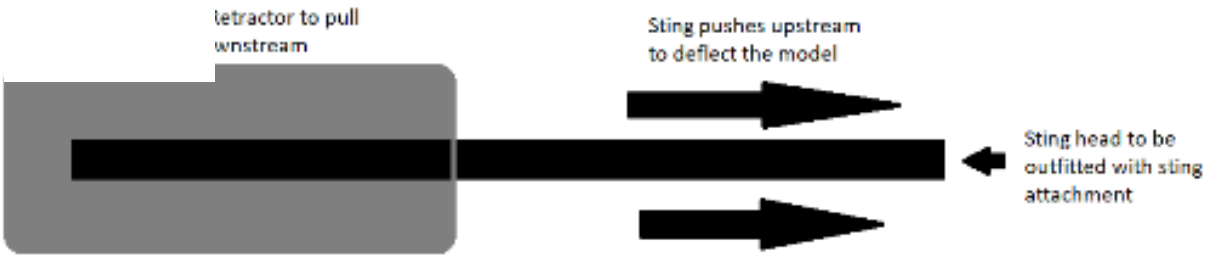

Figure 18: Conceptual drawing of sting

20-degree standard sting

The 20-degree standard sting was based on one of the sting attachments that was previously designed and tested in the MSBS subsonic wind tunnel. The previous design was at a set angle of 5 degrees, but for comparisons with the grabber and edge holder, the design was augmented to 20 degrees. It features a head with a diameter of 0.5 inches and a surface area of 0.209 in^2. The 20-degree standard sting is shown below in Figure 19.

Figure 19: 20-degree standard sting for Stardust MSBS testing.

20-degree edge holder for Stardust

The 20-degree edge holder for Stardust was augmented from an existing edge holder with a deflection angle of 4.5 degrees. The edge holder was designed to hold a thin tensioned nylon sheet that lightly touches the Stardust model enough to set the angle. For this the surface area that is touching the model would be roughly 0.238 in^2. The 20-degree edge holder for Stardust is shown below in Figure 20.

Figure 20: 20-degree edge holder for Stardust MSBS testing.

2.1.3. Magnetically suspended models

The magnetically suspended Stardust model was 3D printed with black filament so that white dots could be placed on it later for tracking motion of the model while testing. The 3D printed Stardust model is shown below in Figure 21.

Figure 21: 3D printed Stardust model. [Heatshield (front) side up]

2.2. Aerodynamic Tests

Multiple tests were conducted in the NASA Langley Subsonic MSBS tunnel. Two targets in the form of white dots were added to the Stardust model to allow the “track2dot” MATLAB function to recover model motion. The camera video was processed post-test with dot locations exported in the form of pitch, axial movement, and vertical movement. Different settings were typically needed for each video, such as adjusting the masking size and threshold to ensure the software was tracking the points sufficiently well. Data collection varied between one second and six seconds. Tabular data was compared from a range of zero to one second although graphed data from MATLAB still shows the entire testing history. Videos were cropped for ease of use. Due to this, the end data value of the x-position and y-position are not comparable for every video. The main emphasis of this study was to see the nominal movement in the axial and vertical directions, so comparisons of that data are valid. For the video data, the units exported by the original MATLAB code were in pixels, so a conversion from pixels to millimeters had to be established. For the conversion, the calibration was conducted by taking a ruler and placing it on tunnel centerline and in the camera view. The calibration image is shown below in Figure 22.

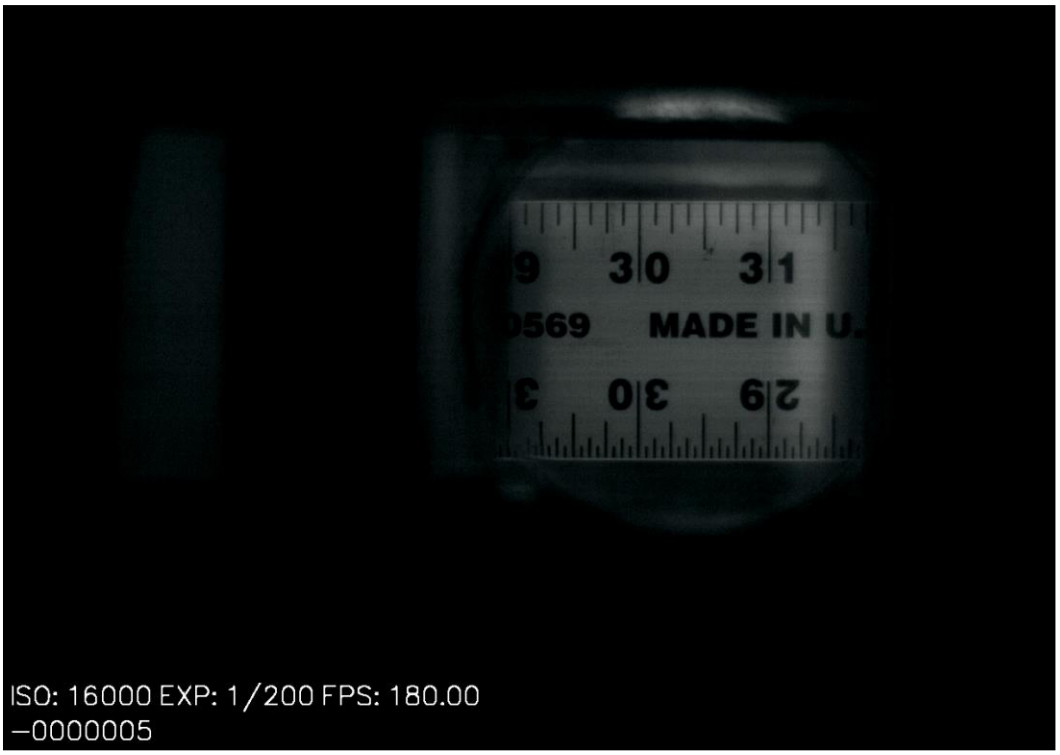

Figure 22: Calibration image for pixel to meter conversion.

The calibration image was then measured with an image processing code in MATLAB that translates user input coordinates into pixels. The codes for this step are shown in Appendix D.3. The calculations are shown below in Equations (2) – (4).

$$xyPixels(2,1) - xyPixels(1,1) = (Length * meter\ to\ inch\ ) * \frac{pixels}{meter} conversion \quad (2)$$

$$923 - 765 = (Length * 0.0254) * \frac{pixels}{meter} conversion \quad (3)$$

$$\frac{923-765}{1*0.0254} = \frac{pixels}{meter} conversion = 6220.47 \quad (4)$$

Uncertainty Analysis

An analysis of the uncertainty of the camera tracking was conducted. For this, the Stardust model was mounted to a traverse sting and the position was moved in both the axial and

vertical direction in 3 millimeter increments. The positions calculated by the “track2dot” MATLAB code were compared to the commanded positions from the MSBS controller. The experimental setup is shown below in Figure 23 and Figure 24, respectively.

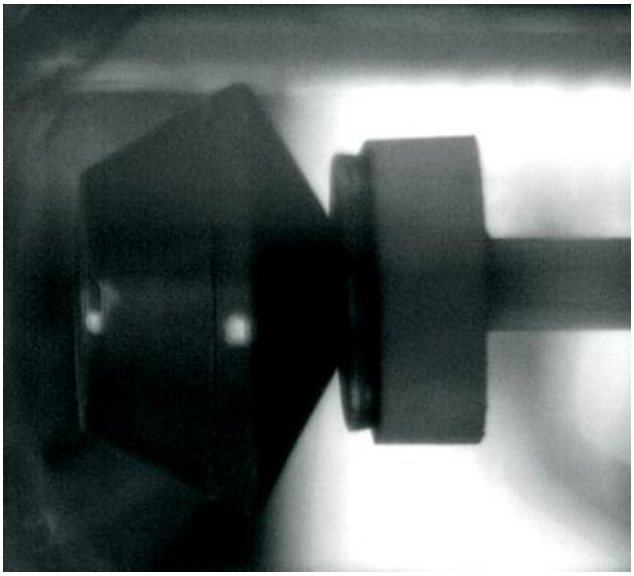

Figure 23: Experimental setup for uncertainty analysis with traverse

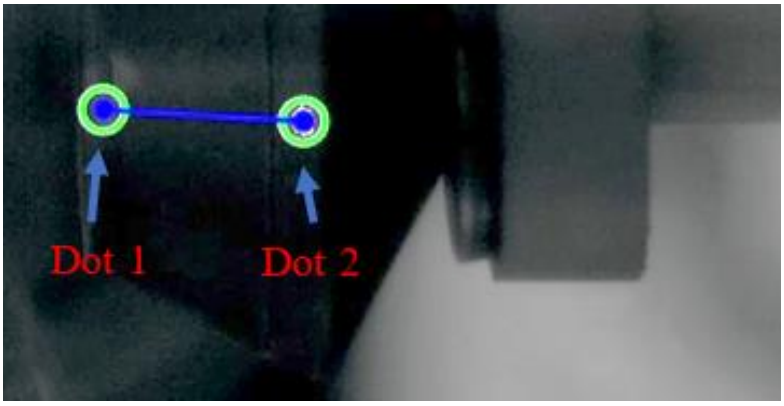

Figure 24: Dot labels for "track2dot" code

The video was analyzed, and the known positions were compared against the experimental tracked positions to find the error and bounds of a linear fit. The time histories for Dot 1 and Dot 2 are shown below in Figure 25 and Figure 26, respectively.

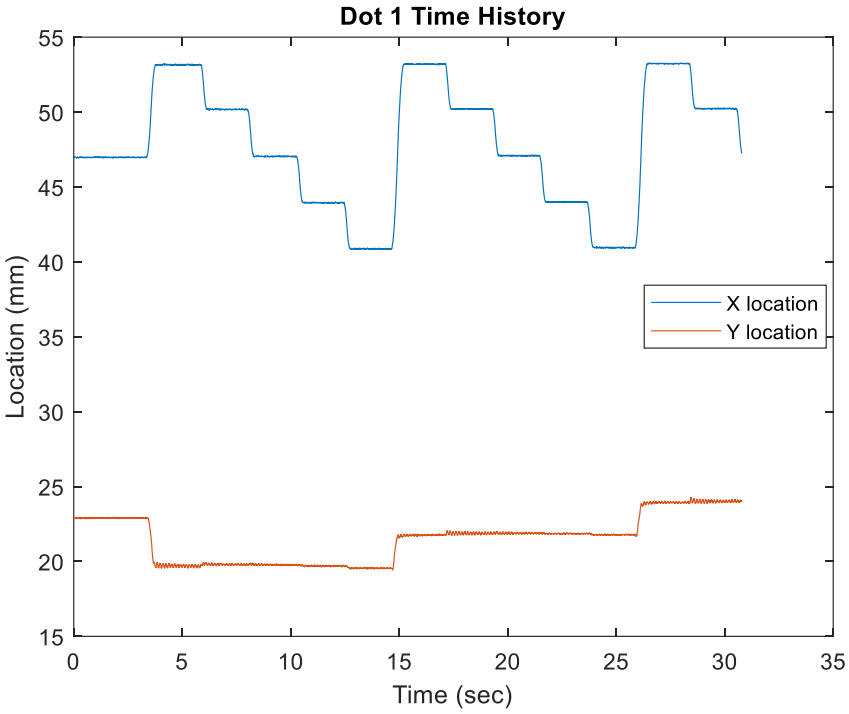

Figure 25: Dot 1 time history for traverse data

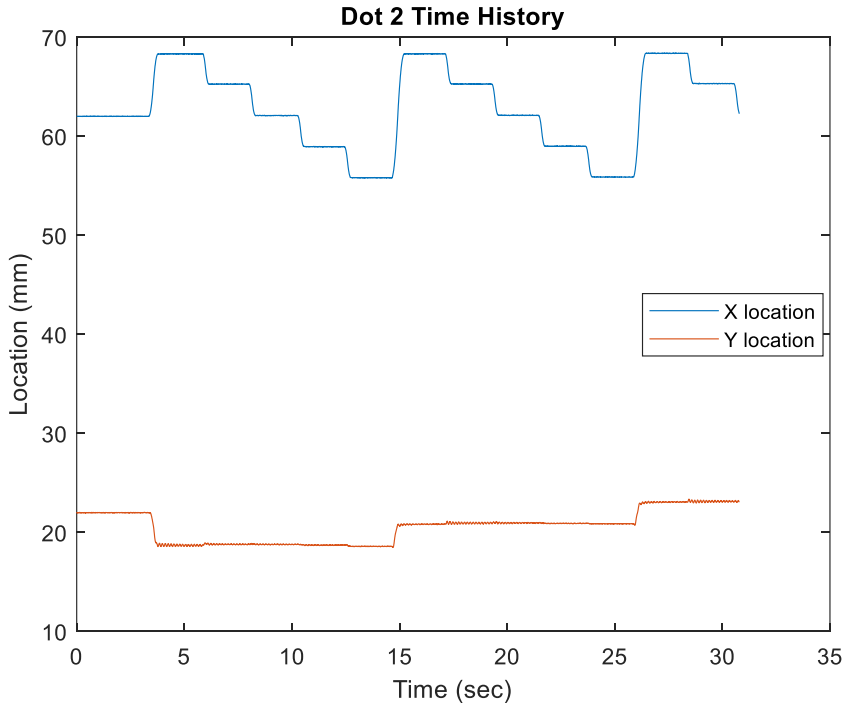

Figure 26: Dot 2 time history for traverse data

For this calculation, the linear fit was analyzed with ± 2 sigma for each dot location, where sigma is the average calculated error. The average sigma value for dot 1 was found to be 0.2124 and the average sigma value for dot 2 was found to be 0.2156 mm. The linear fit was applied to find the slope and $R^2$to determine the goodness of fit of the experimental data to the traverse location. From the calculated error, the pitch uncertainty was determined from Equation 5 below

$$Pitch\ Uncertainty = \frac{Sigma\ of\ Dot\ 1 + Sigma\ of\ Dot\ 2}{Location\ between\ dots\ (mm)} * 180/\pi \quad (5)$$

Where the location between the dots was 15 mm and the sigma for each dot varied from point to point. The analyzed data for linear fits are shown below in Figure 27 and Figure 28.

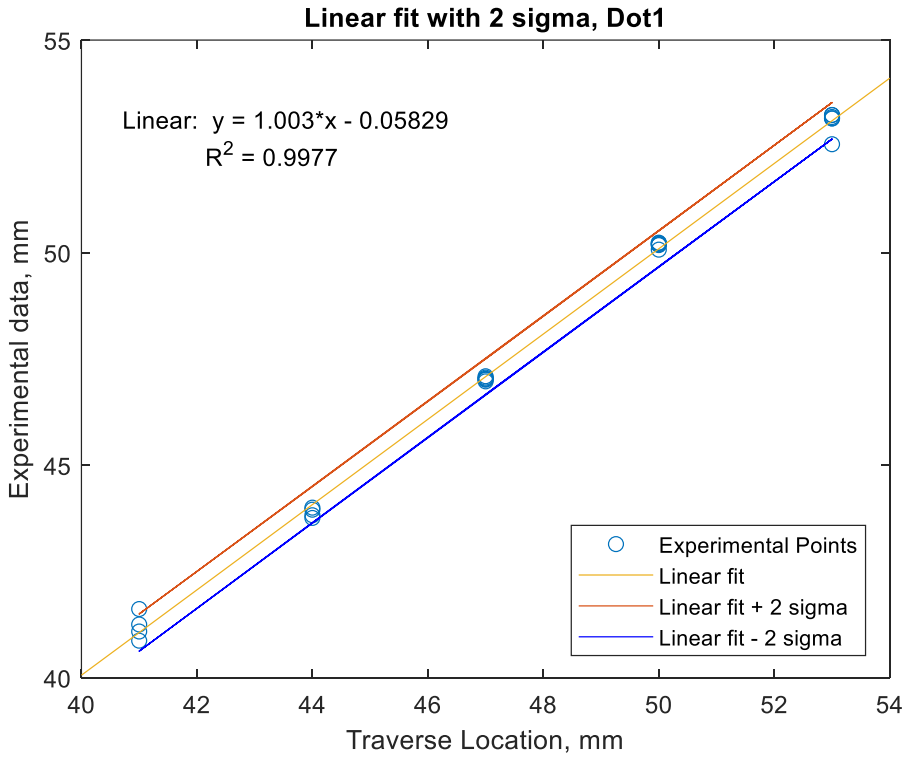

Figure 27: Linear fit with ± 2 sigma for Dot 1

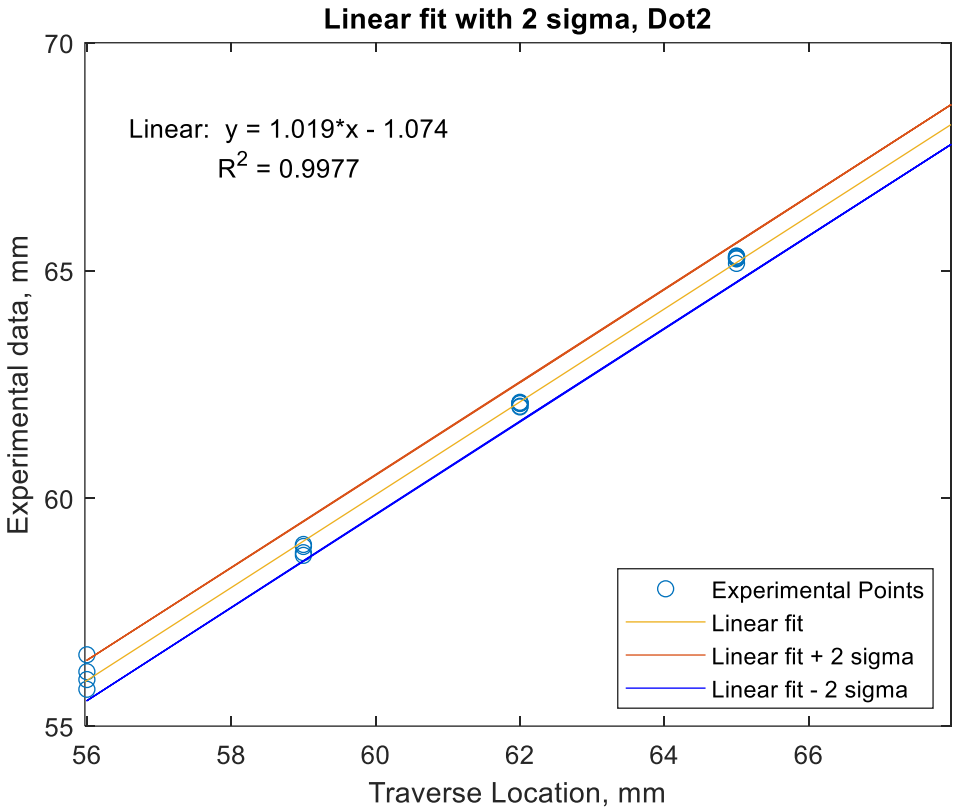

Figure 28: Linear fit with ± 2 sigma from Dot 2

Based on the figures shown above, the experimental points fall within the calculated error bounds for the model. An R^2 value of 0.9977 indicated a good agreement between the locations commanded to the traverse and the observed locations from the video analysis. The calculated error and pitch uncertainty were applied to the trajectory plots as error bars for the aerodynamics runs of the standard sting, edge holder, and Mark 1 grabber. The MATLAB code for plotting the error bars is included in Appendix E.

Mark 1 grabber tests

Multiple tests were conducted in the NASA Langley Subsonic MSBS tunnel. The Stardust model was suspended magnetically and then held by the Mark 1 grabber in the configuration seen below in Figure 29.

Figure 29: Mark 1 grabber holding Stardust capsule for free to oscillate testing.

When testing, the retraction of the Mark 1 grabber was tested numerous times before the Stardust model was levitated to ensure all systems functioned correctly and additional changes were made as needed. Once all systems were verified to be functional and collecting data, the Stardust model was levitated. When ready to begin testing, the Mark 1 grabber was deployed to grip the model and the tunnel was brought to the specified test conditions. The Mark 1 grabber retraction was then triggered causing the grippers to open and the assembly to retract away from the levitated model. Axial data can be analyzed by looking at just one target dot's data as the axial position does not vary much with pitch. Vertical movement varies with pitch therefore the

vertical motion was estimated by focusing on the dot on the nose side of the Stardust model. This dot should only move slightly with the pitch oscillation.

Results and data reduction

Mark 1 grabber: Trial 1

For the first trial, the Mark 1 grabber was slightly too short and did not meet the Stardust at its origin. As shown in Figure 30 below, the Stardust model had to be forced backwards by MSBS controls for the Mark 1 grabber to grip it.

Figure 30: Mark 1 grabber and Stardust configuration for trial 1.

The data gathered from the video of the first data collection is shown below in Figure 31.

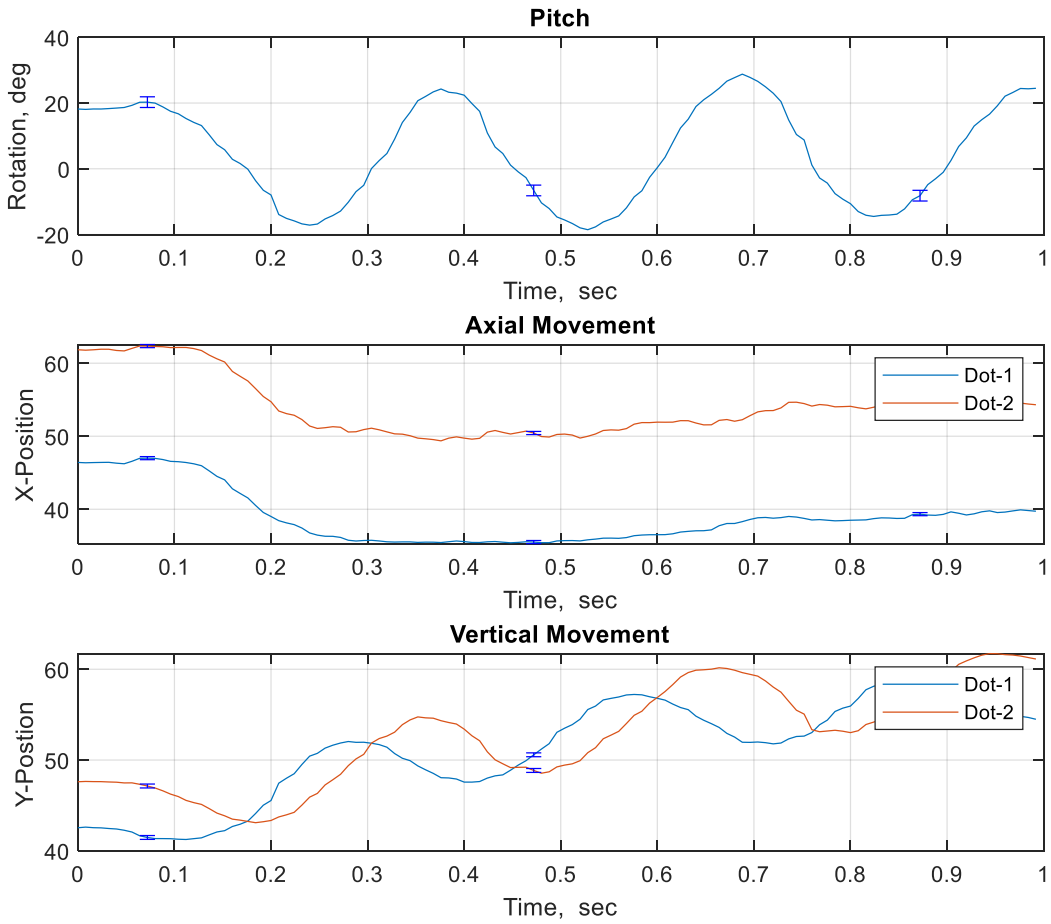

Figure 31: Pitch, axial movements, and vertical movements vs. time for trial 1

In this case, the Mark 1 grabber retraction was triggered at 0.05 seconds. A more in depth look at the data is shown below in Table 1.

Table 1: Axial and vertical movements from trial 1

Axial Movement (Dot 1) (mm)	Vertical Movement (Dot 2) (mm)	Time (sec)
46.40	47.60	0.00
46.23	47.48	0.05
46.56	46.24	0.10
44.52	44.14	0.15
39.55	43.19	0.20

36.76	45.94	0.25
35.68	50.11	0.30
35.53	54.02	0.35
35.57	54.22	0.40
35.58	50.06	0.45
35.42	48.57	0.50
35.80	50.81	0.55
36.39	54.92	0.60
36.88	59.33	0.65
38.05	60.06	0.70
38.79	57.82	0.75
38.57	53.15	0.80
38.53	53.91	0.85
39.28	56.74	0.90
39.44	60.82	0.95
39.53	61.72	0.99

As shown in Table 1, the x-position dips down from 46.4 millimeters with the lowest x-position being 35.42 millimeters and the highest x-position being 46.56 millimeters. This shows the largest axial movement to be 11.14 millimeters. The y-position starts at 47.6 millimeters, with the lowest y-position being 43.19 millimeters and the highest y-position being 61.72 millimeters, giving a total vertical movement of 18.53 millimeters.

Mark 1 grabber: Trial 2

For the second trial, the Mark 1 grabber was adjusted to be longer than the first trial so that the Stardust model would be gripped at the MSBS origin, thus alleviating any axial force caused by pullback. As shown in Figure 32 below, the Stardust model is held by the Mark 1 grabber closer to its axial and vertical origin than in trial 1.

Figure 32: Mark 1 grabber and Stardust configuration for trial 2.

The data gathered from the video of the second data collection is shown below in Figure 33.

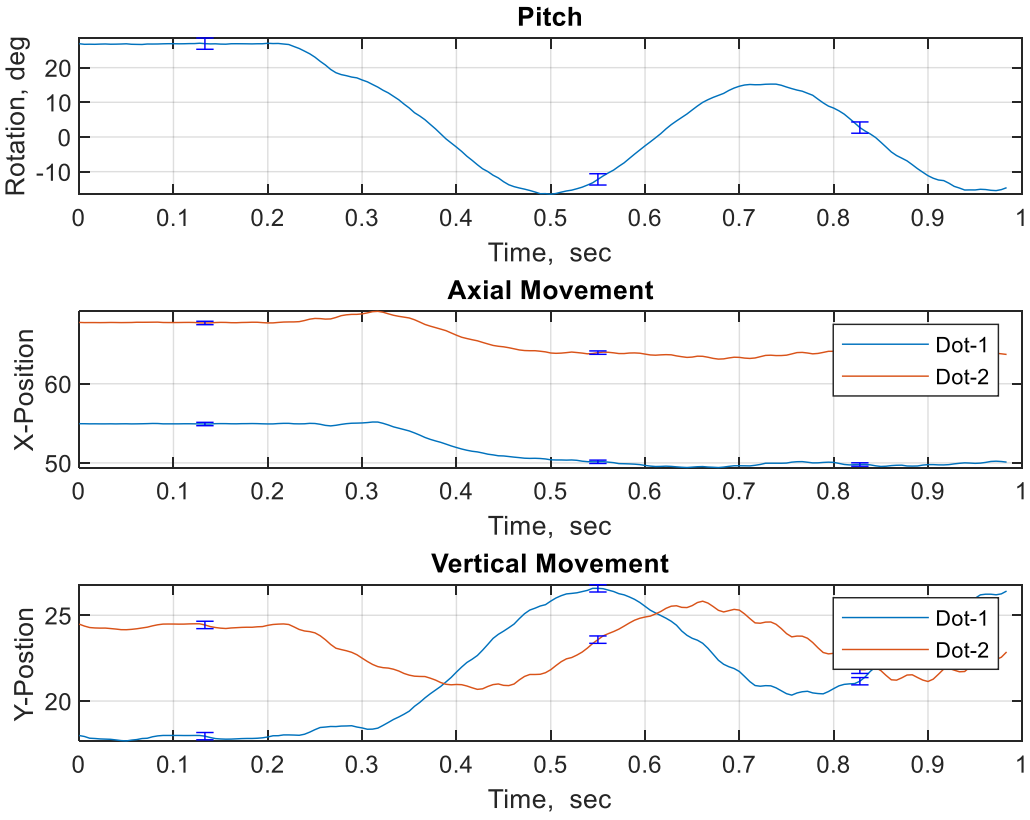

Figure 33: Pitch, axial movements and vertical movements vs. time for trial 2.

These oscillations and positions of the Stardust model are more damped than the first trial. In this case, the Mark 1 grabber retraction was triggered at 0.21 seconds. A more in depth look at the data is shown below in Table 2.

Table 2: Axial and vertical movements from trial 2.

Axial Movement (Dot 1) (mm)	Vertical Movement (Dot 2) (mm)	Time (sec)
54.95	24.48	0.00
54.94	24.16	0.05
54.93	24.49	0.10
54.96	24.25	0.15
54.92	24.41	0.20
54.98	23.97	0.25
55.05	22.50	0.30
54.03	21.51	0.35
51.94	20.97	0.40
50.88	20.91	0.45
50.39	21.83	0.50
50.14	23.58	0.55
49.68	24.90	0.60
49.51	25.56	0.65
49.64	25.30	0.70
49.98	23.93	0.75
50.06	22.78	0.80
49.55	21.77	0.85
49.78	21.14	0.90
49.94	22.30	0.95
50.08	23.17	0.99

As shown in Table 2, the x-position dips down from 54.95 millimeters with the lowest x-position being 49.51 millimeters and the highest x-position being 55.05 millimeters. This shows the largest axial movement to be 5.53 millimeters. The y-position starts at 24.48 millimeters,

with the lowest y-position being 20.91 millimeters and the highest y-position being 25.56 millimeters, giving a total vertical movement of 4.65 millimeters.

Mark 1 grabber: Trial 3

For the third trial, the settings for the Mark 1 grabber were the same as the second trial. The data gathered from the video of the third data collection is shown below in Figure 34.

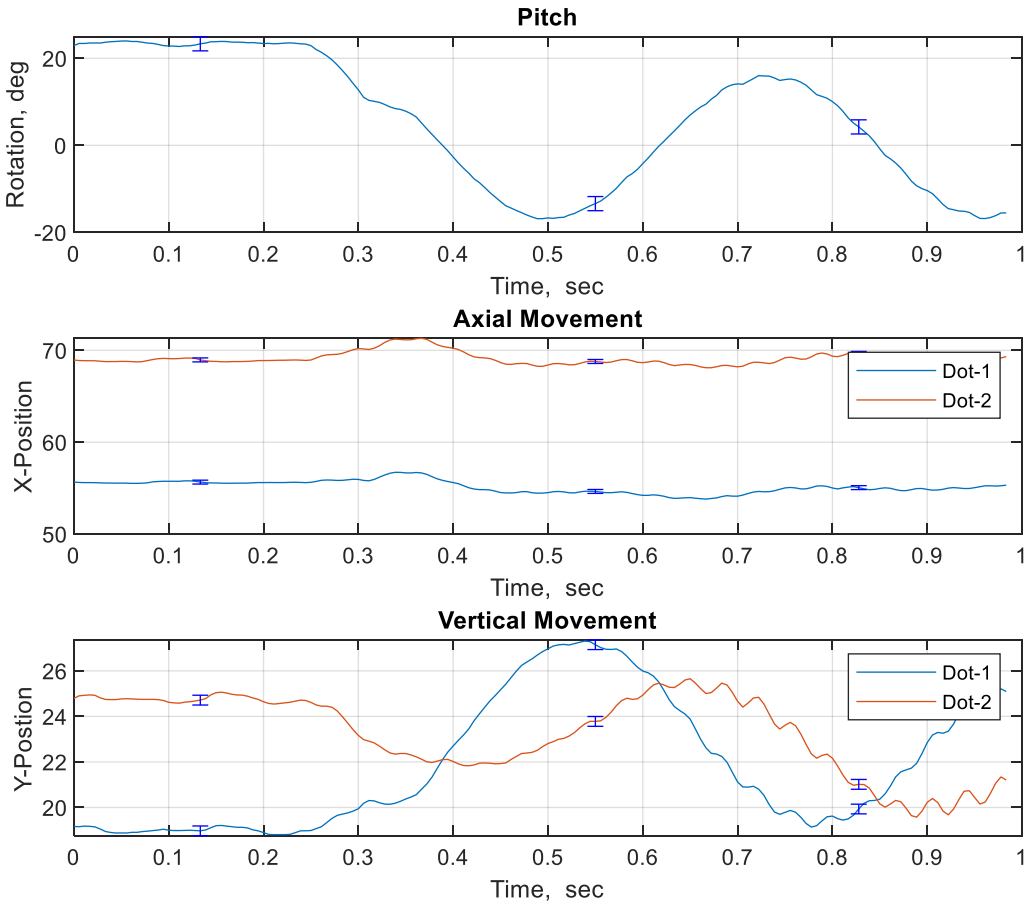

Figure 34: Pitch, axial movements and vertical movements vs. time for trial 3.

Similarly, to the second trial, the axial movement had less oscillatory behavior, which is ideally what is desired, and the vertical position oscillates as expected but not in large

magnitude. In this case, the Mark 1 grabber retraction was triggered at 0.25 seconds. A more in depth look at the data is shown below in Table 3.

Table 3: Axial and vertical movements from trial 3

Axial Movement (Dot 1) (mm)	Vertical Movement (Dot 2) (mm)	Time (sec)
55.65	24.61	0.00
55.55	24.77	0.05
55.74	24.62	0.10
55.56	25.04	0.15
55.60	24.64	0.20
55.63	24.61	0.25
55.95	23.17	0.30
56.66	22.37	0.35
55.61	22.02	0.40
54.52	21.93	0.45
54.51	22.81	0.50
54.64	23.78	0.55
54.21	24.94	0.60
53.96	25.66	0.65
54.12	24.66	0.70
55.02	23.61	0.75
55.02	22.16	0.80
54.96	20.16	0.85
54.86	20.23	0.90
55.05	20.44	0.95
55.45	20.95	0.99

As shown in Table 3, the axial movement fluctuates slightly, moving up to 56.66 millimeters from a starting x-position of 55.65 millimeters, then dipping back down to 53.96 millimeters and then ends at 55.45 millimeters. This shows the largest axial movement to be 2.69 millimeters. The y-position starts at 24.61 millimeters, with the lowest y-position being 20.16 millimeters and the highest y-position being 25.66 millimeters, giving a total vertical movement of 5.50 millimeters.

A commonly observed behavior in video data from the Mark 1 grabber was a delay between the opening of the Mark 1 grabber and the retraction of the sting. This was caused by signal delay as the controller for the retraction of the sting and the actuation of the solenoid are separate systems and do not receive voltage at the exact same time. Although the delay is small, found to be about 0.05 seconds, this cuts into the available time needed for the Mark 1 grabber to be clear from the testing model and could lead to interference and unwanted influence on the model.

Standard sting attachment

When testing, the sting with the standard sting attachment was deployed to push against the Stardust model and then retracted to pull away from the Stardust model to gather data. The configuration for the standard sting attachment is shown below in Figure 35.

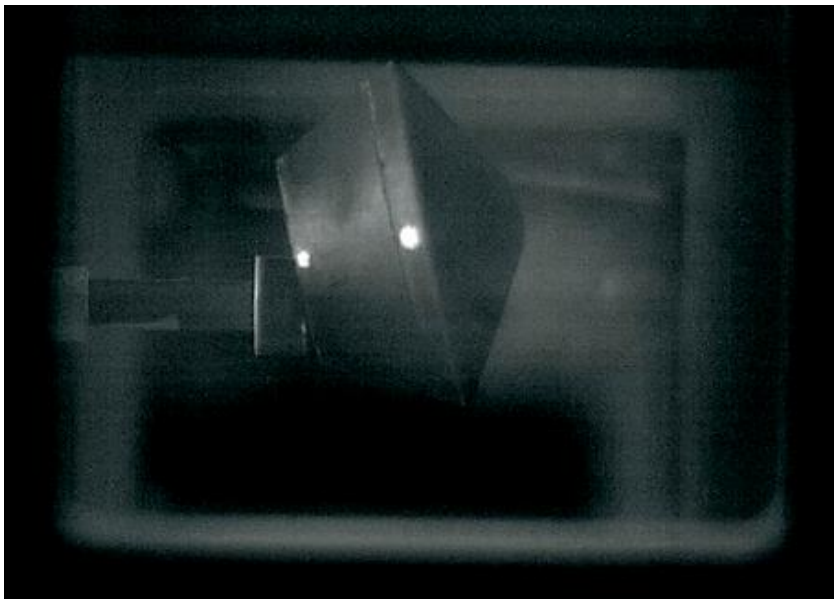

Figure 35: Standard sting holding Stardust capsule for free to oscillate testing.

Results and data reduction

For the standard sting attachment, the pneumatic retractor was deployed to push the sting attachment against the Stardust model to deflect it. The data gathered from the video of this run is shown below in Figure 36.

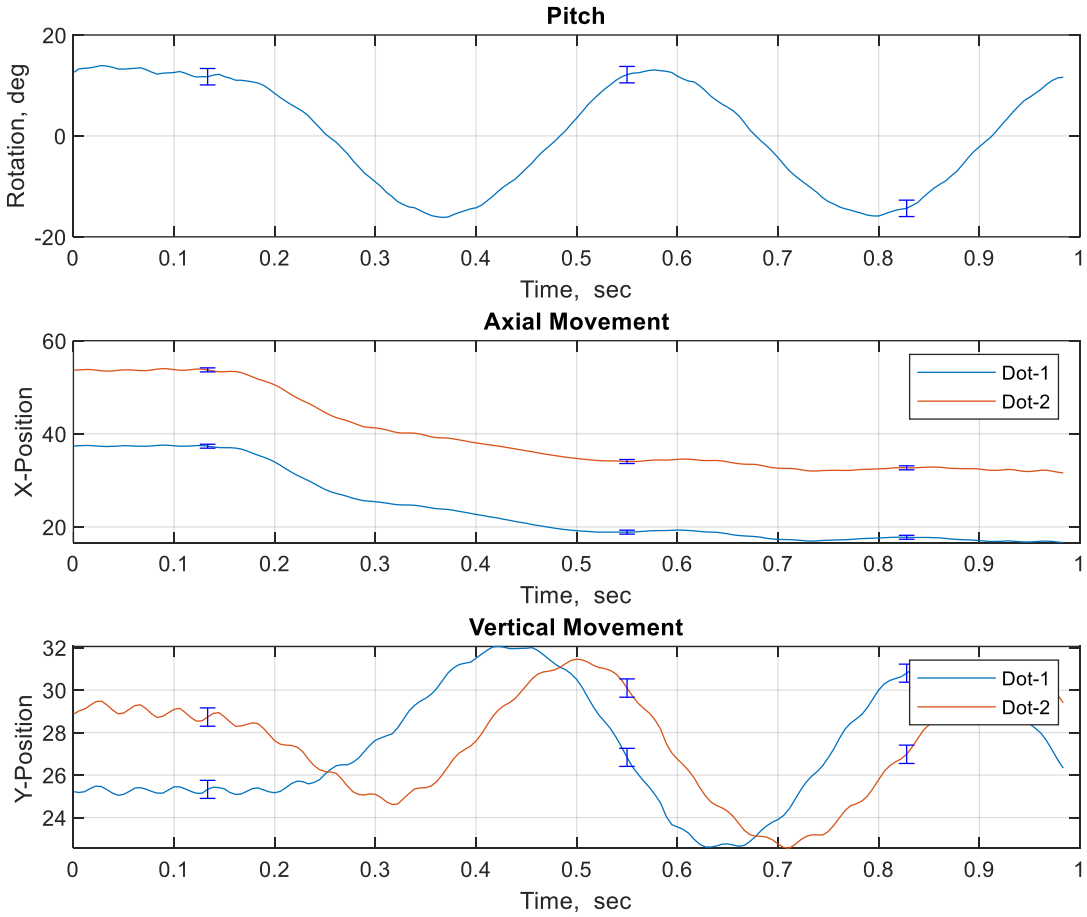

Figure 36: Pitch, axial movements and vertical movements vs. time for standard sting

The axial position is shown to have an initial large dip and then levels out, with the vertical position oscillating as expected. An in depth look at the data is shown below in Table 4.

Table 4: Axial and vertical movements from standard sting test

Axial Movement (Dot 1) (mm)	Vertical Movement (Dot 2) (mm)	Time (sec)
37.34	29.00	0.00
37.42	28.99	0.05
37.41	29.03	0.10
37.01	28.77	0.15
33.97	27.77	0.20
28.16	26.21	0.25
25.41	25.15	0.30
24.30	25.29	0.35
22.68	27.35	0.40
20.76	29.93	0.45
19.19	31.16	0.50
18.86	30.37	0.55
19.27	27.03	0.60
18.50	24.58	0.65
17.31	23.07	0.70
17.09	23.15	0.75
17.59	25.47	0.80
17.73	28.07	0.85
17.06	29.74	0.90
16.73	30.41	0.95
16.76	29.27	0.99

As shown in Table 4, the x-position dips down from 37.34 millimeters to 16.76 millimeters. This shows the largest axial movement to be 20.68 millimeters. The y-position starts at 29 millimeters, with the lowest y-position being 23.07 millimeters and the highest y-position being 31.16 millimeters, giving a total vertical movement of 8.09 millimeters.

Edge holder attachment

When testing, the sting with the edge holder sting attachment was deployed to push against the Stardust model and then retracted to pull away from the Stardust model to gather data. The 3D modeling configuration for the edge holder attachment is shown schematically below in Figure 37 due to insufficient lighting to clearly show the actual experimental setup.

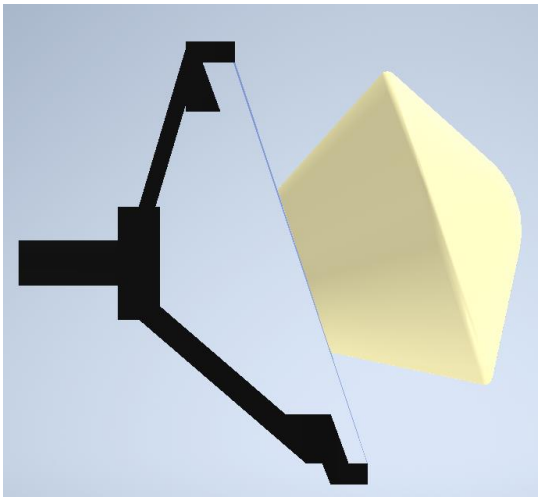

Figure 37: Edge holder holding Stardust capsule for free to oscillate testing.

Results and data reduction

For the edge holder attachment, the pneumatic retractor was deployed to push the edge holder attachment against the Stardust model to deflect it. The data gathered from the video of this run is shown below in Figure 38.

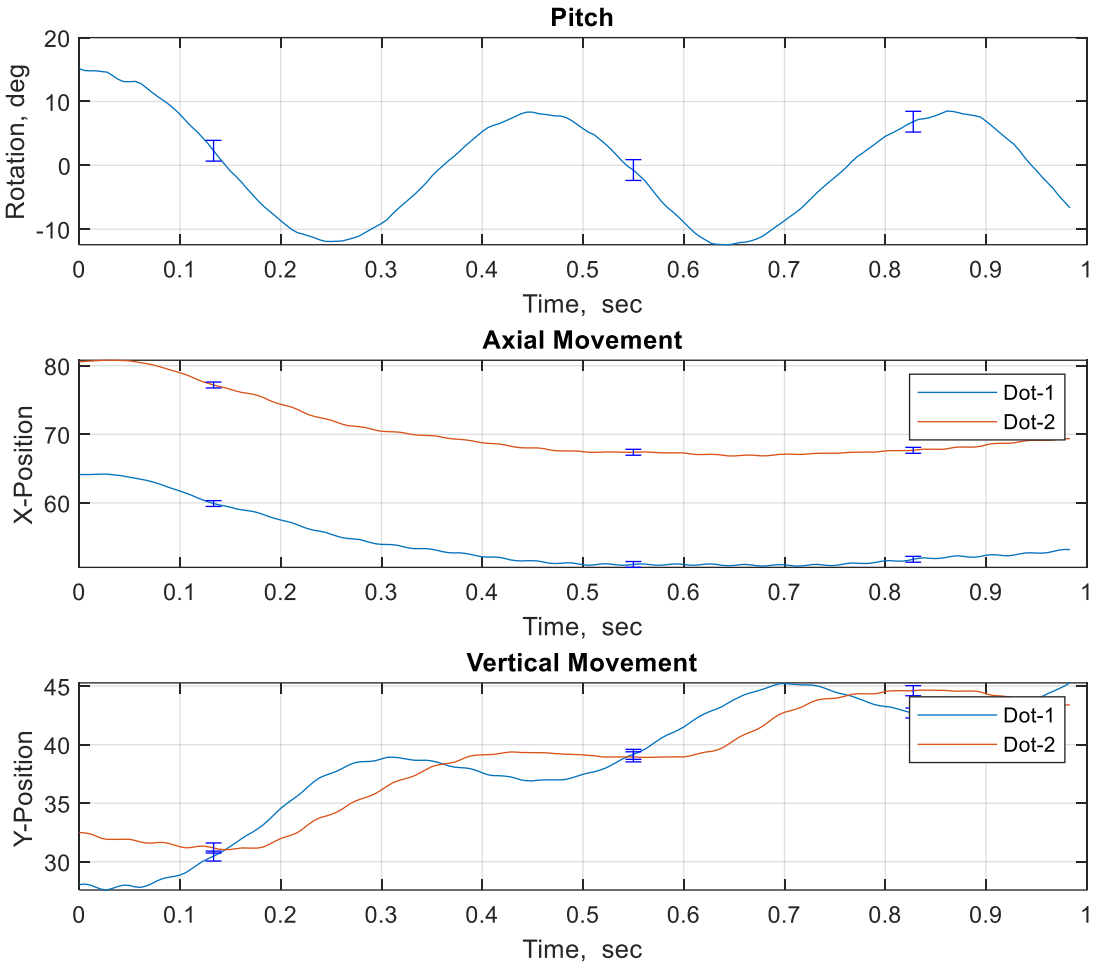

Figure 38: Pitch, axial movements and vertical movements vs. time for edge holder

A more in depth look at the data is shown below in Table 5.

Table 5: Axial and vertical movements from edge holder test

Axial Movement (Dot 1) (mm)	Vertical Movement (Dot 2) (mm)	Time (sec)
61.75	34.64	0.00
60.49	34.65	0.05
56.94	34.40	0.10
53.03	34.62	0.15
50.38	36.48	0.20
48.55	39.16	0.25
46.83	41.71	0.30

45.96	43.38	0.35
46.03	43.50	0.40
45.93	42.89	0.45
45.36	41.53	0.50
44.88	41.24	0.55
45.22	42.60	0.60
45.58	45.23	0.65
45.72	47.77	0.70
45.50	48.60	0.75
46.28	48.61	0.80
46.39	48.64	0.85
46.33	47.44	0.90
46.03	46.15	0.95
45.60	46.56	0.99

As shown in Table 5,the x-position dips down from 61.75 millimeters with the lowest x-position being 44.88 millimeters. This shows the largest axial movement to be 16.87 millimeters. The y-position starts at 34.64 millimeters, with the lowest y-position being 34.4 millimeters and the highest y-position being 48.64 millimeters, giving a total vertical movement of 14.24 millimeters.

2.3. Overall results of Stardust testing in MSBS and discussion

For comparison of the launching methods, the Mark 1 grabber trials were separated as “Mark 1 grabber before adjustment” for trial 1 and “Mark 1 grabber after adjustment” for trials 2 and 3. Trials 2 and 3 were then averaged together to find the average axial and vertical movements for the adjusted Mark 1 grabber as shown below in Table 6.

Table 6: Adjusted Mark 1 grabber trials.

Mark 1 grabber trial	Axial movement (mm)	Vertical movement (mm)
2	5.53	4.65
3	2.69	5.50
Average	4.11	5.075

After finding the average axial and vertical movements for the adjusted Mark 1 grabber, the axial and vertical movements for all launching methods could then be compared. Table 7 below shows the comparison of the Mark 1 grabber before adjustment, Mark 1 grabber after adjustment, standard sting, and edge holder.

Table 7: Comparison of launching methods.

Launching method	Axial movement (mm)	Vertical movement (mm)
Mark 1 grabber before adjustment	11.14	18.53
Mark 1 grabber after adjustment	4.11	5.075
Standard sting	20.68	8.09
Edge holder	16.87	14.24

As shown in Table 7, the axial movement from the adjusted Mark 1 grabber was 10 millimeters less than the standard sting and edge holder, in this case the adjusted Mark 1 grabber has a more desirable result. The vertical influence of the adjusted Mark 1 grabber is somewhat comparable to that of the standard sting, with the adjusted Mark 1 grabber having a vertical movement of 5.075 millimeters and the standard sting having a vertical movement of 8.09 millimeters. In this case, the Mark 1 grabber has a more desirable result. An additional comparison can be done on the frequency of oscillations for the different launching methods. The mapping of the oscillations was done in Simulink with the Sine Wave block. The values for amplitude, frequency, and phase were manually adjusted to represent the pitch oscillation data from the corresponding launcher. The setup for this block is shown in Appendix F. The data gathered from this comparison is shown below in Table 8.

Table 8: Frequency comparison between launchers

Launcher	Edge holder	Standard sting	Mark 1 grabber trial 1	Mark 1 grabber trial 2	Mark 1 grabber trial 3
Amplitude	-20	-20	-20	-20	-20

Frequency	2.492	2.1497	3.0653	2.0298	1.99
Phase	17.5	17.5	17.5	17.5	17.5

In this comparison, finding frequency was the goal, so amplitude and phase were set the same for all the launchers. Table 8 shows that the Mark 1 grabber trials 2 and 3 had a smaller frequency compared to the edge holder, standard sting, and the Mark 1 grabber trial 1. The launcher with the highest frequency of oscillations was the Mark 1 grabber trial 1. This was expected as the vertical movement for this launcher was significantly larger than the others. From this comparison, and the comparison of the vertical and axial movements, it can be concluded that the Mark 1 grabber from trials 2 and 3 affect the model's flight path less than the other launchers.

3. SUBSONIC AND SUPERSONIC MSBS LAUNCH SIMULATION

3.1. Simulation Overview

A simulation was created in Simulink to simulate the 3 degree-of-freedom launch process for a free to oscillate flight testing in the subsonic and supersonic MSBS testing environments. The purpose of this simulation was to explore a worst-case scenario where the model is released at a high aerodynamic load condition. This ensures that the launch mechanism gets clear physically and aerodynamically fast enough to not be hit by the model or corrupt the model's flow field. The Simulink codes for the various subsystems are shown in Appendix G. A top-level block diagram of the simulation process is shown below in Figure 39.

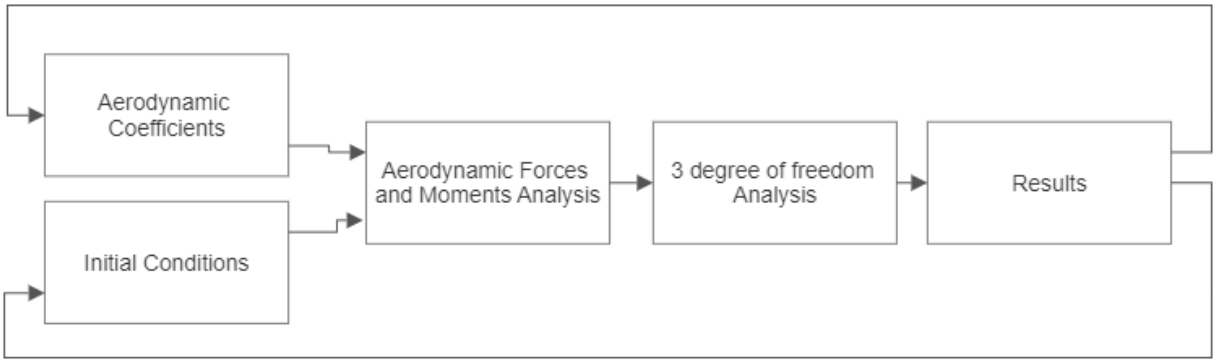

Figure 39: Top level block diagram of the simulation.

3.2. Simulation Setup

Aerodynamic blockset and its output

The aerodynamic forces and moments blockset computes the aerodynamic forces and moments acting on the test model based on the inputs of the aerodynamic coefficients, dynamic pressure, center of pressure, and center of gravity. The outputs of this blockset are forces and moments on the testing body.

Aerodynamic coefficients

The aerodynamic coefficients needed for the simulation are the axial force coefficient, normal force coefficient, rolling moment coefficient, pitching moment coefficient. Since this simulation is for 3 degrees of freedom and hence will only generate axial and vertical movement with the pitching angles, the side force, rolling moment, and yawing moment coefficients can all be set to zero.

Subsonic aerodynamic coefficients

The axial force, normal force, and pitching moment coefficients for the Stardust model, were found based on previous testing by Mitcheltree et al [20]. The initial axial force coefficient was found to be 0.8875, used as a negative since the x-axis is oriented into wind, and the slope of the coefficient measurements was given as 0.001 deg^{-1} as shown in Figure 40.

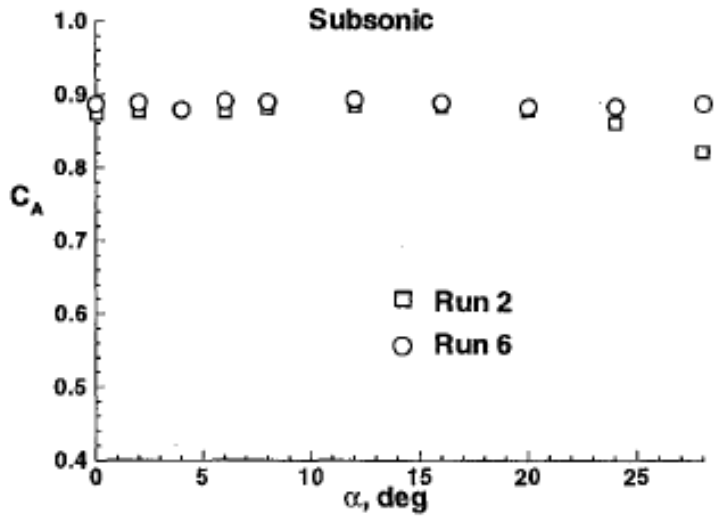

Figure 40: Subsonic axial force coefficient measurements from Mitcheltree et al.[20]

The slope of the coefficient measurements is given as 0.0031 deg^{-1} as shown in Figure 41.

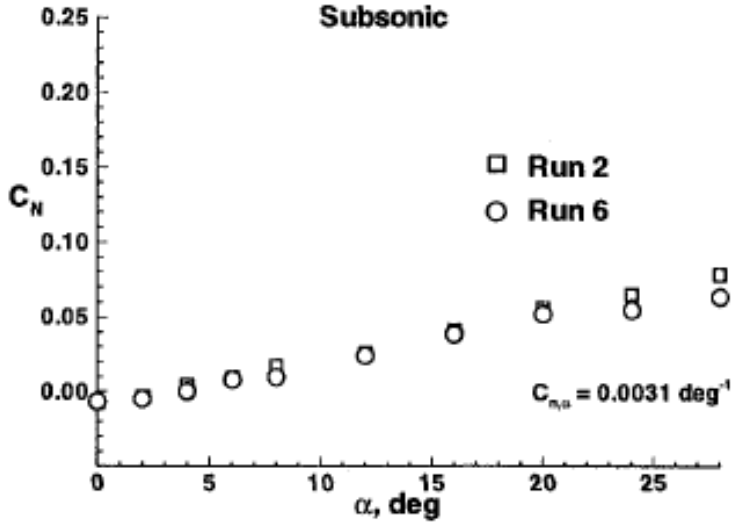

Figure 41: Subsonic normal force coefficient measurements from Mitcheltree et al.[20]

The slope of the coefficient measurements is given as -0.00276 deg^{-1} as shown in Figure 42.

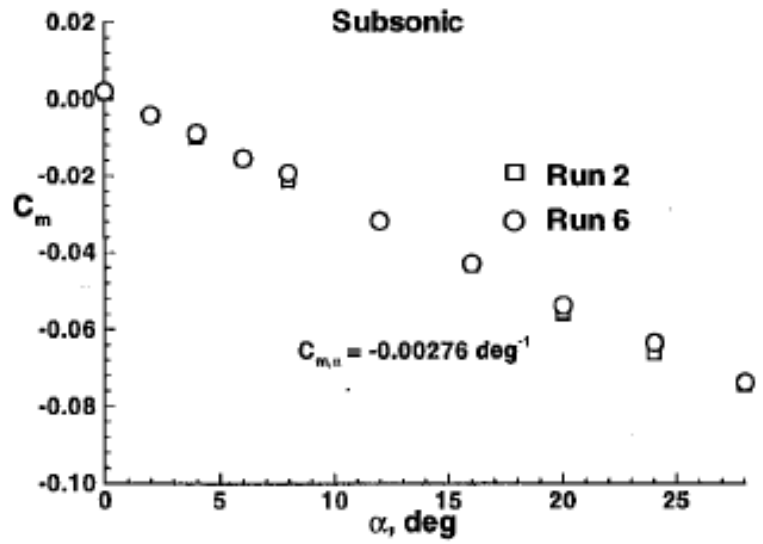

Figure 42: Subsonic Pitching Moment Coefficient measurements from Mitcheltree et al.[20]

For the pitching moment, additional coefficients need to be included. The pitch damping coefficient, C_{mq} is included when calculating and modeling flight of blunt bodies. For dynamic

stability testing, C_{mq} and $C_{m\dot{\alpha}}$ are typically combined into a pitch damping sum. For the purposes of this simulation, C_{mq} and $C_{m\dot{\alpha}}$ were both calculated separately and then later combined. Equations (6) – (8) show the equations for calculating the aerodynamic coefficients needed for this simulation.

$$C_{Aa} * \alpha + C_{A0} = C_A \quad (6)$$

$$C_{Na} * \alpha + C_{N0} = C_N \quad (7)$$

$$\left(C_{m\dot{\alpha}} * \dot{\alpha}\right) + \left(C_{ma} * \alpha\right) + \left(C_{mq} * q\right) + C_{m0} = C_m \quad (8)$$

For the axial and normal coefficient, C_A and C_N respectfully, the equations for iterative values were straightforward. For pitching moment coefficient, C_m, the pitching moment slope had to be multiplied by the value for pitch, in this case alpha, and summed with product of the slope for C_{mq} and the resulting pitch rate of the model, to produce the instantaneous value for the pitching moment coefficient. As this portion of the equations has a mixture of nondimensionalized variables and dimensioned variables, care must be taken to nondimensionalize the needed values before calculations. The pitch rate was nondimensionalized using Equation (9) below.

$$\hat{q} = \left(\frac{q+\dot{\alpha}}{2}\right)\left(\frac{D}{2V_\infty}\right) \quad (9)$$

and then the slope for C_{mq} was calculated by extrapolating data from Figure 43 [5].

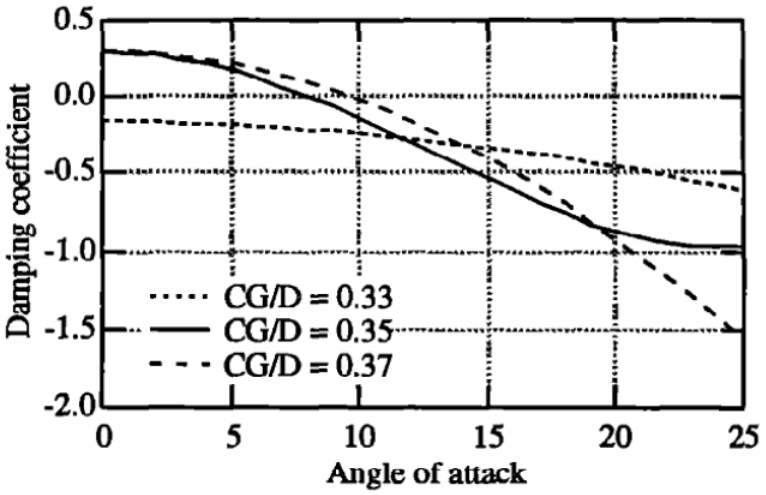

Figure 43: C_{mq} values as functions of location of CG.

The model geometry that was used for this research had a CG location of 0.35 of the diameter that was measured heatshield to the backshell. Data points were curve fitted and the resulting trendline equation, shown below in Equation 10, was imported into the simulation to calculate C_{mq} based on the input of angle of attack.

$$C_{mq_\alpha} = 0.0002\alpha^3 - 0.009\alpha^2 + 0.0244\alpha + 0.2937 \quad (10)$$

The subsystem for this step is also shown in Appendix G. The initial coefficient values for the simulation are shown below in Table 9.

Table 9: Initial coefficient values for subsonic MSBS simulation.

Axial force coefficient (C_A)		Normal force coefficient (C_N)		Pitching moment coefficient (C_m)	
Slope	Initial value	Slope	Initial value	Slope	Initial value
0.001 deg^{-1}	0.8875	0.0031 deg^{-1}	0	-0.00276 deg^{-1}	0

Supersonic aerodynamic coefficients

The aerodynamic coefficients for supersonic testing were also found from Mitcheltree et al. [20] The slopes of the coefficients were assumed to be the same as the subsonic coefficients. Figure 44, Figure 45, and Figure 46 show the values for the coefficients at Mach 2.5.

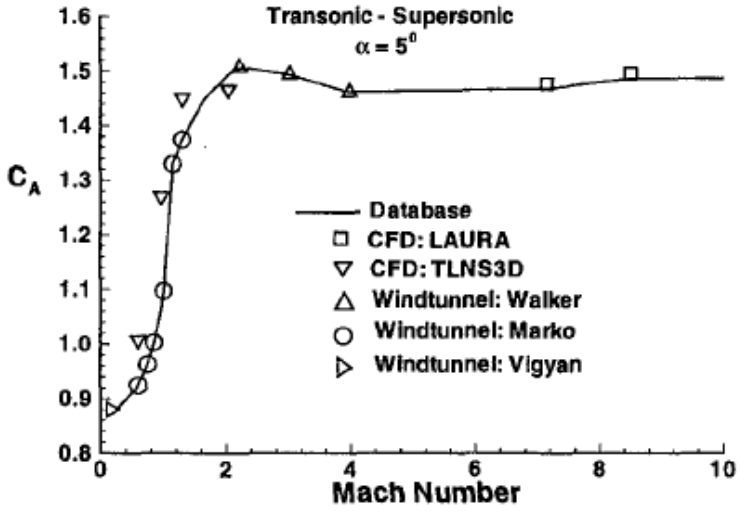

Figure 44: Supersonic axial force coefficient measurements from Mitcheltree et al.[20]

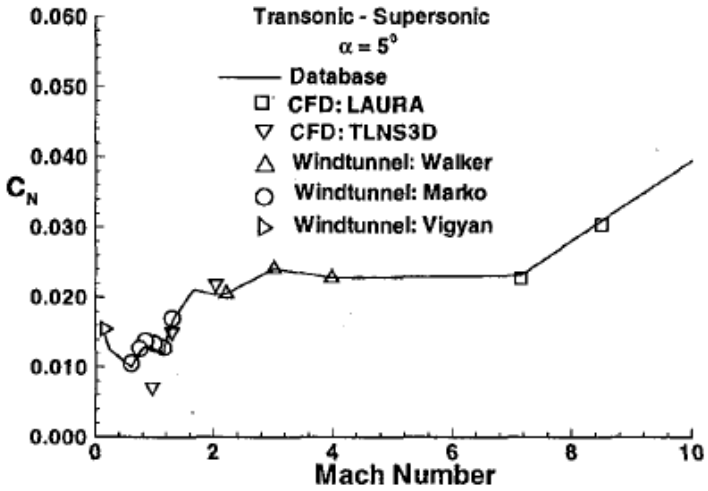

Figure 45: Supersonic normal force coefficient measurements from Mitcheltree et al.[20]

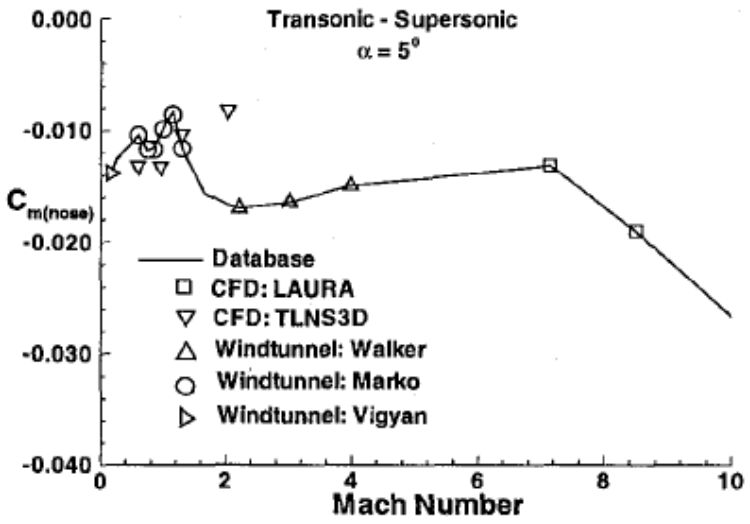

Figure 46: Supersonic pitching moment coefficient measurements from Mitcheltree et al.[20]

C_{mq} was calculated the same way as the subsonic simulation due to relative agreement between damping in the subsonic regime and in the supersonic regime. The initial coefficient values for the simulation are shown below in Table 10.

Table 10: Initial coefficient values for supersonic MSBS simulation.

Axial force coefficient (C_A)		Normal force coefficient (C_N)		Pitching moment coefficient (C_m)	
Slope	Initial value	Slope	Initial value	Slope	Initial value
0.001 deg^{-1}	-1.5	0.0031 deg^{-1}	0	-0.00276 deg^{-1}	0

Subsonic initial conditions

For the purposes of simulating the Stardust model, the CG and CP of this model was 0.35 of the diameter and 0.26 of the diameter, respectively from the heatshield. The starting velocity was chosen to be 25 m/s. The density of the air is 1.225 kg/m3. The density and velocity values were input into the Simulink code to calculate the correct dynamic pressure for the wind tunnel. The model parameters for the testing body were based on the 1.75-inch (44.45 mm) Stardust model. In the simulation, the reference span, length and area were the model diameter, model depth, and frontal area, respectively. The sample time for the simulation was set to 1 second to coincide with the release time of the grabber. The starting values for the subsonic simulation are shown in Table 11 below.

Table 11: Starting values for subsonic simulation.

CG (x,y,z) (m)	CP (x,y,z) (m)	Velocity (m/s)	Density (kg/m^3)	Reference span (m)	Reference length (m)	Reference area (m^2)
0.0155575, 0, 0	0.011557, 0, 0	25	1.225	0.04445	0.028956	$1.55*10^{-3}$

Supersonic initial conditions

For the supersonic simulation, many of the initial conditions remained the same. The starting dynamic pressure for supersonic speeds was chosen to be 13 kPa. The starting velocity was calculated from Mach and dynamic pressure, in the supersonic case Mach 2.5 was chosen for comparison to expected supersonic MSBS speeds. This gave a starting velocity of 577.8 m/s. This value was derived from a sub atmospheric upstream stagnation pressure and ambient stagnation temperature, based on the capabilities of the NASA Glenn supersonic wind tunnel. The sample time for the simulation was set to 1 second to coincide with the release time of the grabber. The starting values for the supersonic simulation are shown in Table 12 below.

Table 12: Starting values for supersonic simulation.

CG (x,y,z) (m)	CP (x,y,z) (m)	Velocity (m/s)	Reference span (m)	Reference length (m)	Reference area (m^2)	Dynamic pressure (kPa)
0.0155575, 0,0	0.011557, 0,0	577.8	0.04445	0.028956	$1.55*10^{-3}$	13

Three degrees of freedom and body axes blockset and outputs.

The 3 degree of freedom blockset integrates the three-degrees-of-freedom equations of motion using the input of F_x, F_z, and M_y. The outputs of this blockset are the pitch attitude, pitch angular rate, pitch angular acceleration, location of body, velocity and acceleration of the body in x and z.

Output of simulations

The results that are exported from the simulation are the body attitude, body velocity, accelerations of the body in the x and y axis, the horizontal displacement of the model, the vertical displacement of the model, dynamic pressure, and Mach number in wind axes.

3.3. Results for Subsonic Simulation

Body attitude

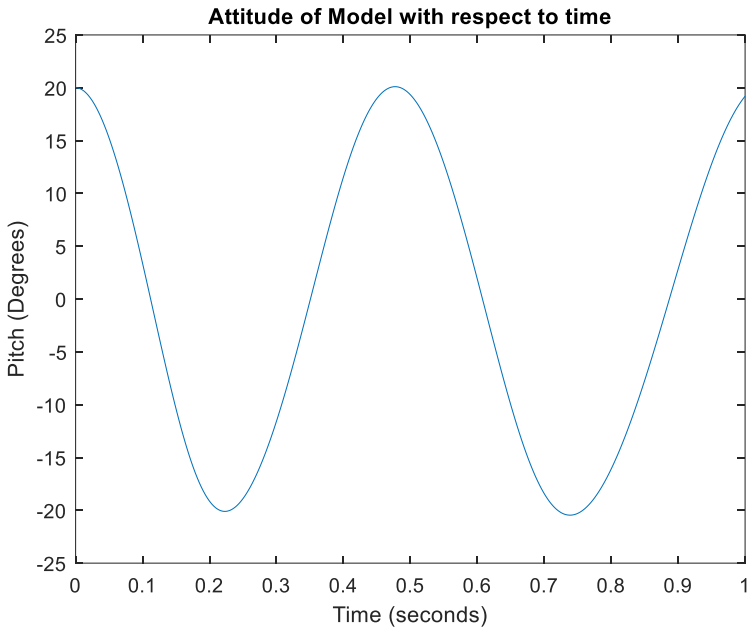

Figure 47: Body attitude for subsonic MSBS.

Body velocity

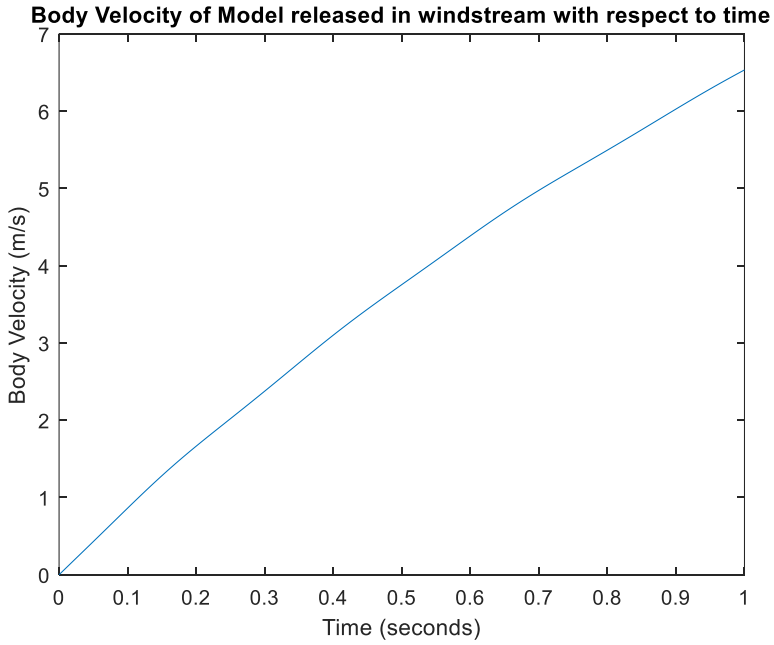

Figure 48: Body velocity for subsonic MSBS.

Body accelerations

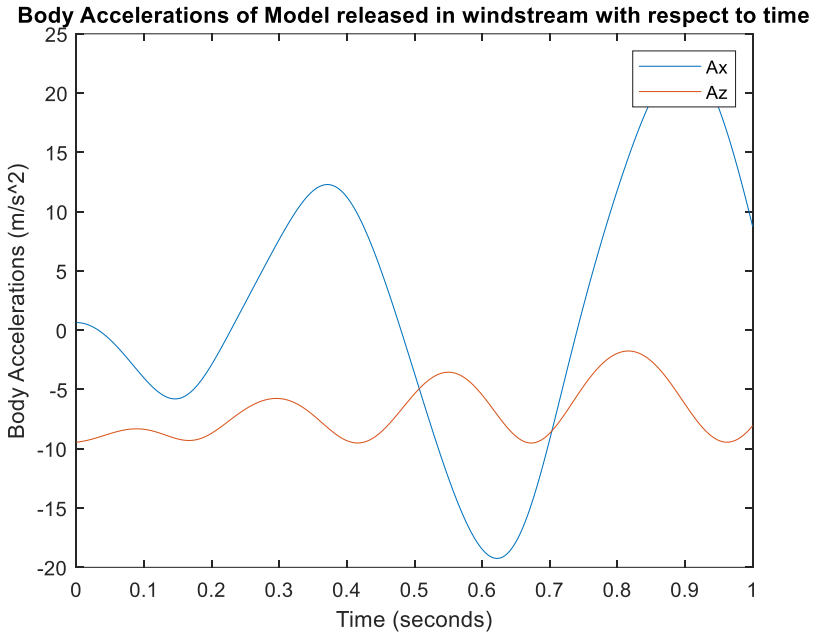

Figure 49: Body accelerations for subsonic MSBS.

Displacement

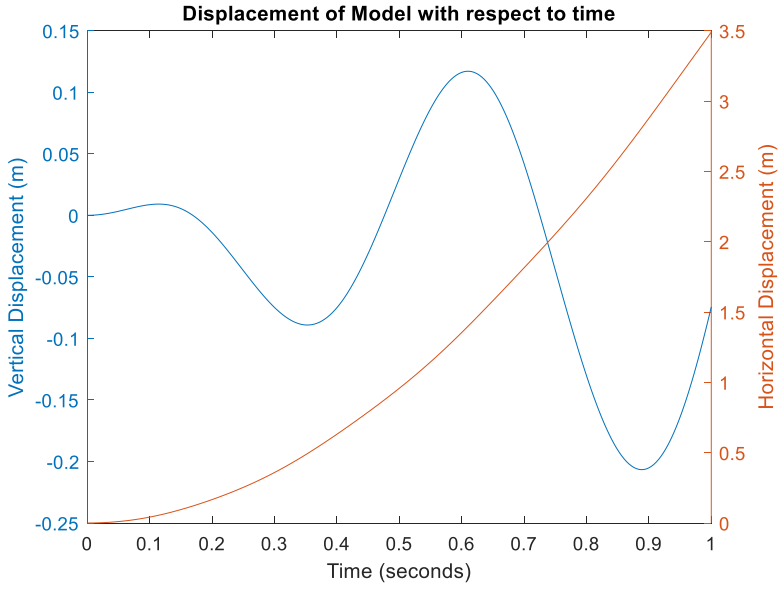

Figure 50: Displacement of model for subsonic MSBS.

Model dynamic pressure

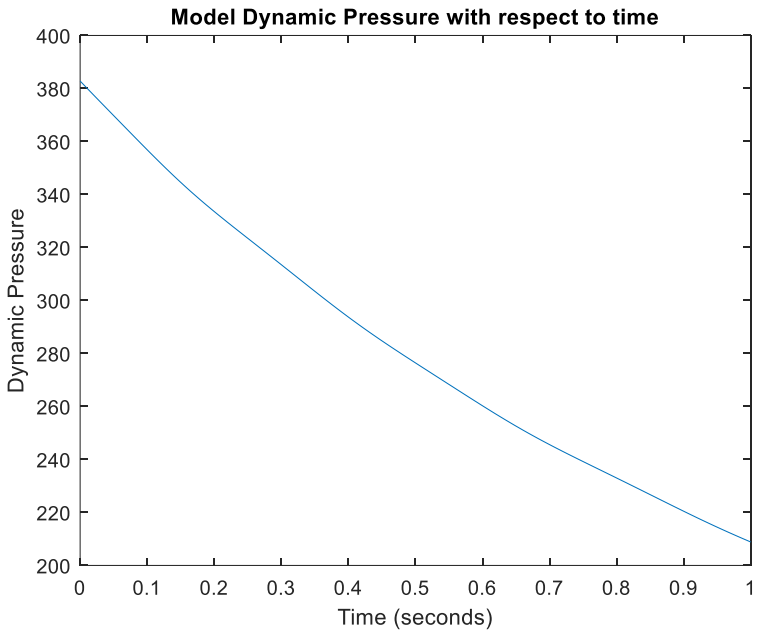

Figure 51: Model Dynamic pressure for subsonic MSBS.

Model Mach number

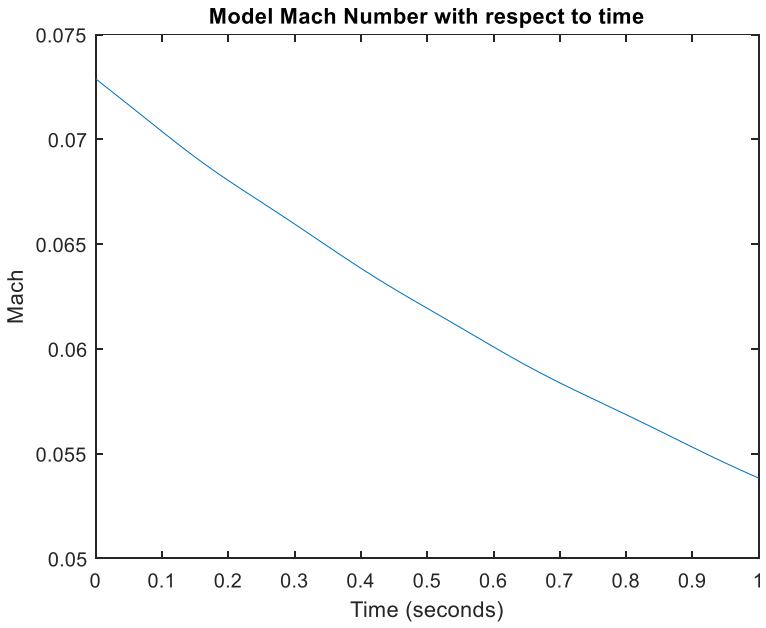

Figure 52: Model Mach number for subsonic MSBS.

3.4. Subsonic simulation discussion

This simulation exhibits a case in which the model is released into the windstream without suspension at subsonic conditions. The results of the subsonic simulation show the model having a gradual increase in velocity, which is as expected. The horizontal displacement behaves much the same with a slow start and then gradual rise. To compare these results to the Mark 1 grabber, the data of the retraction was plotted against the model's ideal path to show whether the model would hit the grabber upon release and loss of magnetic suspension as seen below in Figure 53.

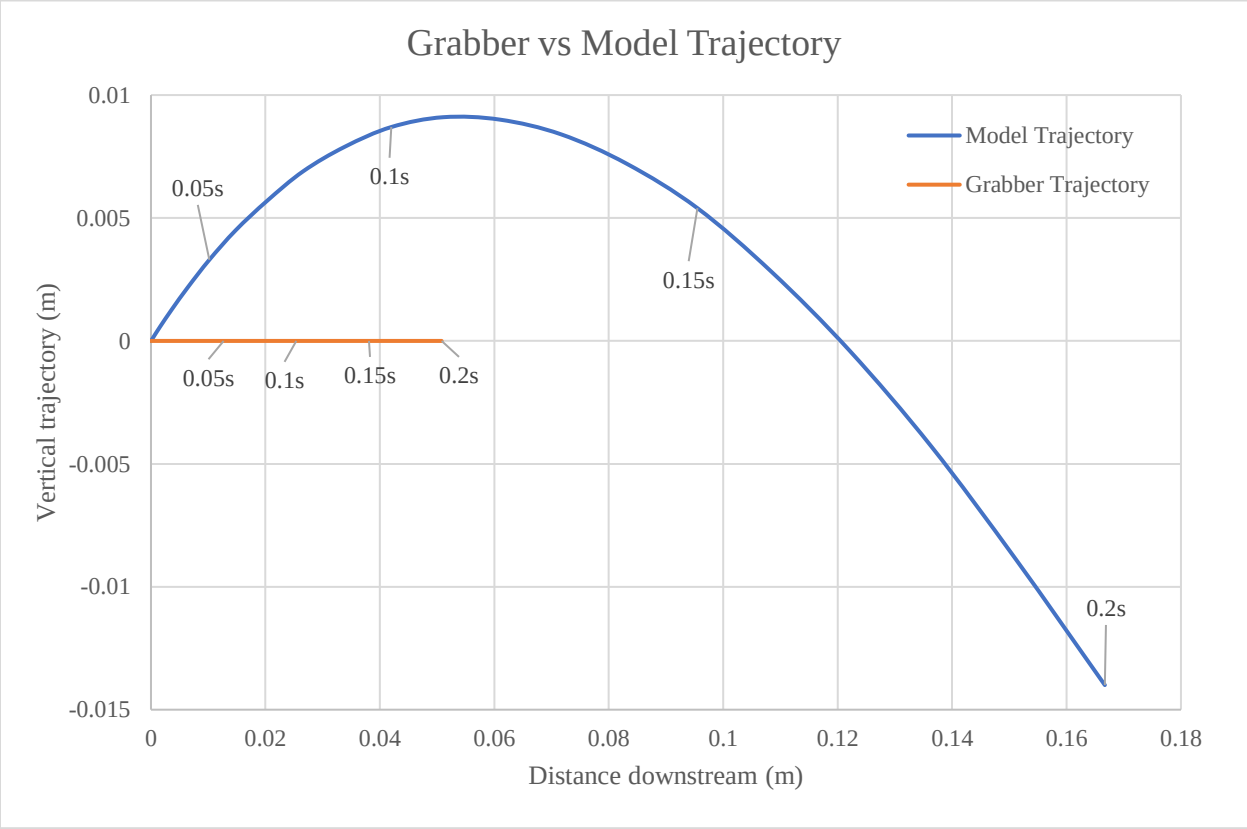

Figure 53: Model movement unsuspended vs. Grabber retraction.

Actual launch sequences feature the MSBS catching the model before it be fly downstream, in these cases the grabber must retract in a window of 0.1 seconds, as found from the experimentation previously discussed, to not interfere with the oscillation of the model.

3.5. Results for unsuspended supersonic simulation

Unsuspended supersonic case: body attitude.

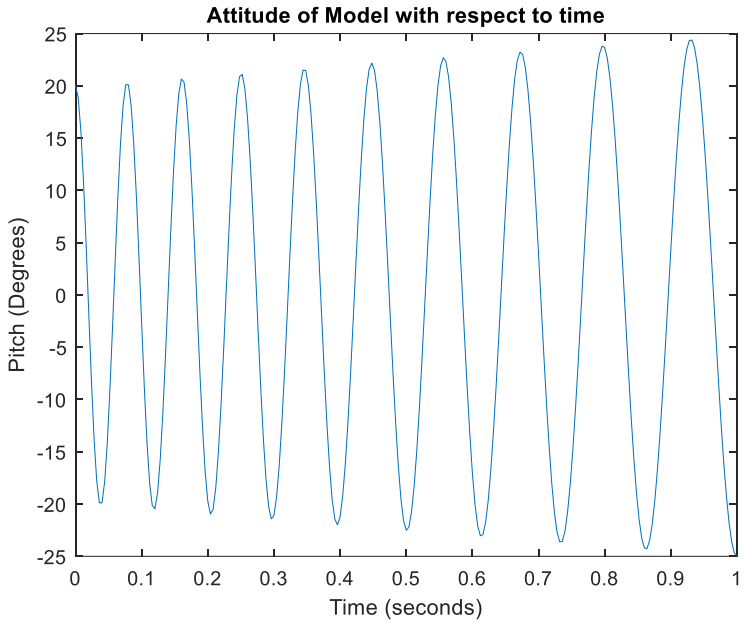

Figure 54: Body attitude for unsuspended supersonic MSBS.

Unsuspended supersonic case: body velocity.

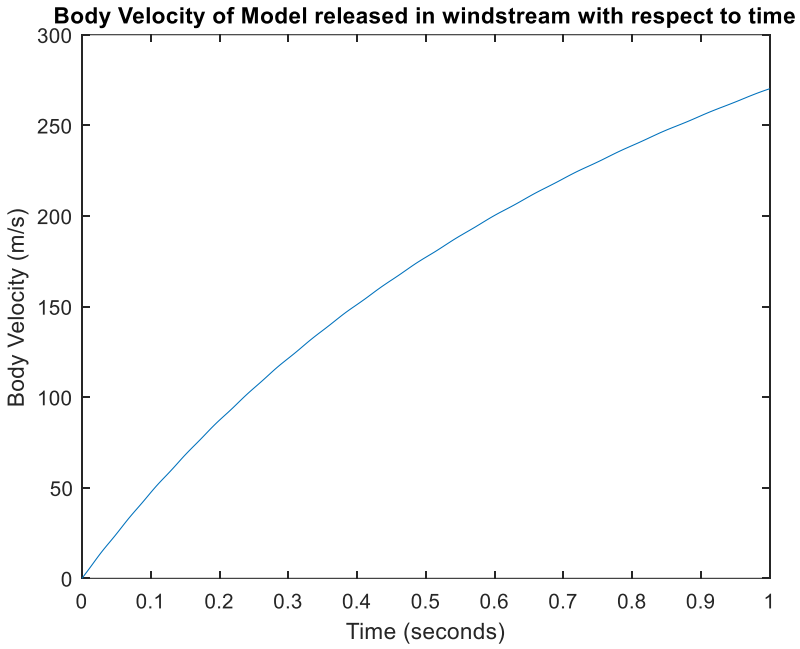

Figure 55: Body velocity for unsuspended supersonic MSBS.

Unsuspended supersonic case: body accelerations.

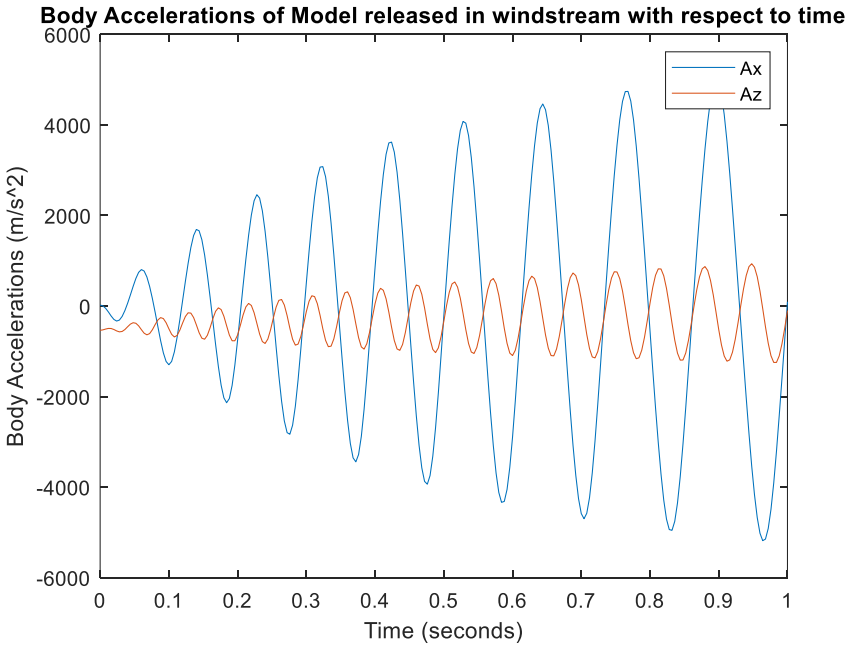

Figure 56: Body accelerations for unsuspended supersonic MSBS.

Unsuspended supersonic case: displacement.

Figure 57: Displacement of model for unsuspended supersonic MSBS.

Unsuspended supersonic case: model dynamic pressure.

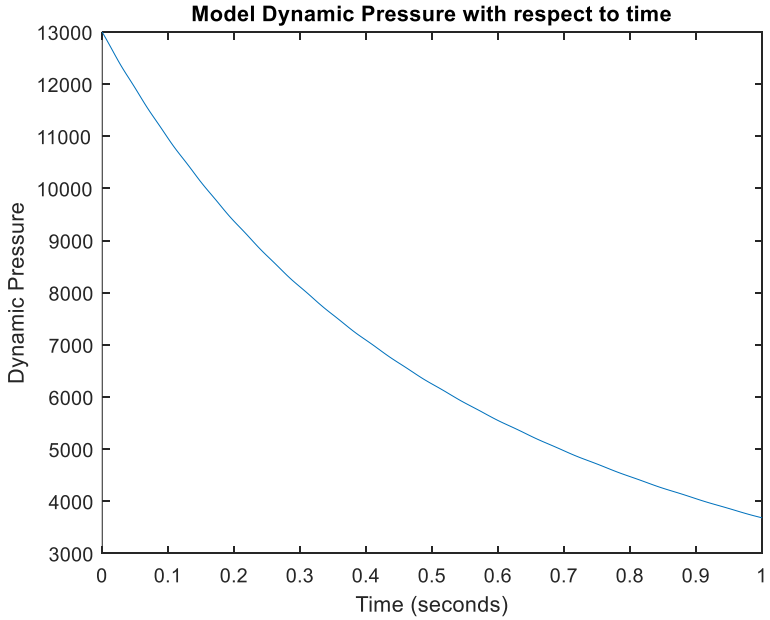

Figure 58: Model dynamic pressure for unsuspended supersonic MSBS.

Unsuspended supersonic case: model Mach number.

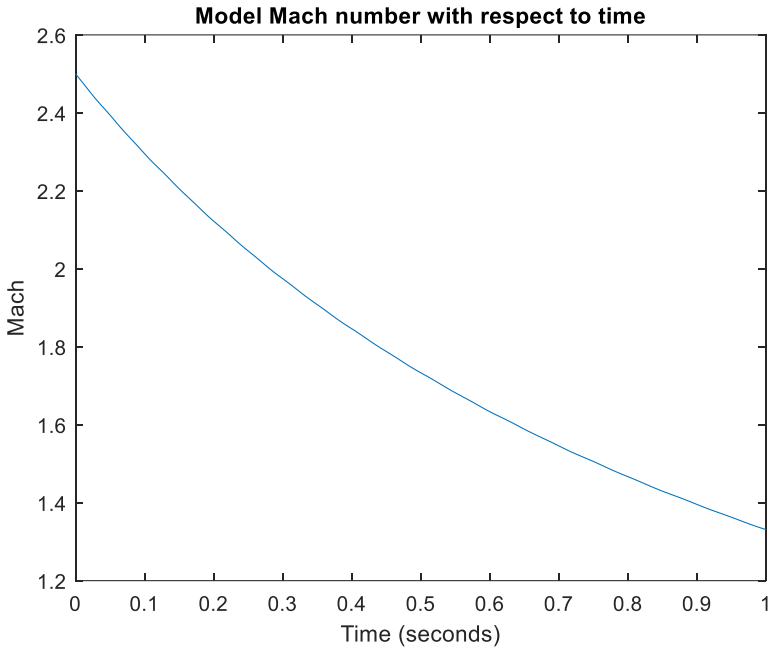

Figure 59: Model Mach number for unsuspended supersonic MSBS.

3.6. Unsuspended supersonic simulation discussion

This simulation exhibits a case in which the model is released unsuspended into the windstream at supersonic conditions. In these cases, the behavior of the model is similar to the subsonic simulation, with the differences being the magnitude of the results. For example, in the subsonic simulation, an unsuspended model will travel 3.5 meters in 1 second, whereas in the supersonic simulation, the model will travel 160 meters in 1 second. For this case, there is not grabber data available at supersonic speeds, so it can be assumed that the retraction of a grabber for a supersonic setting would need to be sped up to match the magnitude of the supersonic speeds. Due to the speed of the model moving downstream, a grabber retracting out of the way would be unrealistic. Due to this, simulation cases were conducted to simulate a model released with ±10% drag preload. The ±10% drag preload references the input of the MSBS to stabilize the model along the system centroid. In a real test, the MSBS should engage to compensate for

the model movement, but as this has not been tested in supersonic conditions. The results for the velocities and displacement of the model for the ±10% drag preload cases are shown below in Figure 60 through Figure 63.

-10 preload case: body velocity

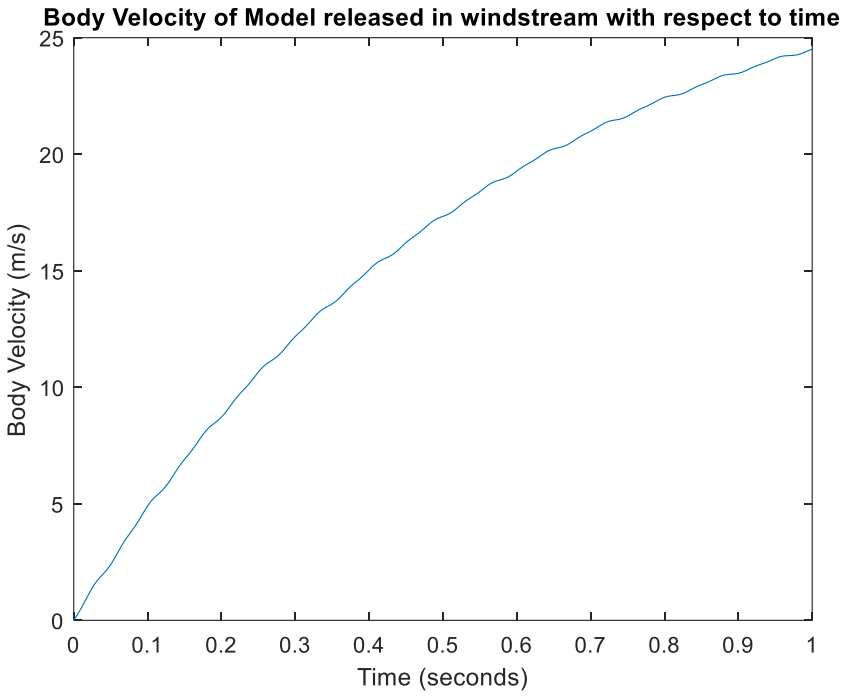

Figure 60: Velocity of model for -10% preload case

-10 preload case: displacement

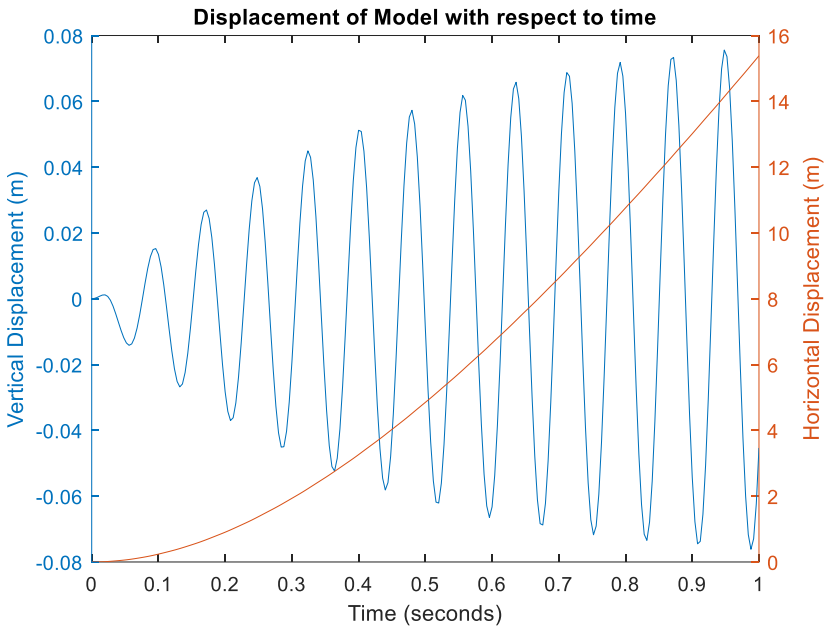

Figure 61: Displacement of model for -10% preload case

+10 preload case: body velocity

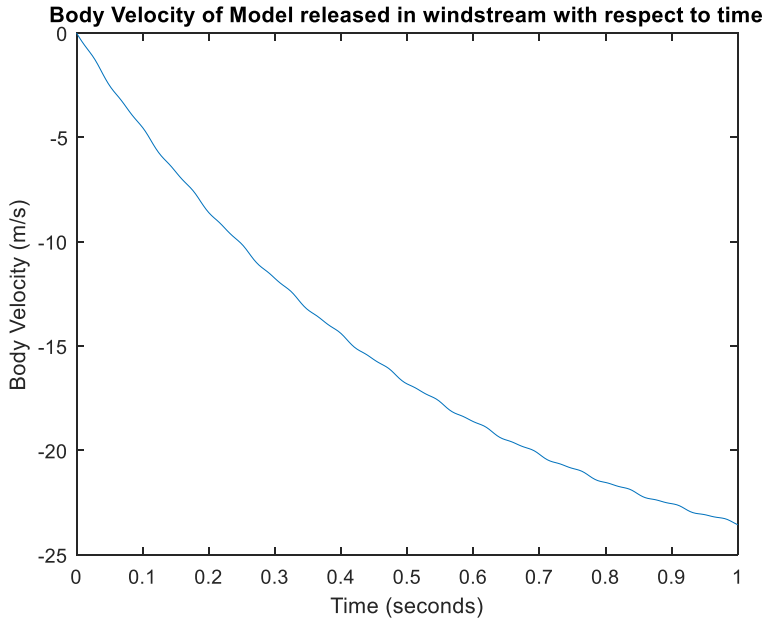

Figure 62: Velocity of model for +10 preload case

+10 preload case: displacement

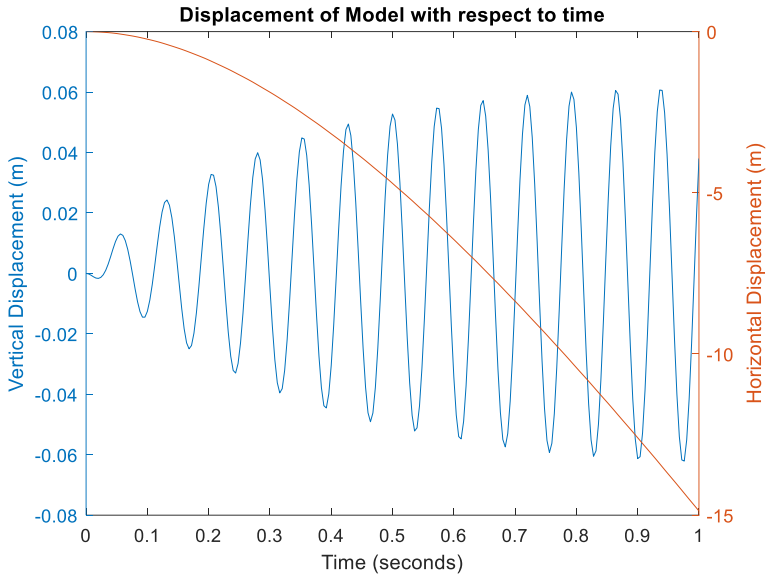

Figure 63: Displacement of model for +10 preload case

As shown in the graphs above, for the -10% and +10% preloads, the model velocities are much lower than the unsuspended case since this assumes the MSBS is counteracting the axial force on the model. As shown in Figure 64, the behavior of the -10% preload case still flies downstream but at a slower rate than the unsuspended case, while the +10% preload case flies upstream.

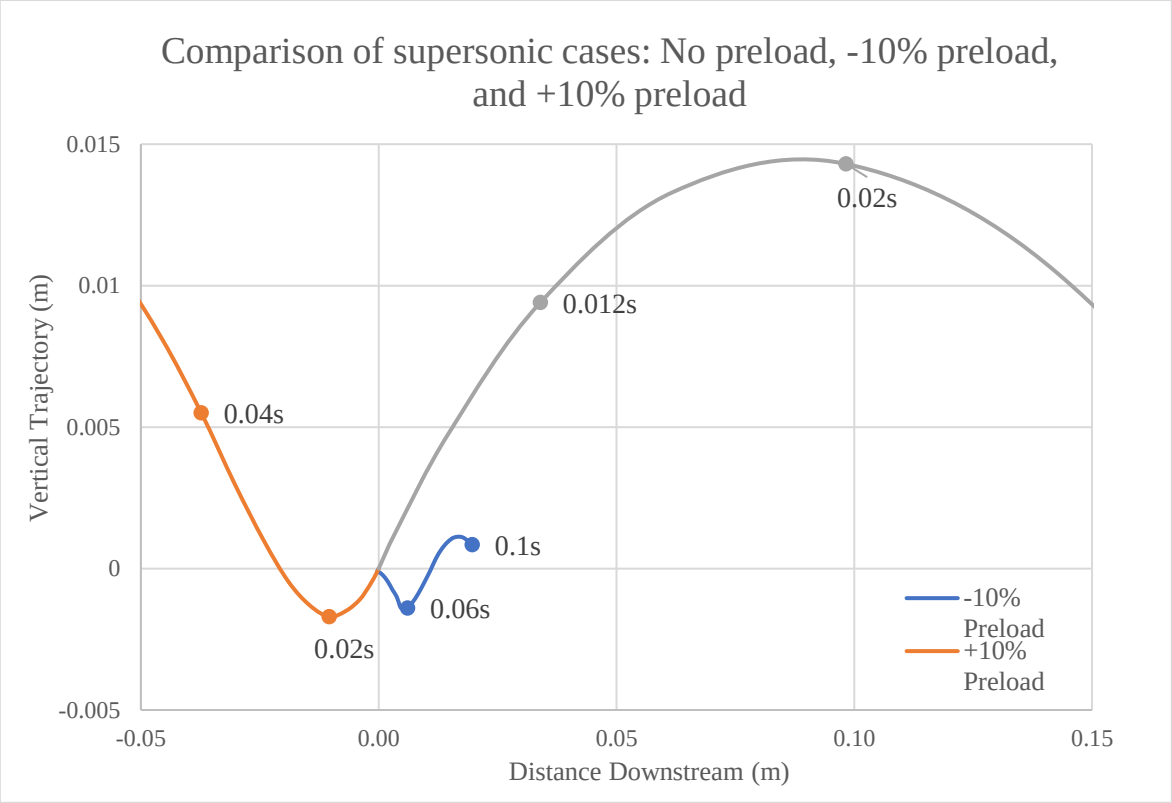

Figure 64: Comparison of supersonic cases.

In actual tests the MSBS would modulate the speed of the model, instead of having one constant counteracting force. Overall, this gives an insight into the magnitude of displacements and velocities that will be observed in future supersonic testing. The rest of the results for these cases are in Appendix G.

4. SUPERSONIC DESIGN FOR FUTURE WORK

4.1. Mark 2 grabber

The Mark 2 grabber was designed to hold the magnetically suspended model at a predetermined angle, in this case 20 degrees, in a high dynamic pressure flow with a very rapid release. The concept relies more on direct mechanical action rather than sequenced solenoid actuation used in the Mark 1 grabber. The Mark 2 grabber employs a one-motion retraction that works by the pneumatic retractor, similar to the retractor used in subsonic testing, pulling an internal rod to open the grippers that then hits a stop and pulls the whole assembly backwards. Another consideration for the design of the Mark 2 grabber is the rigidity required to withstand the initial conditions of the tunnel start in the 225 cm^2 supersonic tunnel and successfully hold the tested model until release. A visual representation of this concept is shown below in Figure 65.

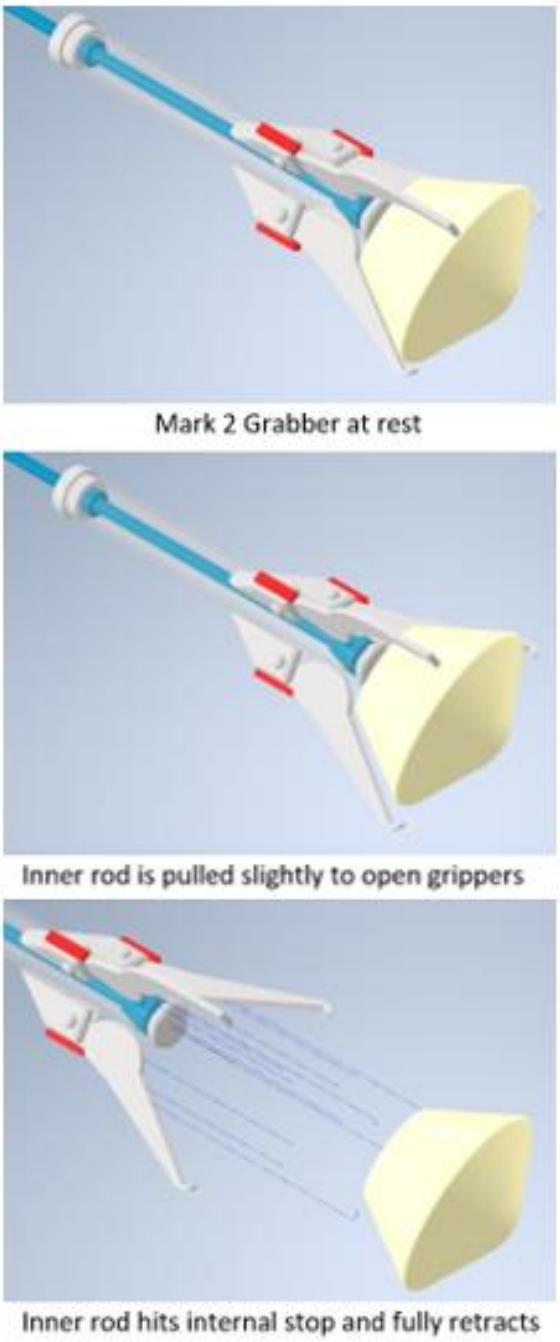

Figure 65: Representation of one-motion retraction.

This mechanism for retraction is desirable for supersonic testing due to the reduced frontal area, increased strength and potentially faster actuation. The proposed supersonic setting is the NASA Glenn Supersonic Wind Tunnel (SWT). This wind tunnel has a 225 cm^2 cross

sectional area for the test section. Using MSBS for this tunnel would allow for upper supersonic speeds to be tested without the need for more expensive tests such as a ballistic range test [21]. Since the Mark 2 grabber was designed with this tunnel in mind, it is streamlined to minimize blockage, whereas the Mark 1 grabber was limited in sizing changes due to the need for a powerful enough solenoid to actuate the grippers. The Mark 2 grabber assembly has an overall length of nine inches and is composed of six main parts: outer rod, inner rod, connector rod, aero fairing cap, stop cap, and grippers. A schematic of the Mark 2 grabber is shown below in Figure 66.

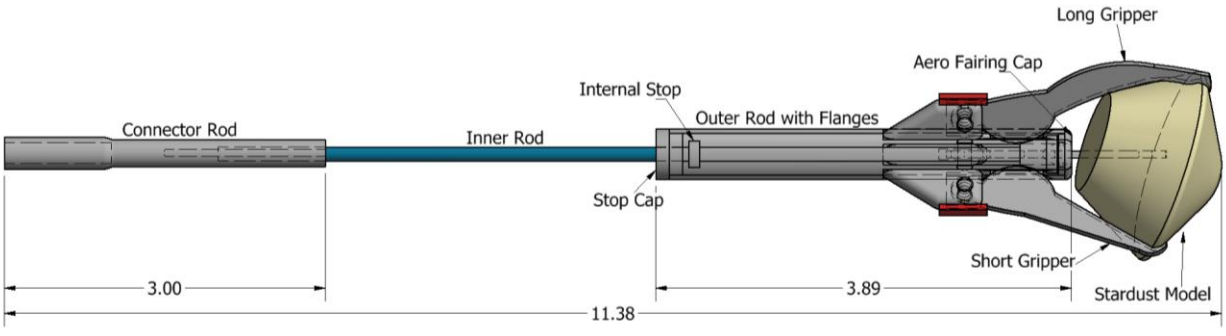

Figure 66: Schematic of Mark 2 grabber

Outer rod

The outer rod was designed with a length of 3.7 inches, 0.5-inch diameter, and 3 side flanges that the grippers mount to. The outer rod has cutouts next to the flanges to allow the grippers to be pulled inside. The end of the rod has space for the inner rod, with the aero faring cap and stopping cap fitting on the ends. The outer rod was fabricated from 3D printed nylon for ease of prototyping and durability of material. The outer rod is shown below in Figure 67.

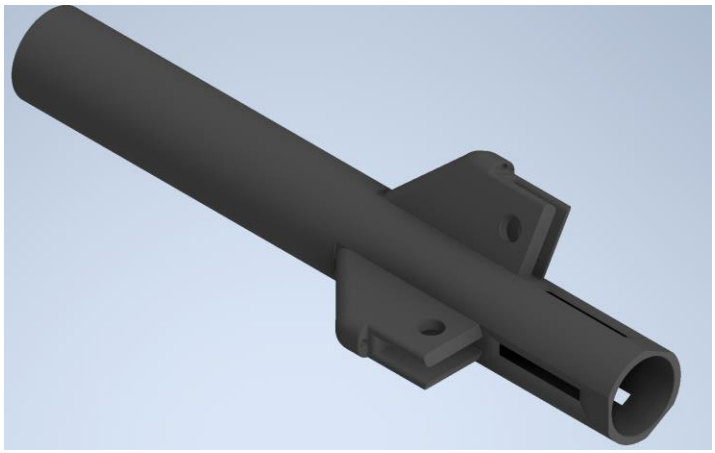

Figure 67: Mark 2 outer rod with flanges.

Inner rod

The inner rod was designed to fit inside the outer rod with a conical feature that acts as a cam that pushes the grippers apart when the inner rod is retracted. The composition of the inner rod is a 1/16-inch carbon fiber rod with 3D printed wedge and ring that were epoxied to the rod. The total length of the carbon fiber rod is dependent on the overall length required for the tunnel; in this case the inner rod was made to be 6.5 inches. While the length of the carbon fiber can vary, the distance between the wedge and internal ring must stay at 3 inches for the mechanism to function. The carbon fiber was used for the rod as it is lightweight and sturdy while nylon was used for the 3D printed features for ease of machinability. The ring in the middle acts as a stop and has a longer piece that fastens into the connector rod. The inner rod is shown below in Figure 68.

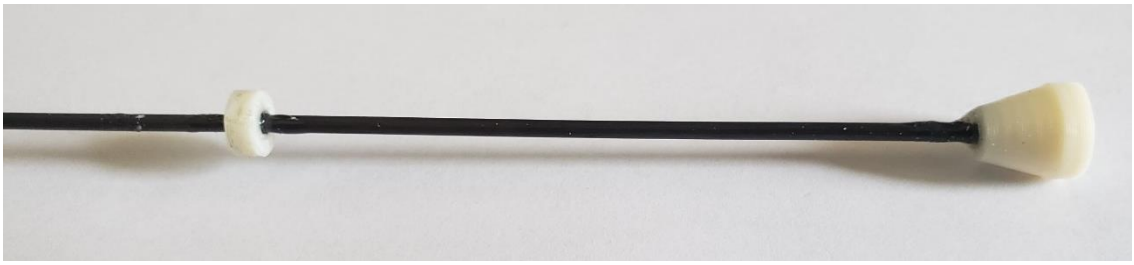

Figure 68: Mark 2 inner rod with 3D printed parts attached with epoxy.

Connector rod

The connector rod is a fastener that connects the inner rod to the pneumatic retractor. The connector rod is 3.7-inches in length and features a long hollow section that the inner rod friction fits into, and one threaded section for the pneumatic retractor to screw into. The connector rod was also 3D printed from nylon. The connector rod is shown below in Figure 69.

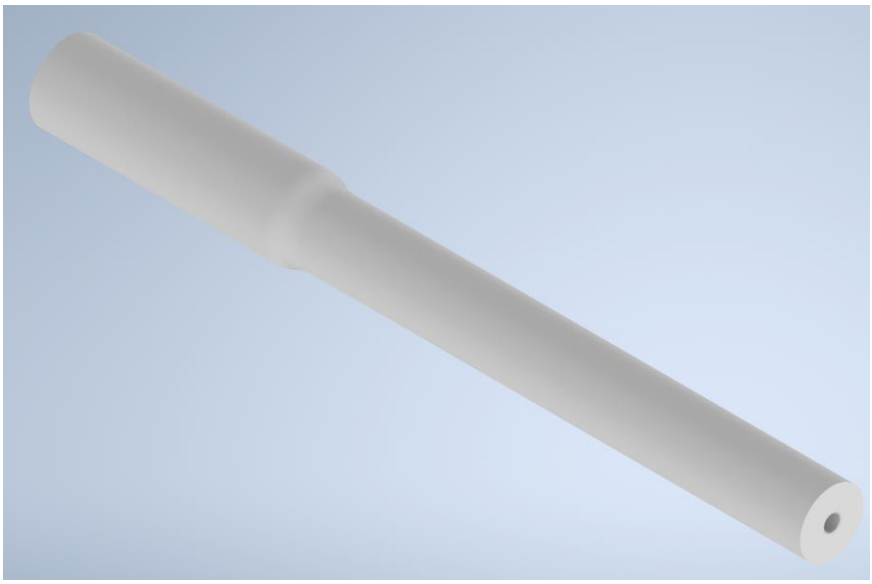

Figure 69: Mark 2 connector rod from inner rod to retractor.

Aero fairing cap

The aero fairing cap is incorporated on the upstream section of the outer rod. This piece acts as aero fairing to shed flow along the sides of the grabber to reduce blockage. It has a nominal diameter of 0.472 inches and features fillets that will assist in better aerodynamics. The aero faring cap was created from 3D printed ABS plastic. The aero fairing cap is shown below in Figure 70.

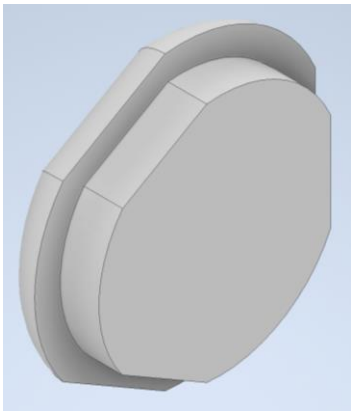

Figure 70: Mark 2 aero fairing cap.

Stop cap

The stop cap is attached to the downstream section of the outer rod and acts as a stop for the ring on the inner rod. When retracted the inner rod is pulled until the ring hits the stop cap, and then the entire assembly of the grabber is pulled backwards. It has an outer diameter of 0.472 inches, with the clearance hole diameter of 0.125 inches for the inner rod to slide through. The stop cap was 3D printed from ABS plastic. The stop cap is shown below in Figure 71.

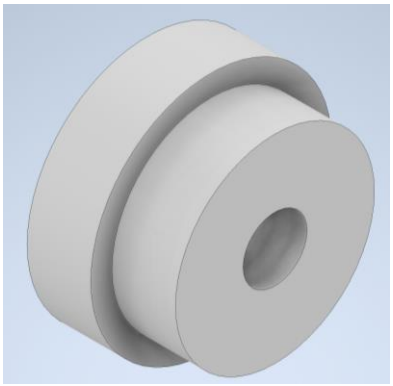

Figure 71: Mark 2 stop cap.

Mark 2 grabber grippers

Similarly, to the Mark 1 design, the Mark 2 grippers had to be two different sizes. As this design is more streamlined than the Mark 1 design, the grippers had to be redesigned to be much thinner and longer than the Mark 1 grabber. By modeling the Stardust model in Autodesk

Inventor, the gripper lengths were chosen to be 2.42 inches for the long gripper, and 2.01 inches for the short grippers. Each gripper features a mounting hole that is held to the outer rod flanges by a small pin. The long and short grippers were 3D printed from nylon for rigidity. For the release motion of the grabber, the wedge on the inner rod pushes the grippers apart. For the capture motion of the grabber, there are small music wire springs that pull the grippers closed once the wedge is pushed back to its original position. The long and short grippers are shown below in Figure 72.

Figure 72: Mark 2 3D printed long gripper and short grippers for MSBS testing.

Mark 2 grabber assembly

For the Mark 2 assembly, the inner rod is set in place inside the outer rod with wedge and internal ring attached. The stop cap and aero fairing cap were then attached to the upstream and downstream portions of the outer rod. The inner rod was then fastened into the connector rod with epoxy. The Mark 2 grabber assembly is shown below in Figure 73.

Figure 73: Mark 2 grabber prototype Assembly.

Mark 2 grabber setup

The setup for the Mark 2 grabber in the subsonic MSBS tunnel at NASA Langley would be more straightforward than the Mark 1 grabber. The only step for setup is to the fasten the connector rod portion of the assembly into the threaded section of the pneumatic retractor. Further work for the Mark 2 grabber would include testing and revision of current design, and further implementation in the NASA Glenn SWT.

5. FUTURE WORK

Future work for this project would include the further augmentation of the Mark 1 grabber for testing, further design and implementation of a Mark 2 grabber in a subsonic testing setting, and further augmentation of the supersonic MSBS simulation. As discussed previously, there was some feedback delay between the signal being sent to open the Mark 1 grabber and the signal to retract the sting. This is a design aspect that would have to be investigated more to limit the chance of the tested model hitting the Mark 1 grabber, and to gather more accurate dynamic stability data. Another design aspect that could be investigated is the robustness of the Mark 1 grabber and the possibility for streamlining the design into a more elegant one that would incur less blockage overall. For the Mark 2 grabber, further design and testing would need to be conducted to get it to working condition and resize it for a use in the NASA Langley Subsonic MSBS and future use in the NASA Glenn supersonic wind tunnel.

6. CONCLUSIONS

The main goal of this thesis was to design and implement a new launching method into the existing subsonic MSBS wind tunnel at NASA Langley. The design and implementation were successful as the Mark 1 grabber is being used for ongoing dynamic stability testing. The other goal of this thesis was to compare data from the Mark 1 grabber to previous launching methods. It was compared to previous launching methods based on axial and vertical influence. As shown in the result section for the launching methods, the adjusted Mark 1 grabber performed better than the edge holder in terms of axial and vertical influence. The adjusted Mark 1 grabber outperformed the standard sting for axial influence but did not perform better than the standard sting in terms of vertical influence. From the simulation, the release speed required for the launching method to be away from the model was found to be acceptable. The preliminary conclusion of these results shows that the Mark 1 grabber inflicts less overall influence on the testing models than other launching methods.

The secondary goal of this thesis was to design a Mark 2 grabber for a supersonic setting. The Mark 2 grabber, albeit not tested, is a preliminary design into the general idea of how a supersonic Mark 2 grabber would look and function. As discussed previously, the Mark 2 grabber is a purely mechanical design, therefore, feedback delay between the controller and the actuation is entirely based on the design of the Mark 2 grabber itself, and not a signal delay as in the Mark 1 grabber. This design featured internal stops and a pull rod that would wedge open the grippers when the sting was retracted and then close the grippers when the sting fully redeploys. An issue found with the current design was the redeployment and test capabilities. The redeployment of the grippers conceptually has been determined but converting that to a usable product is unfinished. Another issue of the current design for the Mark 2 grabber is the feasibility

of testing. Unlike the Mark 1 grabber, the controls for the actuation and the retraction are not separate, which means that to test, the sting would have to be fully retracted and redeployed to regrip the testing model if the test conditions such as angle of attack, were not correct.

The tertiary goal of this thesis was to create a simulation for testing of a blunt body in a subsonic and supersonic MSBS setting. A simulation was created with Simulink to calculate the displacements, accelerations, body velocity, and the attitude of the blunt body in a worst-case setting.

Overall, the goals of this thesis were met. A functional launching method was designed to yield better results than previous launching methods, with room for improvement, and inflict less interference for Stardust and any future entry vehicles to be tested. A simulation was created and used for a baseline for a clearance time and ideal values of data gathered.

REFERENCES

[1] Schoenenberger, M., Cox, D., Schott, T., Mackenzie, A., Ramirez, O., Britcher, C., Neill, C., Weinmann, M., and Johnson, D., “Preliminary Aerodynamic Measurements from a Magnetic Suspension and Balance System in a Low-Speed Wind Tunnel” AIAA Aviation in *AIAA Paper 2018-3323,*, Atlanta, Georgia, 2018.

[2] Neill, C., "Comparison of Support Methods for Static Aerodynamic Testing and Validation of a Magnetic Suspension and Balance System.," Thesis, Department of Mechanical and Aerospace Engineering, Old Dominion University, May 2019.

[3] Karatekin, O., Charbonnier, JM., Wang, F., and Dehant, V., “Dynamic Stability of Atmospheric Entry Probes”, Proceedings of the International Workshop Planetary Probe Atmospheric Entry and Descent Trajectory Analysis and Science, Lisbon, Portugal, October 2003.

[4] Kazemba, C., Braun, R. D., Schoenenberger, M., Clark, I. G., “Dynamic Stability Analysis of Blunt Body Entry Vehicles Through the Use of a Time-lagged Aftbody Pitching Moment”, AE8900 MS Special Problems Report, Georgia Institute of Technology, Atlanta, Georgia, May 2012.

[5] Kazemba, C., Braun, R., Clark, I., and Schoenenberger, M., “Survey of Blunt Body Dynamic Stability in Supersonic Flow”, AIAA Atmospheric Flight Mechanics Conference in *AIAA Paper 2012-4509.,* Minneapolis, Minnesota, August 2012.

[6] Desai, P., Mitcheltree, R., Cheatwood, F., “Entry Trajectory Issues for the Stardust Sample Return Capsule”, International Symposium on Atmospheric Reentry Vehicles and Systems, France, March 1999.

[7] Baillion, M.., Blunt Bodies Dynamic Derivatives, *AGARD Report 808: Capsule Aerothermodynamics,* Vol. 8, No. 1 – 20.

[8] Chapman, G. T. and Yates, L. A, "Dynamics of Planetary Probes: Design and testing issues", 36th AIAA Aerospace Sciences Meeting and Exhibit in *AIAA paper 98-0797,* Reno, New York. January 1998.

[9] Ericsson, L., and Reding, J., "Re-Entry Capsule Dynamics," AIAA Atmospheric Flight Mechanics Conference in *AIAA Paper 70-563.,* Tullahoma, Tennessee, May 1970.

[10] Covert, E., "Magnetic suspension and balance systems", IEEE Aerospace and Electronics Systems Magazine, vol. 3, no. 5, 1988.

[11] Boyden, R. P., and Tcheng, P., "Status of Magnetic Suspension Technology", Langley Symposium on Aerodynamics, vol. 1, NASA CP-2397, December 1986.

[12] Schoenenberger, M., Finke, C., Britcher, C., Cox, D., Schott, T., "Static and Dynamic Testing of Blunt Bodies in a Subsonic Magnetic Suspension Wind Tunnel", 15th International Conference on Flow Dynamics, Sendai, Japan, November 2018.

[13] Stephens, T., "Design, Construction, and Evaluation of a Magnetic Suspension and Balance Systems for Wind Tunnels", NASA CR-66903, November 1969.

[14] Boyden, R. P., "A Review of Magnetic Suspension and Balance Systems," 15th Aerodynamic Testing Conference in *AIAA Paper 1988-2009,* May 1988.

[15] Schoenenberger, M. and Queen, E. M., "Limit Cycle Analysis Applied to the Oscillations of Decelerating Blunt-Body Entry Vehicles" NATO OTAN R&T, RTO-MP-AVT-152.

[16] Mitcheltree, R., and Fremaux, C., “Subsonic Dynamics of Stardust Sample Return Capsule”, Hampton, VA, NASA Technical Memorandum, NASA-TM-110329, March 1997.

[17] Schoenenberger, M., Cox, D., Britcher, C., “Preliminary Measurement of Pitch Damping of Blunt Entry Vehicles in a Subsonic Magnetic Suspension Wind Tunnel”, 18th International Conference on Flow Dynamics, October 2021.

[18] Britcher, C., and Schoenenberger, M., “Feasibility of Dynamic Stability Measurements of Planetary Entry Capsules Using MSBS”, 12th International Conference on Flow Dynamics, Sendai, Japan, 27-29 October 2015.

[19] Britcher, C., Schoenenberger, M., Cox, D., “Demonstration of a Magnetic Suspension and Balance System with Transverse Magnetization”, 16th International Conference on Flow Dynamics, Sendai, Japan, November 2019.

[20] R.A. Mitcheltree, R.G. Wilmoth, F.M. Cheatwood, G.J. Brauckmann, F.A. Greene, “Aerodynamics of Stardust Sample Return Capsule”, Journal of Spacecraft and Rockets, vol. 36, no. 3, *AIAA A97-31764*, June 1999.

[21] Sevier, A., “Feasibility Study for Testing the Dynamic Stability of Blunt Bodies with a Magnetic Suspension and Balance System in a Supersonic Wind Tunnel”, Thesis, Department of Mechanical and Aerospace Engineering, Case Western Reserve University, May 2017.

APPENDIX A. MSBS TESTING DESIGNS

A.1 Vertical support strut top drawing

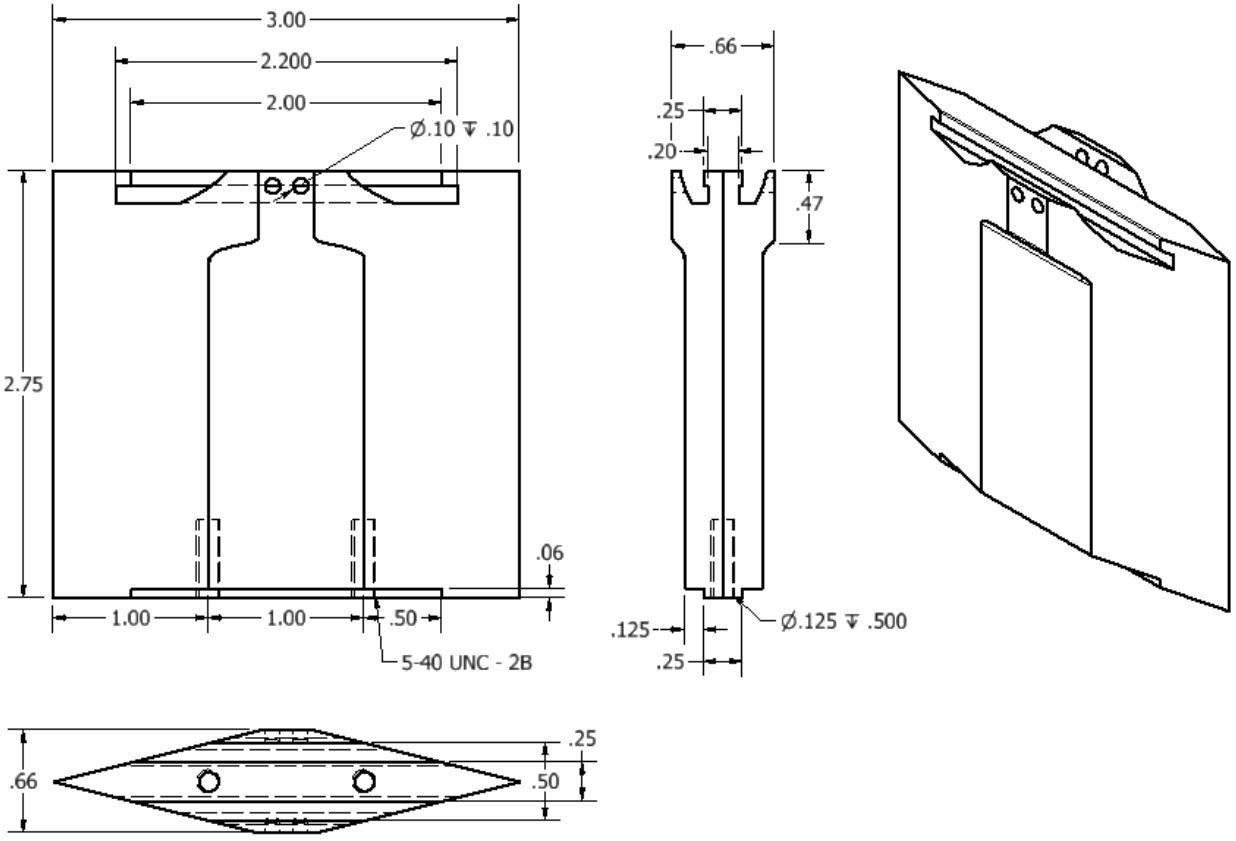

Figure 74: Vertical support strut top. Dimensions in inches.

A.2 Vertical support strut bottom drawing

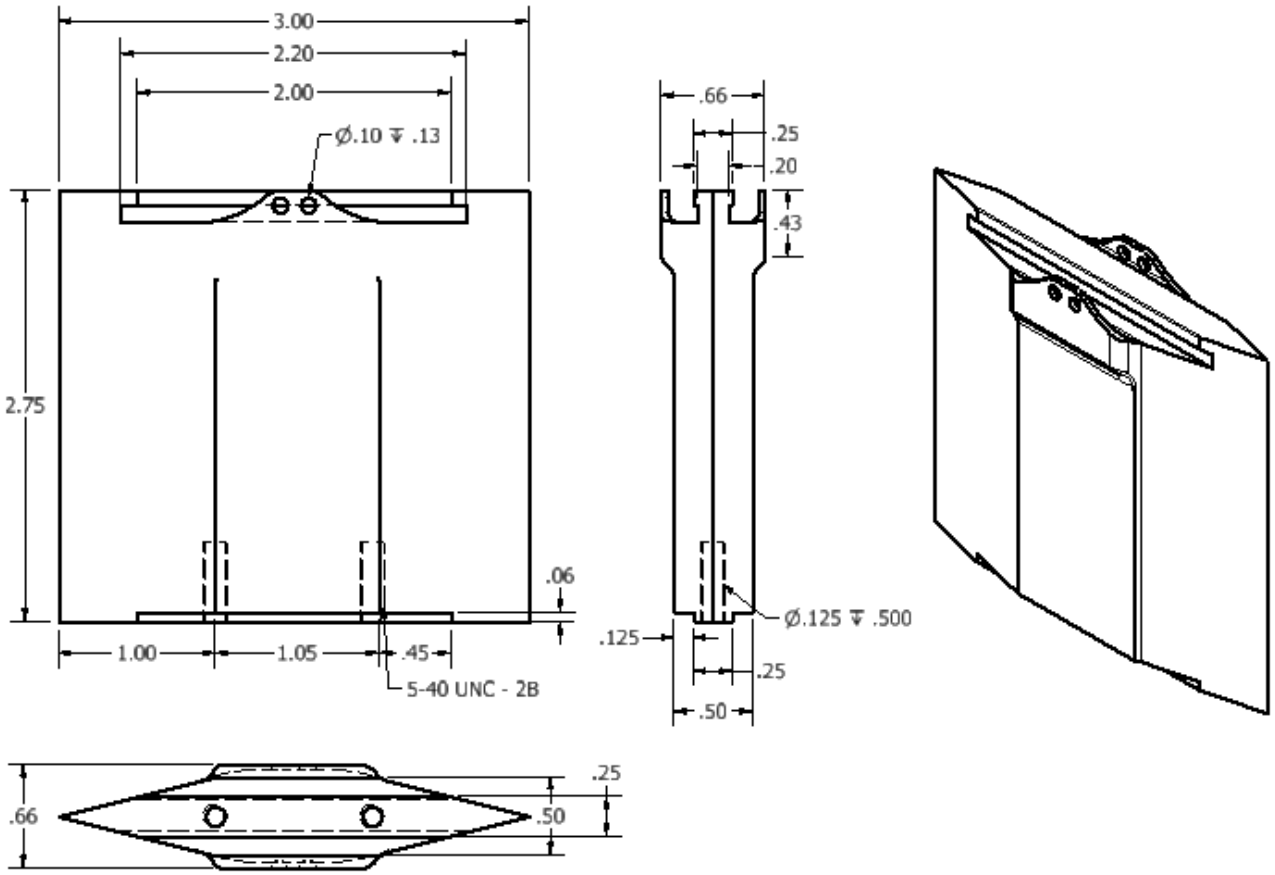

Figure 75: Vertical support strut bottom. Dimensions in inches.

A.3 Vertical support strut assembly drawing

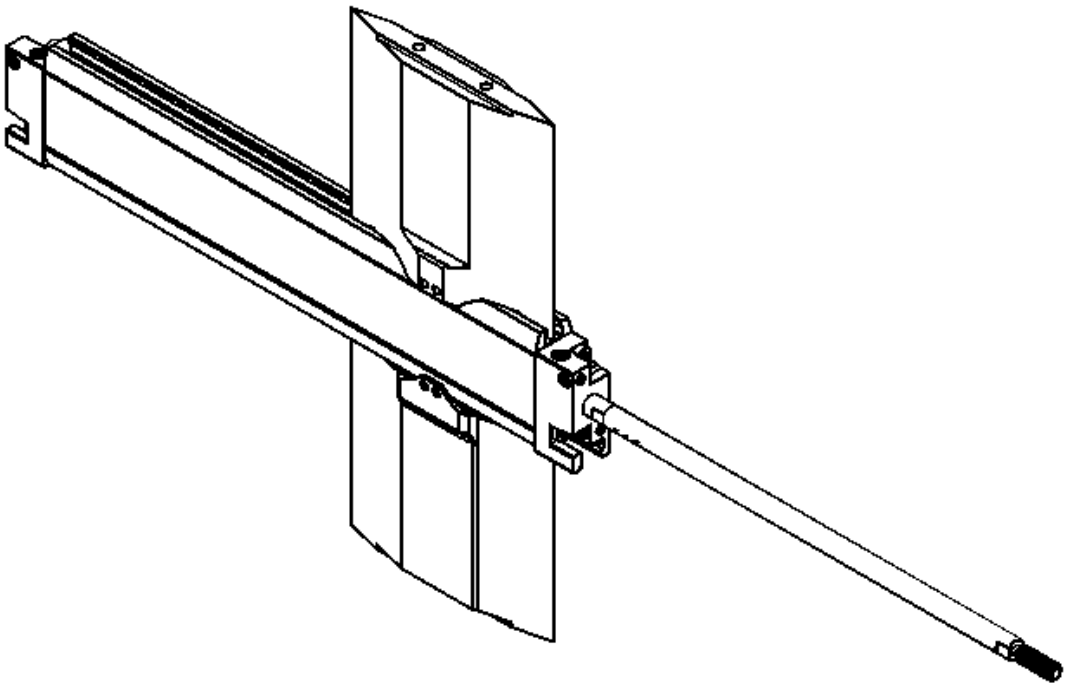

Figure 76: Vertical support strut assembly.

The strut assembly is secured to the wind tunnel via two mounting holes. The pneumatic retractor slides into place and is secured via four mounting holes on each strut part.

A.4 Mark 1 grabber components drawings

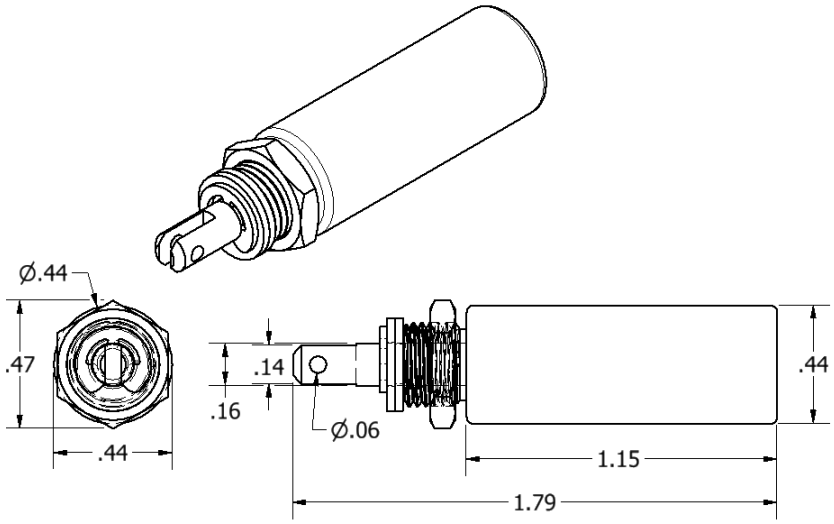

Figure 77: Solenoid for Mark 1 grabber. Dimensions in inches.

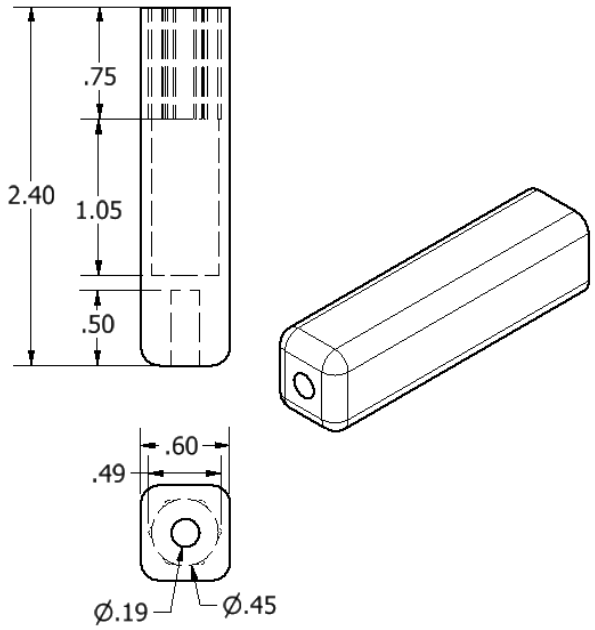

Figure 78: Solenoid housing for Mark 1 grabber. Dimensions in inches.

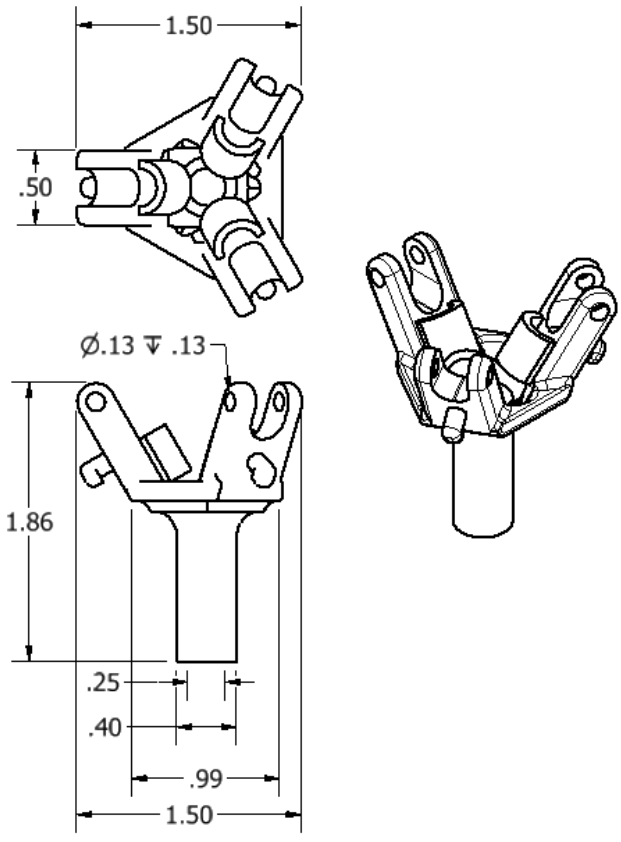

Figure 79: Grabber base for Mark 1 grabber. Dimensions in inches.

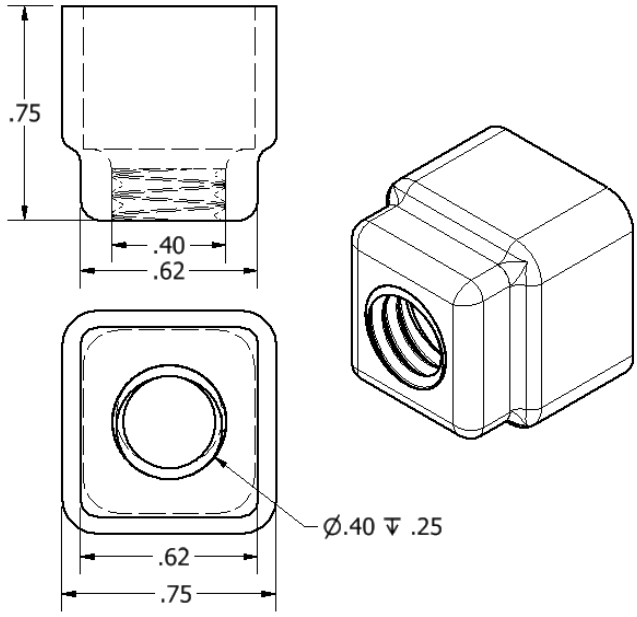

Figure 80: Connector for solenoid housing for Mark 1 grabber. Dimensions in inches.

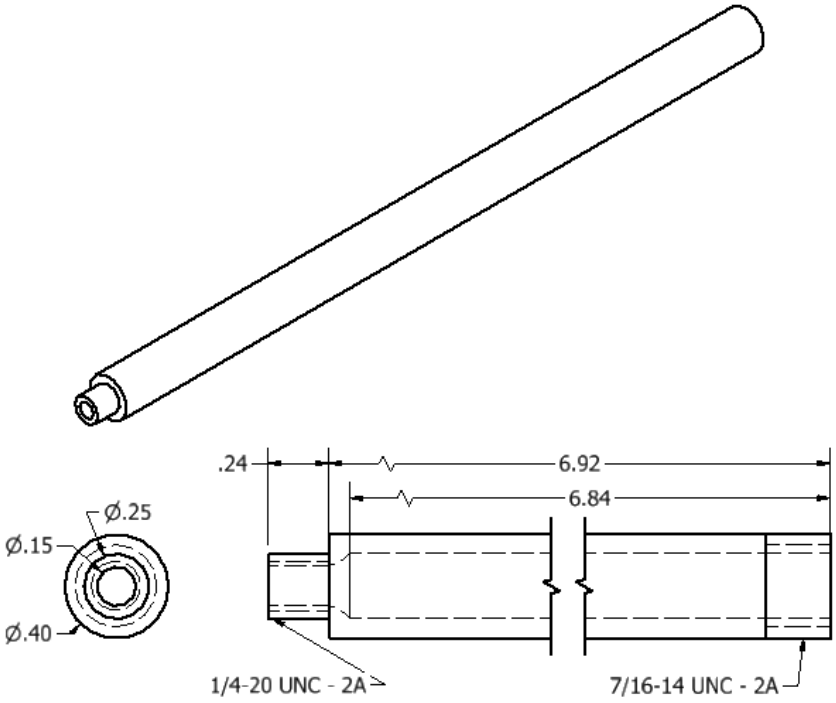

Figure 81: Connector rod for Mark 1 grabber. Dimensions in inches.

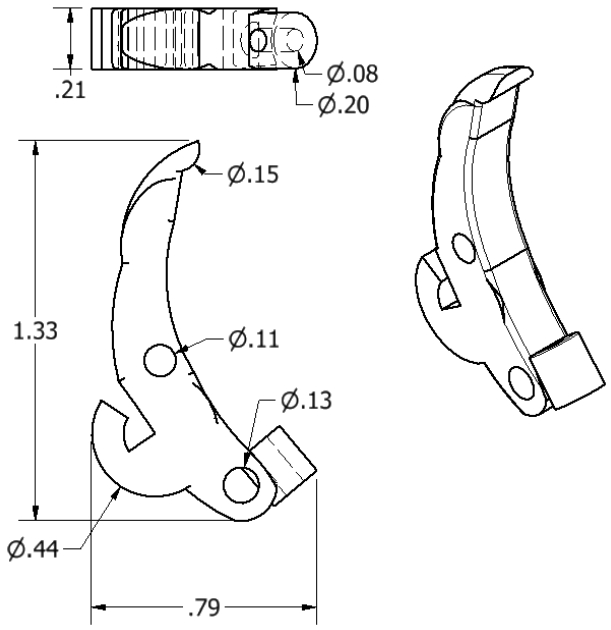

Figure 82: Long gripper for Mark 1 grabber. Dimensions in inches.

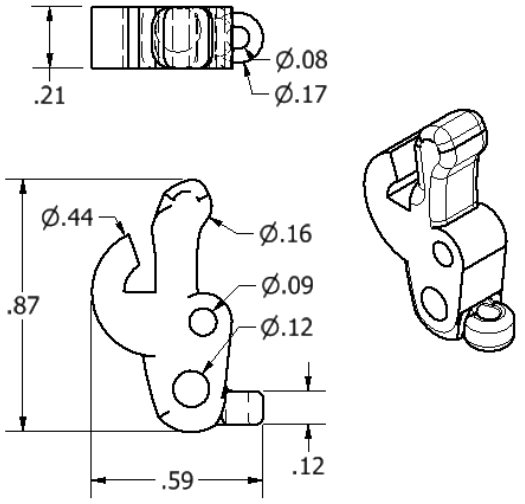

Figure 83: Short gripper for Mark 1 grabber. Dimensions in inches.

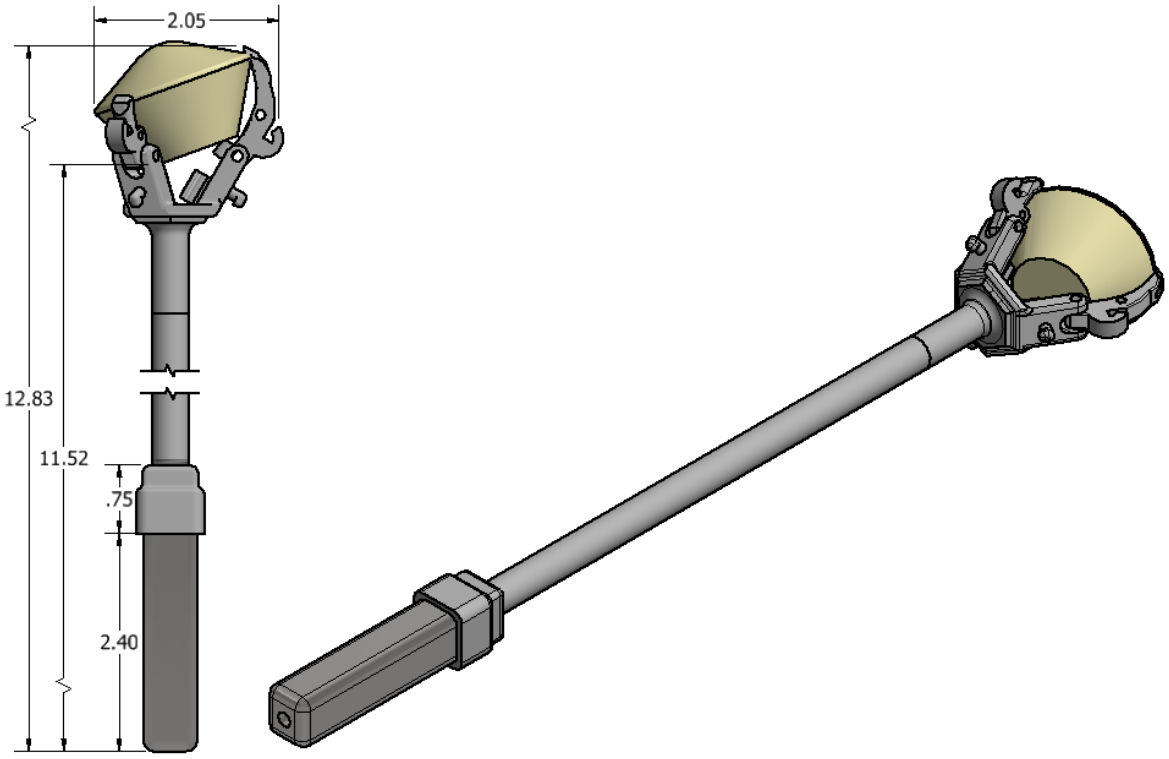

Figure 84: Schematic of assembly of Mark 1 grabber. Dimensions in inches.

APPENDIX B. MAGNETICALLY SUSPENDED MODEL DRAWING

B.1 Magnetically suspended stardust model

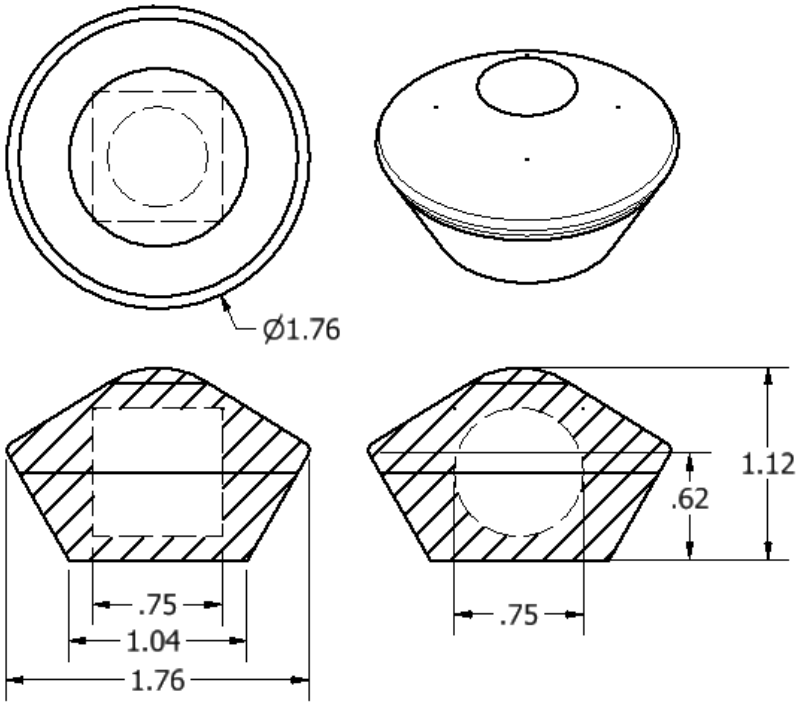

Figure 85: Stardust model with cavity for cylindrical ¾ inch magnet. Dimensions in inches.

APPENDIX C. STING TIPS AND EDGE HOLDERS FOR STARDUST TESTING

C.1 Standard sting attachment

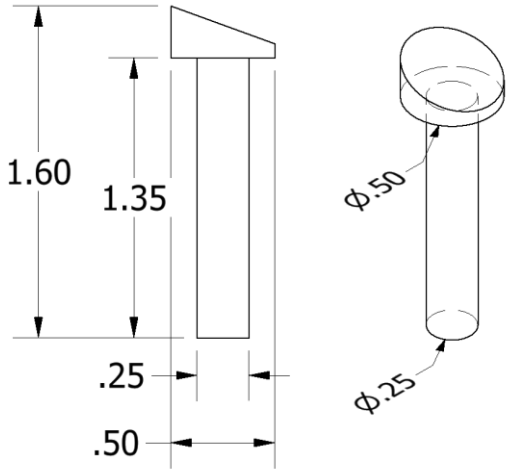

Figure 86: Sting attachment for Stardust testing. Dimensions in inches.

C.2 Edge holder

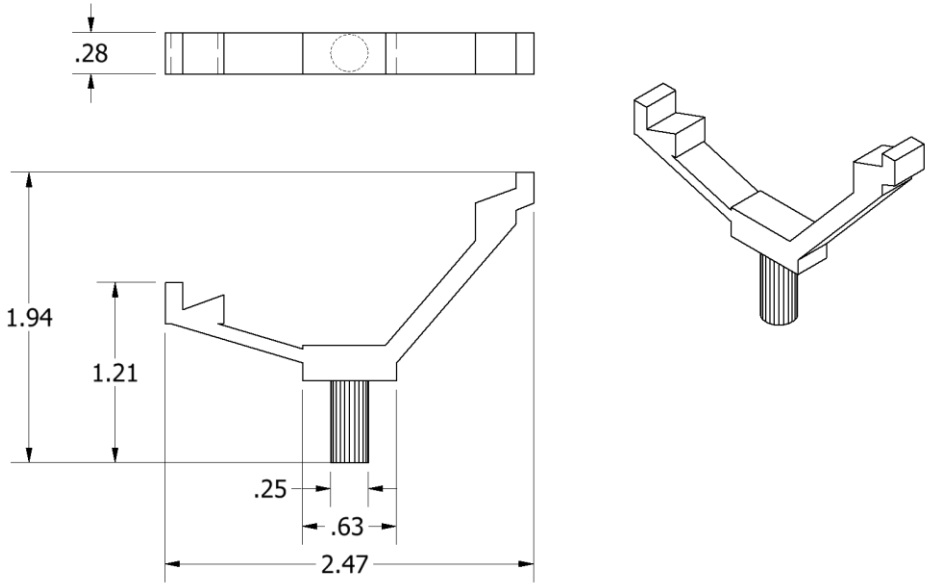

Figure 87: Edge holder for Stardust testing. Dimensions in inches.

APPENDIX D. MATLAB CODES FOR LAUNCHING METHOD CALCULATIONS

D.1 Track2dot function

```
function [rotation,position1,position2] =
track2dot(filename,threshold,cropWindow,maskRadius,frameRange,frameStep,videoOut);
%function [rotation,position1,position2] =
track2dot(filename,threshold,cropWindow,maskRadius,frameRange,frameStep,videoOut);
%
%
% Provides positions and angle history for two-target video tracking
% Initial targets must be selected in first video frame
% Angle is the line from target-1 to target-2 (size of the targets
does not matter).
%
% filename: Name of movie file
% threshold: Value (0-255) value for thresholding image into
black/white
% cropWindow Region of original video file to use in processing
% maskRadius Radius around targets to search in processing the
next frame
% frameRange Lower and upper frame numbers for processing
% frameStep Steps > 1 skip frames in file, lowers sample rate on
output data
% videoOut name for an output video file
%
% All options except the filename have default values and can be left
off, or passed an empty matrix:[]
%
% Load file
VidObj=VideoReader(filename);
% Defaults
if ~exist('cropWindow','var') || isempty(cropWindow) cropWindow=[1 1
VidObj.Width VidObj.Height]; end
if ~exist('threshold','var') || isempty(threshold) threshold=160; end
if ~exist('maskRadius','var') || isempty(maskRadius)
maskRadius=30; end
if ~exist('Vid','var') || isempty(frameRange) frameRange=[1
VidObj.Duration*VidObj.FrameRate]; end
if ~exist('frameStep','var') || isempty(frameStep) frameStep=1; end
if ~exist('videoOut','var') || isempty(videoOut) videoOut=[]; end
% Initialize
frameNdx=[];
rot=[];
pos1=[];
pos2=[];
cnt=0;
missedFrameCount=0;
% Create obj for output video file
if ~isempty(videoOut),
voutObj = VideoWriter(videoOut,'MPEG-4');
%voutObj = VideoWriter(videoOut,'Uncompressed AVI');
open(voutObj);
end
```

```
% Total number of frames in output
nFrames = ??? %number of frames in the video being analyzed
% Forward in file to 1st frame
title(' Seeking start frame, please wait...','FontSize',16);
for i=1:frameRange(1)
PicCrop = imcrop(VidObj.readFrame, cropWindow);
end
for i = 1:nFrames,
% Create grayscale image to process
img2d=rgb2gray(PicCrop);
% If first-frame prompt for mask
if (i==1),
clf
imshow(img2d);
title('Click to Locate both Targets','FontSize',16);
centers=ginput(2);
[xgrid,ygrid]=meshgrid([1:size(img2d,2)],[1:size(img2d,1)]);
end
% Generate mask to isolate targets
mask1=0*img2d;
mask1 =uint8((xgrid-centers(1,1)).^2 + (ygrid-centers(1,2)).^2 <
maskRadius^2);
mask2=0*img2d;
mask2 = uint8((xgrid-centers(2,1)).^2 + (ygrid-centers(2,2)).^2 <
maskRadius^2);
% Mask image, convert to binary for contiguous region identification
bw1 = (img2d.*mask1) > threshold;
bw2 = (img2d.*mask2) > threshold;
% Take centroid of largest blob in masked regions
foundCount=0;
LabeledImage = bwlabel(imfill(bw1,'holes'),8);
BlobMeasurements = regionprops(LabeledImage, 'basic');
if ~isempty(BlobMeasurements)
[~,ndx]=max([BlobMeasurements(:).Area]);
centers(1,:)=BlobMeasurements(ndx).Centroid;
foundCount=foundCount+1;
end
LabeledImage = bwlabel(imfill(bw2,'holes'),8);
BlobMeasurements = regionprops(LabeledImage, 'basic');
if ~isempty(BlobMeasurements)
[~,ndx]=max([BlobMeasurements(:).Area]);
centers(2,:)=BlobMeasurements(ndx).Centroid;
foundCount=foundCount+1;
end
% If both ends were found,calculate values, else skip frame
if foundCount==2,
missedFrameCount=0;
delta=diff(centers);
angle=atan2(-delta(2),delta(1));
imshow(imfuse(imfuse(bw1,bw2,'blend'),PicCrop,'blend'));
viscircles(centers, maskRadius*[1;1],'Color','g');
line(centers(:,1),centers(:,2),'LineWidth',2,'Color','b','Marker','o','MarkerFaceColor','drawnow;
% Augment frameNdx vector with current frame count
% This allows interpolation below to fill in missing frames
frameNdx=[frameNdx,i];
rot =[rot;angle];
```

```
% Convert to Y +Up
pos1 =[pos1; [centers(1,1), cropWindow(4)-centers(1,2)] ];
pos2 =[pos2; [centers(2,1), cropWindow(4)-centers(2,2)] ];
else % didn't find two targets, render and increment missed
counter
imshow(PicCrop)
viscircles(centers,maskRadius*[1;1],'Color','g');
% Missed 4 frames in a row, bail.
missedFrameCount=missedFrameCount+1;
if missedFrameCount>3,
fprintf(2,'Poor tracking, adjust thresholds or mask size\n');
break;
end
end
% Add frame to output video
if ~isempty(videoOut), writeVideo(voutObj,getframe(gcf)), end
% Forward to next frame, skipping as required
for j=1:frameStep,
PicCrop = imcrop(VidObj.readFrame, cropWindow);
end
end
% Generate output data
% Interpolate through skipped frames, if necessary
if (length(frameNdx)<nFrames && length(frameNdx)>1 )
rotation=interp1(frameNdx,rot,[1:max(frameNdx)]');
rotation=unwrap(rotation)*180/pi;
position1=interp1(frameNdx,pos1,[1:max(frameNdx)]');
position2=interp1(frameNdx,pos2,[1:max(frameNdx)]');
else
rotation=unwrap(rot)*180/pi;
position1=pos1;
position2=pos2;
end
% Close video output file
if ~isempty(videoOut), close(voutObj); end
```

Published with MATLAB® R2018a

D.2 Template code for video analysis

```
figure(1),
% % % No crop, default settings (takes a long time....)
% [r,p1,p2]=track2dot('???.mov');
% t=[0:length(r)-1]*1/180;
% Loosely cropped, every 6th frame for 30 Hz data
%[r,p1,p2]=track2dot('???.mov',[],[1 80 500 840],16,[122 400],6);
%t=[0:length(r)-1]*6/180;
% High threshold, Tight crop, tight mask radius, frame range, every
frame (default), with a video output
[r,p1,p2]=track2dot('???.mov', 150, [500 100 600 500], 20, [17 150],
[],'processedVideo');
t=[0:length(r)-1]'*1/180;
figure(2),clf
subplot(3,1,1)
plot(t,r)
```

```
grid on
ylabel('Rotation, deg');
title('Pitch')
subplot(3,1,2)
plot(t,[p1(:,1),p2(:,1)])
grid on
ylabel('X-Position');
title('Axial Movement')
legend('Dot-1','Dot-2');
subplot(3,1,3)
plot(t,[p1(:,2),p2(:,2)]);
grid on
ylabel('Y-Postion');
title('Vertical Movement')
legend('Dot-1','Dot-2');
xlabel('Time, sec');
```

Published with MATLAB® R2018a

D.3 Conversion from pixels to inches

```
>> VidObj=VideoReader('ruler.mov');
singleFrame = VidObj.readFrame;
imshow(singleFrame);
xyPixels = ginput(2);
xyPixels

xyPixels =

  765.0000  265.0000
  923.0000  265.0000

>> format long g
>> (xyPixels(2,1)-xyPixels(1,1))/0.0254

ans =

          6220.47244094488
```

APPENDIX E: UNCERTAINTY ANALYSIS

E.1 Code to plot error bars on trajectory plots

```
%Pitch Uncertainty average = 0.0285
%SigmaDot1 average = 0.2125
%SigmaDot2 average = 0.2156

figure
plot(t,r), hold on
errorbar((t(25,:)),[r(25,1)],0.0285,'b'), hold on
errorbar((t(100,:)),[r(100,1)],0.0285,'b'), hold on
errorbar((t(150,:)),[r(150,1)],0.0285,'b'), hold on
grid on
ylabel('Rotation, deg');
title('Pitch')
xlabel('Time,  sec');

figure
plot(t,[p1(:,1),p2(:,1)]), hold on
errorbar((t(25,:)),[p1(25,1)],0.2125,'b'), hold on
errorbar((t(100,:)),[p1(100,1)],0.2125,'b'), hold on
errorbar((t(150,:)),[p1(150,1)],0.2125,'b'), hold on
errorbar((t(25,:)),[p2(25,1)],0.2156,'b'), hold on
errorbar((t(100,:)),[p2(100,1)],0.2156,'b'), hold on
errorbar((t(150,:)),[p2(150,1)],0.2156,'b'), hold on
grid on
ylabel('X-Position');
title('Axial Movement')
legend('Dot-1','Dot-2');
xlabel('Time,  sec');

figure
plot(t,[p1(:,2),p2(:,2)]), hold on
errorbar((t(25,:)),[p1(25,2)],0.2125,'b'), hold on
errorbar((t(100,:)),[p1(100,2)],0.2125,'b'), hold on
errorbar((t(150,:)),[p1(150,2)],0.2125,'b'), hold on
errorbar((t(25,:)),[p2(25,2)],0.2156,'b'), hold on
errorbar((t(100,:)),[p2(100,2)],0.2156,'b'), hold on
errorbar((t(150,:)),[p2(150,2)],0.2156,'b'), hold on
grid on
ylabel('Y-Position');
title('Vertical Movement')
legend('Dot-1','Dot-2');
xlabel('Time,  sec');
```

APPENDIX F: FREQUENCY OF OSCILLATIONS BLOCK

F.1 Sine wave block in Simulink

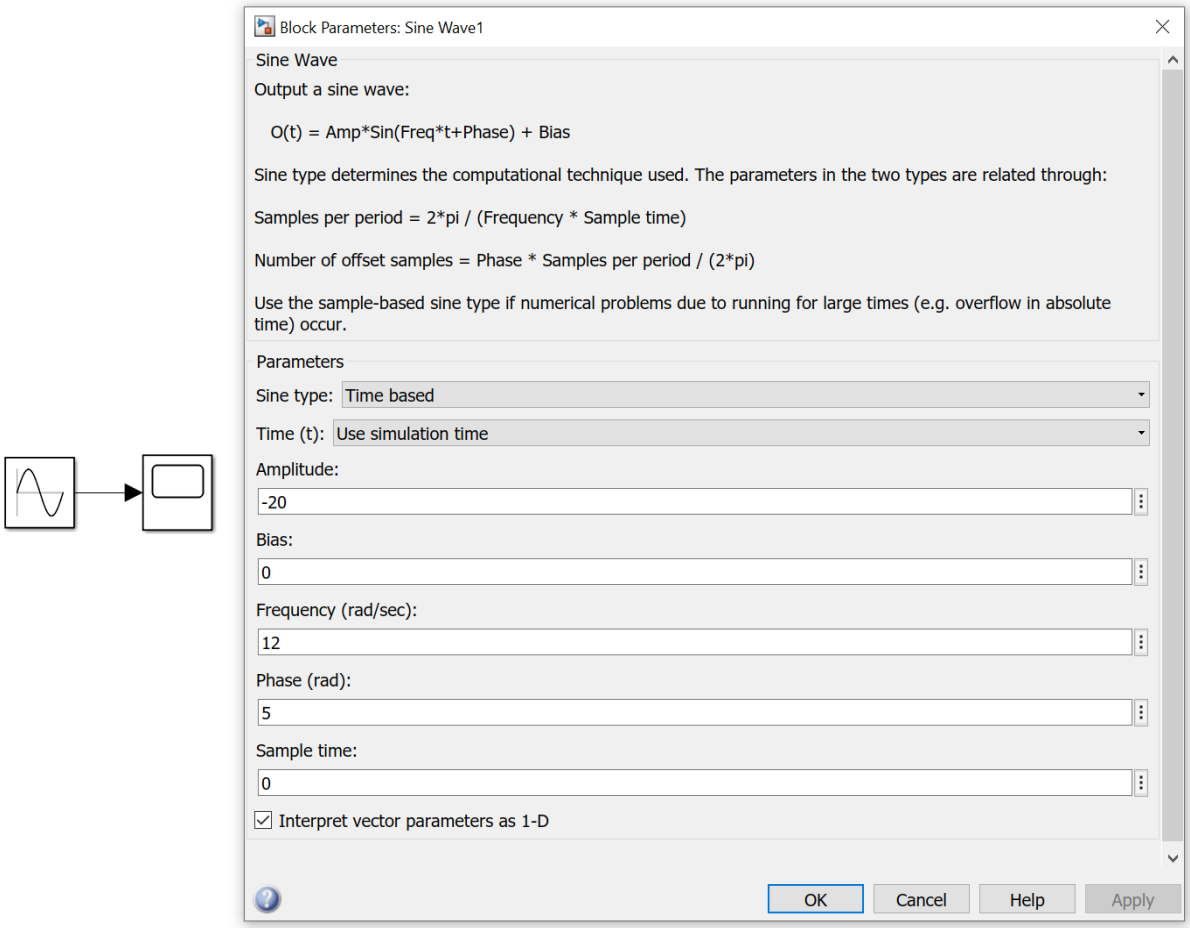

Figure 88: Sine wave block parameters.

APPENDIX G: SUBSONIC AND SUPERSONIC SIMULATIONS

G.1 Simulink model for Subsonic and Supersonic Simulations

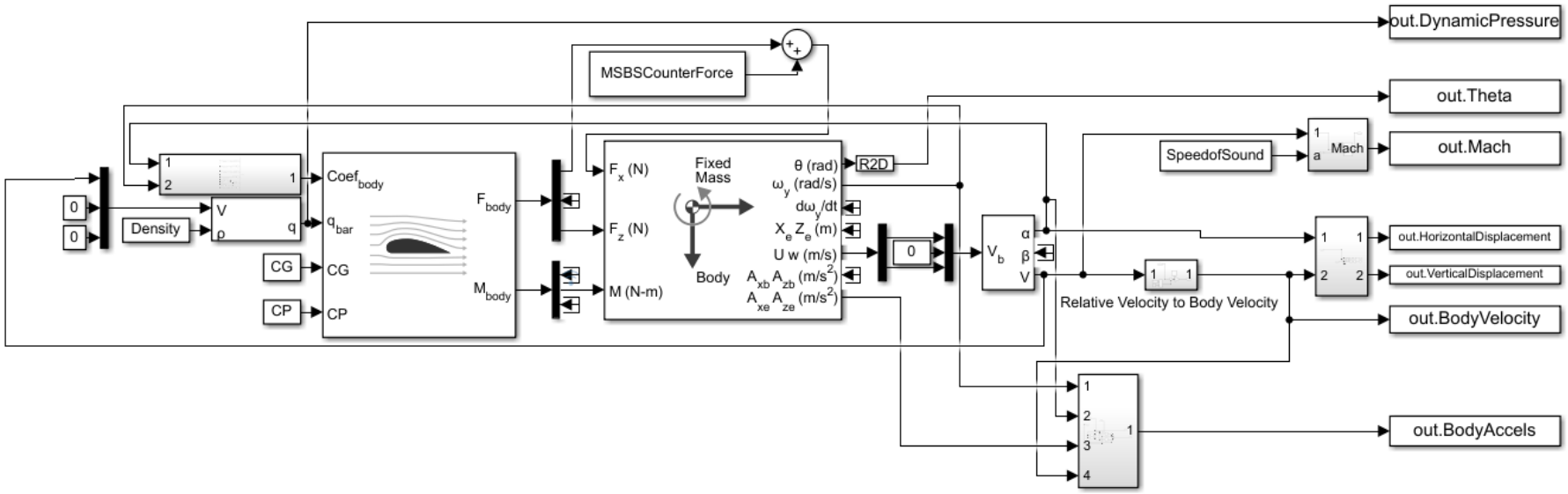

Figure 89: Simulink model for Subsonic and Supersonic Simulations.

G.2 Aerodynamic coefficients subsystem in Simulink

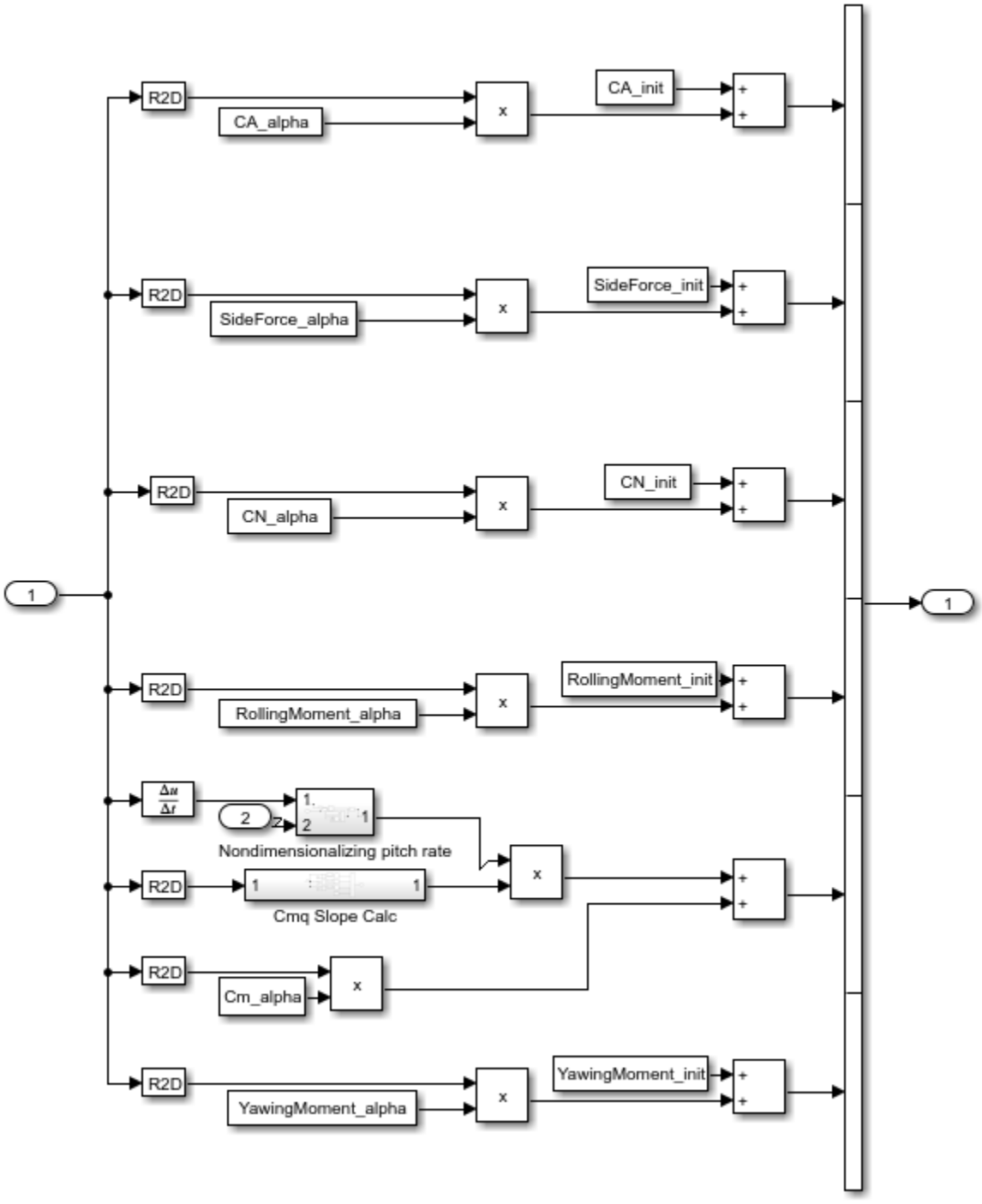

Figure 90: Aerodynamic coefficient subsystem

G.3 Cm_q subsystems in Simulink

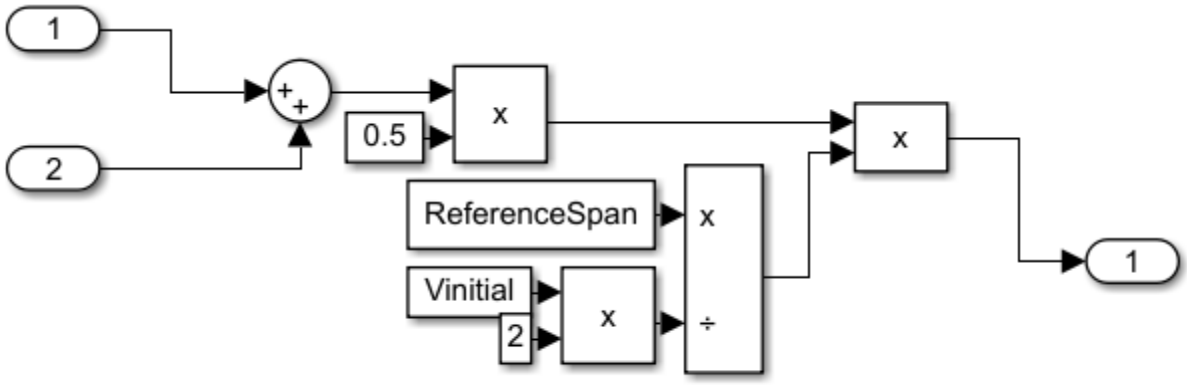

Figure 91: Pitch rate nondimensionalizing subsystem

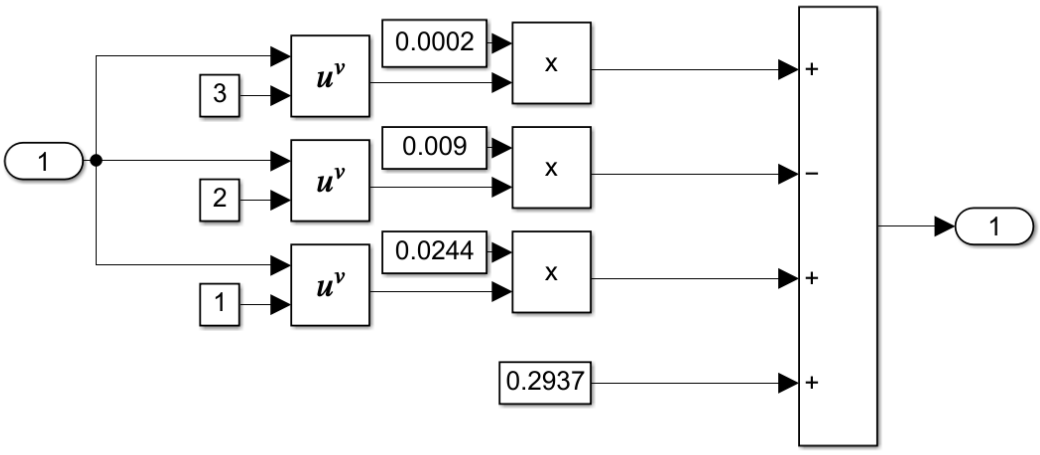

Figure 92: C_{mq} slope subsystem

G.4 Aerodynamic Forces and Moments Subsystem in Simulink

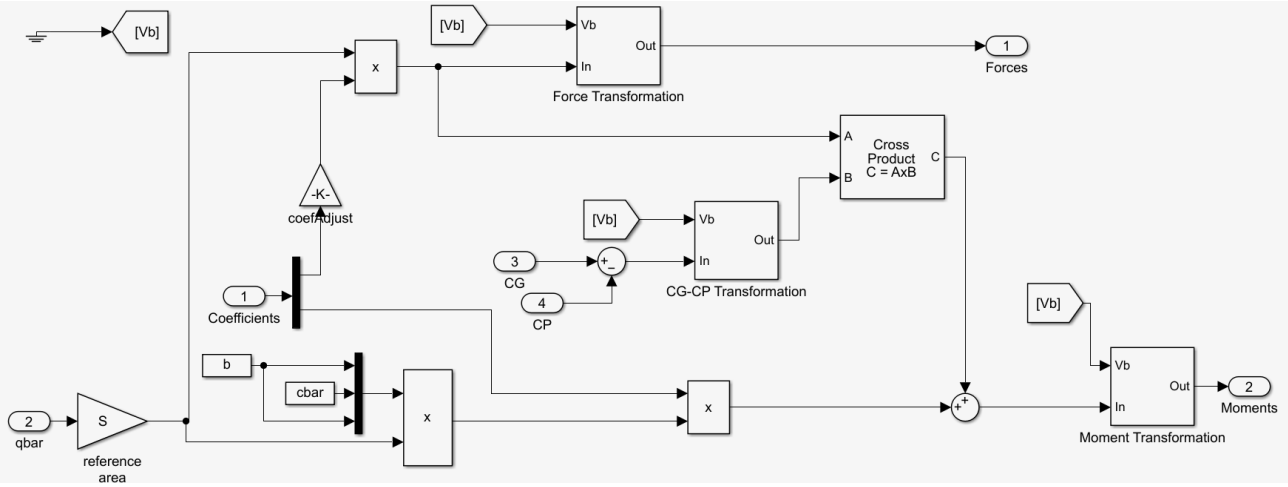

Figure 93: Aerodynamic Forces and Moments Subsystem.

G.5 3DOF Body Axes Subsystem in Simulink

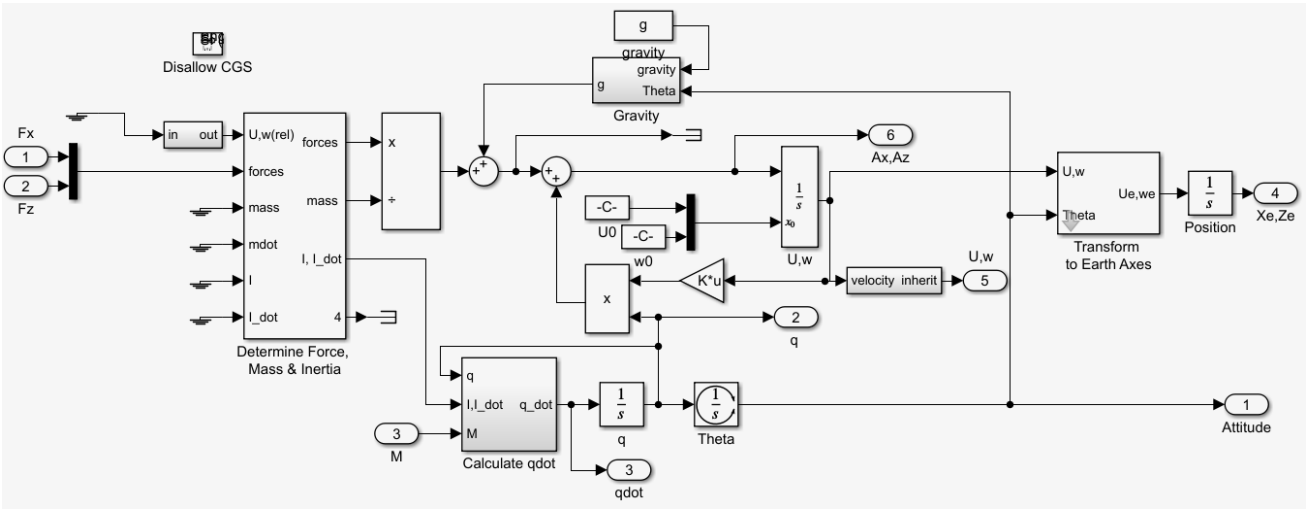

Figure 94: Three Degree of Freedom Body Axes Subsystem.

G.6 Subsonic MATLAB Code

```
%Model Specifications
%If testing the 1.75 inch Stardust model, then don't change these values
%If testing a different model, these values will change

%All values have been converted from imperial to metric for Simulink

ReferenceArea = 1.55*10^-3;             %Largest Area of "Face" of Model in meters^2
ReferenceSpan = 0.04445;                %Largest Diameter of Model in meters
ReferenceLength = 0.028956;             %Distance from Backshell to Nose in meters
Mass = 0.057;                           %Mass of model including plastic shells and
neodymium core in kilograms
Inertia = 0.00001126407;                %Moment of Inertia calculated using Model
Analysis in Autodesk Inventor.
CG = [0.0155575, 0, 0];                 %Center of Gravity of Model in meters (y and
z directions are the radius of the heat shield). This value was found from Model
Analysis in Autodesk Inventor
CP =[0.011557, 0, 0];                   %Center of Pressure of Model in meters (y and
z directions are the radius of the heat shield). This value was found from Model
Analysis in Autodesk Inventor

%Subsonic Coefficients

CA_init = -0.8875;                      %Axial Force Coefficient
CA_alpha = -0.001;                      %Axial Force Coefficient Slope
CN_init = 0;                            %Normal Force Coefficient
CN_alpha = 0.0031;                      %Normal Force Coefficient Slope
Cm_alpha = -0.00276;                    %Pitching Moment Coefficient Slope

%Coefficients not used for 3Dof but still needed for calcs

SideForce_init = 0;                     %Side Force Coefficient
SideForce_alpha = 0;                    %Side Force Coefficient Slope
RollingMoment_init = 0;                 %Rolling Moment Coefficient
RollingMoment_alpha = 0;                %Rolling Moment Coefficient Slope
YawingMoment_init = 0;                  %Yawing Moment Coefficient
YawingMoment_alpha = 0;                 %Yawing Moment Coefficient Slope

%Initial Conditions for Supersonic Flow
%Change starting velocity, alpha, theta and density if applicable
Time = 1;                               %Set the value for time of simulation
Vinitial  = 25;                         %Starting wind velocity for supersonic tunnel
conditions in meters/second
Density = 1.225;                        %Density of Air, if testing in different
medium then change this value in kilograms/meters^2
Alpha = 20;                             %Starting incidence in degrees
Theta = 20;                             %Starting attitude in degrees
SpeedofSound = 343;                     %Speed of sound in air in meters/second
MSBSCounterForce = 0;                   %In worst case where model is release
unsuspended
%MSBSCounterForce = 0.486;              %90% of initial drag value
```

```
%MSBSCounterForce = 0.594;              %110% of initial drag value, uncomment if
using this instead

%Running initial conditions through simulation
sim('ModelReleasedwithoutSuspension', Time)

%Plot outputs of Body Velocity, Body Accelerations, Mach, and Displacement

figure(1)
plot(ans.BodyVelocity);
title('Body Velocity of Model released in windstream with respect to time')
xlabel('Time (seconds)')
ylabel('Body Velocity (m/s)')

figure(2)
plot(ans.BodyAccels);
title('Body Accelerations of Model released in windstream with respect to time')
xlabel('Time (seconds)')
ylabel('Body Accelerations (m/s^2)')
legend({'Ax','Az'},'Location', 'Northeast')

figure(3)
plot(ans.Mach);
title('Mach in wind axes with respect to time')
xlabel('Time (seconds)')
ylabel('Mach')

figure(4)
plot(ans.HorizontalDisplacement);
title('Horizontal Displacement of Model with respect to time')
xlabel('Time (seconds)')
ylabel('Displacement (m)')

figure(5)
plot(ans.DynamicPressure);
title('Dynamic Pressure with respect to time')
xlabel('Time (seconds)')
ylabel('Dynamic Pressure')

figure(6)
yyaxis left
plot(ans.VerticalDisplacement);
ylabel ('Vertical Displacement (m)')
yyaxis right
plot(ans.HorizontalDisplacement);
ylabel('Horizontal Displacement (m)')
xlabel('Time (seconds)')
title('Displacement of Model with respect to time')

figure(7)
plot(ans.Attitude);
title('Attitude of Model with respect to time')
xlabel('Time (seconds)')
ylabel('Pitch (Degrees)')
```

```
%Output simulation data to spreadsheet

varNames = {'Body Velocity', 'Ax', 'Az', 'Mach', 'Horizontal Displacement' ,'Vertical
Displacement', 'Attitude'};                %Set variable names based on desired
outputs
filename = 'SubsonicSimulationData.xlsx';
%Send this data to spreadsheet
OutputtoTimeTable = timeseries2timetable(ans.BodyVelocity, ans.BodyAccels, ans.Mach,
ans.HorizontalDisplacement, ans.VerticalDisplacement, ans.Attitude);

SimData = splitvars(OutputtoTimeTable);
%Splits any variables into separate columns (beneficial is exporting multivariable
outputs such as body accelerations)

SimDataRenamed = renamevars(SimData, ["Data", "Data_1_1", "Data_1_2", "Data_2",
"Data_3", "Data_4", "Data_5"], varNames);   %Correcting the simulation results names
based on previously chosen variable names.

writetimetable(SimDataRenamed, filename, 'Sheet', 1);   %Export corrected simulation
data to excel for post processing.

open("SubsonicSimulationData.xlsx")     %Open the spreadsheet that the results were
sent to. Note: if the spreadsheet is already open in another tab then an error will
populate the command window.
clear;
```

G.7 Supersonic MATLAB Code

```
%Model Specifications
%If testing the 1.75 inch Stardust model, then do not change these values
%If testing a different model, these values will change

%All values have been converted from imperial to metric for Simulink

ReferenceArea = 1.55*10^-3;             %Largest Area of "Face" of Model in meters^2
ReferenceSpan = 0.04445;                %Largest Diameter of Model in meters
ReferenceLength = 0.028956;             %Distance from Backshell to Nose in meters
Mass = 0.057;                           %Mass of model including plastic shells and
neodymium core in kilograms
Inertia = 0.00001126407;                %Moment of Inertia calculated using Model
Analysis in Autodesk Inventor.
CG = [0.0155575, 0, 0];   %Center of Gravity of Model in meters (y and z directions
are the radius of the heat shield). This value was found from Model Analysis in
Autodesk Inventor
CP =[0.011557, 0, 0];     %Center of Pressure of Model in meters (y and z directions
are the radius of the heat shield). This value was found from Model Analysis in
Autodesk Inventor

%Supersonic Coefficients

CA_init = -1.5;                         %Axial Force Coefficient
```

```
CA_alpha = -0.001;                      %Axial Force Coefficient Slope
CN_init = 0;                            %Normal Force Coefficient
CN_alpha = 0.0031;                      %Normal Force Coefficient Slope
Cm_alpha = -0.00276;                      %Pitching Moment Coefficient Slope

%Coefficients not used for 3Dof but still needed for calcs

SideForce_init = 0;                     %Side Force Coefficient
SideForce_alpha = 0;                    %Side Force Coefficient Slope
RollingMoment_init = 0;                 %Rolling Moment Coefficient
RollingMoment_alpha = 0;                %Rolling Moment Coefficient Slope
YawingMoment_init = 0;                  %Yawing Moment Coefficient
YawingMoment_alpha = 0;                 %Yawing Moment Coefficient Slope

%Initial Conditions for Supersonic Flow
%Change starting velocity, alpha, theta and density if applicable
Time = 1;                               %Set the value for time of simulation
Vinitial  = 577.8; %857.5; %202.8;      %Starting wind velocity for supersonic tunnel
conditions in meters/second
Density = 0.07787; %1.225;%0.046899;    %Density of Air, if testing in different
medium then change this value in kilograms/meters^2
Alpha = 20;                             %Starting incidence in degrees
Theta = 20;                             %Starting attitude in degrees
SpeedofSound = 231.13;                     %Speed of sound in air in meters/second
MSBSCounterForce = 0;                   %In worst case where model is release
unsuspended
%MSBSCounterForce = 27.198;             %90% of initial drag value (30.22 N)
%MSBSCounterForce = 33.242;              %110% of initial drag value, uncomment if
using this instead

%Running initial conditions through simulation
sim('ModelReleasedwithoutSuspension', Time)

%Plot outputs of Body Velocity, Body Accelerations, Mach, and Displacement

figure(1)
plot(ans.BodyVelocity);
title('Body Velocity of Model released in windstream with respect to time')
xlabel('Time (seconds)')
ylabel('Body Velocity (m/s)')

figure(2)
plot(ans.BodyAccels);
title('Body Accelerations of Model released in windstream with respect to time')
xlabel('Time (seconds)')
ylabel('Body Accelerations (m/s^2)')
legend({'Ax','Az'},'Location', 'Northeast')

figure(3)
plot(ans.Mach);
title('Mach in wind axes with respect to time')
xlabel('Time (seconds)')
ylabel('Mach')

figure(4)
```

```
plot(ans.HorizontalDisplacement);
title('Horizontal Displacement of Model with respect to time')
xlabel('Time (seconds)')
ylabel('Displacement (m)')

figure(5)
plot(ans.DynamicPressure);
title('Dynamic Pressure with respect to time')
xlabel('Time (seconds)')
ylabel('Dynamic Pressure')

figure(6)
yyaxis left
plot(ans.VerticalDisplacement);
ylabel ('Vertical Displacement (m)')
yyaxis right
plot(ans.HorizontalDisplacement);
ylabel('Horizontal Displacement (m)')
xlabel('Time (seconds)')
title('Displacement of Model with respect to time')


figure(7)
plot(ans.Attitude);
title('Attitude of Model with respect to time')
xlabel('Time (seconds)')
ylabel('Pitch (Degrees)')

%Output simulation data to spreadsheet

varNames = {'Body Velocity', 'Ax', 'Az', 'Mach', 'Horizontal Displacement' ,'Vertical
Displacement', 'Attitude'};                %Set variable names based on desired
outputs
filename = 'SupersonicSimulationData.xlsx';
%Send this data to spreadsheet
OutputtoTimeTable = timeseries2timetable(ans.BodyVelocity, ans.BodyAccels, ans.Mach,
ans.HorizontalDisplacement, ans.VerticalDisplacement, ans.Attitude);

SimData = splitvars(OutputtoTimeTable);
%Splits any variables into separate columns (beneficial is exporting multivariable
outputs such as body accelerations)

SimDataRenamed = renamevars(SimData, ["Data", "Data_1_1", "Data_1_2", "Data_2",
"Data_3", "Data_4", "Data_5"], varNames);   %Correcting the simulation results names
based on previously chosen variable names.

writetimetable(SimDataRenamed, filename, 'Sheet', 1);   %Export corrected simulation
data to excel for post processing.


open("SupersonicSimulationData.xlsx")     %Open the spreadsheet that the results were
sent to. Note: if the spreadsheet is already open in another tab then an error will
populate the command window.
clear;
```

G.8 Exported data from subsonic simulation

Table 13: Data from subsonic simulation

Time	Body Velocity (m/s)	Ax (m/s^2)	Az (m/s^2)	Mach	Horizontal Displacement (m)	Vertical Displacement (m)	Attitude (degrees)
0 sec	0.000	0.65	-9.45	0.073	0.00E+00	0.00E+00	20.00
0.004 sec	0.035	0.63	-9.42	0.073	6.50E-05	2.37E-05	19.97
0.008 sec	0.069	0.60	-9.38	0.073	2.60E-04	9.45E-05	19.87
0.012 sec	0.104	0.55	-9.34	0.073	5.84E-04	2.12E-04	19.71
0.016 sec	0.138	0.48	-9.29	0.073	1.00E-03	3.75E-04	19.48
0.02 sec	0.172	0.39	-9.23	0.072	1.60E-03	5.82E-04	19.20
0.024 sec	0.207	0.28	-9.17	0.072	2.30E-03	8.31E-04	18.85
0.028 sec	0.241	0.16	-9.11	0.072	3.20E-03	1.10E-03	18.45
0.032 sec	0.275	0.02	-9.04	0.072	4.20E-03	1.40E-03	17.98
0.036 sec	0.309	-0.14	-8.97	0.072	5.30E-03	1.80E-03	17.46
0.04 sec	0.344	-0.32	-8.89	0.072	6.50E-03	2.20E-03	16.89
0.044 sec	0.378	-0.51	-8.82	0.072	7.90E-03	2.60E-03	16.27
0.048 sec	0.413	-0.71	-8.75	0.072	9.40E-03	3.10E-03	15.59
0.052 sec	0.447	-0.93	-8.68	0.072	1.11E-02	3.50E-03	14.87
0.056 sec	0.482	-1.15	-8.62	0.072	1.29E-02	4.00E-03	14.10
0.06 sec	0.516	-1.39	-8.55	0.071	1.48E-02	4.50E-03	13.29
0.064 sec	0.551	-1.64	-8.50	0.071	1.69E-02	5.00E-03	12.44
0.068 sec	0.585	-1.89	-8.45	0.071	1.91E-02	5.50E-03	11.55
0.072 sec	0.620	-2.16	-8.40	0.071	2.15E-02	6.00E-03	10.63
0.076 sec	0.655	-2.42	-8.37	0.071	2.40E-02	6.40E-03	9.67
0.08 sec	0.689	-2.70	-8.34	0.071	2.66E-02	6.90E-03	8.68
0.084 sec	0.724	-2.97	-8.33	0.071	2.94E-02	7.30E-03	7.67
0.088 sec	0.759	-3.24	-8.32	0.071	3.23E-02	7.70E-03	6.62
0.092 sec	0.793	-3.51	-8.32	0.071	3.54E-02	8.10E-03	5.56

0.096 sec	0.828	-3.78	-8.34	0.071	3.86E-02	8.40E-03	4.47
0.1 sec	0.862	-4.04	-8.36	0.070	4.20E-02	8.70E-03	3.37
0.104 sec	0.897	-4.29	-8.39	0.070	4.55E-02	8.90E-03	2.26
0.108 sec	0.931	-4.53	-8.44	0.070	4.92E-02	9.00E-03	1.13
0.112 sec	0.965	-4.76	-8.49	0.070	5.30E-02	9.10E-03	0.00
0.116 sec	0.999	-4.97	-8.55	0.070	5.69E-02	9.10E-03	-1.13
0.12 sec	1.033	-5.16	-8.62	0.070	6.10E-02	9.00E-03	-2.27
0.124 sec	1.067	-5.33	-8.69	0.070	6.52E-02	8.90E-03	-3.40
0.128 sec	1.101	-5.48	-8.77	0.070	6.95E-02	8.60E-03	-4.53
0.132 sec	1.134	-5.60	-8.85	0.070	7.40E-02	8.30E-03	-5.64
0.136 sec	1.167	-5.70	-8.93	0.070	7.85E-02	7.80E-03	-6.74
0.14 sec	1.200	-5.76	-9.01	0.069	8.32E-02	7.30E-03	-7.82
0.144 sec	1.233	-5.79	-9.08	0.069	8.81E-02	6.60E-03	-8.87
0.148 sec	1.266	-5.79	-9.15	0.069	9.30E-02	5.90E-03	-9.90
0.152 sec	1.298	-5.75	-9.20	0.069	9.80E-02	5.00E-03	-10.90
0.156 sec	1.330	-5.68	-9.25	0.069	1.03E-01	4.00E-03	-11.86
0.16 sec	1.361	-5.57	-9.28	0.069	1.09E-01	2.90E-03	-12.78
0.164 sec	1.393	-5.43	-9.30	0.069	1.14E-01	1.70E-03	-13.65
0.168 sec	1.424	-5.26	-9.30	0.069	1.19E-01	3.57E-04	-14.48
0.172 sec	1.455	-5.05	-9.28	0.069	1.25E-01	-1.10E-03	-15.26
0.176 sec	1.485	-4.81	-9.25	0.069	1.31E-01	-2.60E-03	-15.99
0.18 sec	1.516	-4.55	-9.19	0.069	1.36E-01	-4.30E-03	-16.66
0.184 sec	1.546	-4.26	-9.12	0.068	1.42E-01	-6.00E-03	-17.28
0.188 sec	1.576	-3.94	-9.04	0.068	1.48E-01	-7.90E-03	-17.83
0.192 sec	1.605	-3.60	-8.93	0.068	1.54E-01	-9.80E-03	-18.33
0.196 sec	1.635	-3.25	-8.81	0.068	1.60E-01	-1.18E-02	-18.76
0.2 sec	1.664	-2.87	-8.68	0.068	1.67E-01	-1.39E-02	-19.13
0.204 sec	1.693	-2.49	-8.54	0.068	1.73E-01	-1.61E-02	-19.44
0.208 sec	1.722	-2.09	-8.38	0.068	1.79E-01	-1.84E-02	-19.69

0.212 sec	1.751	-1.68	-8.22	0.068	1.86E-01	-2.07E-02	-19.88
0.216 sec	1.779	-1.27	-8.05	0.068	1.93E-01	-2.31E-02	-20.01
0.22 sec	1.808	-0.85	-7.88	0.068	1.99E-01	-2.56E-02	-20.07
0.224 sec	1.836	-0.42	-7.71	0.068	2.06E-01	-2.80E-02	-20.08
0.228 sec	1.865	0.00	-7.53	0.068	2.13E-01	-3.06E-02	-20.04
0.232 sec	1.893	0.43	-7.36	0.067	2.20E-01	-3.31E-02	-19.94
0.236 sec	1.921	0.87	-7.19	0.067	2.27E-01	-3.57E-02	-19.79
0.24 sec	1.949	1.30	-7.03	0.067	2.35E-01	-3.84E-02	-19.58
0.244 sec	1.978	1.73	-6.87	0.067	2.42E-01	-4.10E-02	-19.33
0.248 sec	2.006	2.16	-6.72	0.067	2.50E-01	-4.36E-02	-19.03
0.252 sec	2.034	2.60	-6.57	0.067	2.57E-01	-4.62E-02	-18.68
0.256 sec	2.062	3.03	-6.44	0.067	2.65E-01	-4.89E-02	-18.29
0.26 sec	2.090	3.46	-6.31	0.067	2.73E-01	-5.15E-02	-17.85
0.264 sec	2.119	3.89	-6.20	0.067	2.81E-01	-5.40E-02	-17.38
0.268 sec	2.147	4.32	-6.10	0.067	2.89E-01	-5.66E-02	-16.86
0.272 sec	2.176	4.75	-6.01	0.067	2.97E-01	-5.91E-02	-16.31
0.276 sec	2.204	5.18	-5.93	0.067	3.06E-01	-6.15E-02	-15.72
0.28 sec	2.233	5.61	-5.87	0.066	3.14E-01	-6.39E-02	-15.10
0.284 sec	2.261	6.03	-5.82	0.066	3.23E-01	-6.63E-02	-14.44
0.288 sec	2.290	6.46	-5.78	0.066	3.32E-01	-6.86E-02	-13.75
0.292 sec	2.319	6.88	-5.76	0.066	3.41E-01	-7.08E-02	-13.03
0.296 sec	2.348	7.29	-5.76	0.066	3.50E-01	-7.29E-02	-12.28
0.3 sec	2.377	7.70	-5.77	0.066	3.59E-01	-7.49E-02	-11.50
0.304 sec	2.406	8.11	-5.79	0.066	3.68E-01	-7.68E-02	-10.70
0.308 sec	2.435	8.51	-5.84	0.066	3.78E-01	-7.86E-02	-9.87
0.312 sec	2.464	8.90	-5.90	0.066	3.88E-01	-8.03E-02	-9.02
0.316 sec	2.493	9.27	-5.97	0.066	3.97E-01	-8.19E-02	-8.15
0.32 sec	2.522	9.64	-6.06	0.066	4.07E-01	-8.33E-02	-7.25
0.324 sec	2.551	9.99	-6.17	0.065	4.17E-01	-8.46E-02	-6.34

0.328 sec	2.581	10.33	-6.29	0.065	4.28E-01	-8.57E-02	-5.41
0.332 sec	2.610	10.64	-6.42	0.065	4.38E-01	-8.67E-02	-4.47
0.336 sec	2.639	10.94	-6.57	0.065	4.48E-01	-8.75E-02	-3.51
0.34 sec	2.669	11.21	-6.73	0.065	4.59E-01	-8.82E-02	-2.55
0.344 sec	2.698	11.46	-6.91	0.065	4.70E-01	-8.87E-02	-1.57
0.348 sec	2.727	11.68	-7.09	0.065	4.81E-01	-8.90E-02	-0.59
0.352 sec	2.756	11.86	-7.28	0.065	4.92E-01	-8.91E-02	0.39
0.356 sec	2.786	12.02	-7.47	0.065	5.03E-01	-8.91E-02	1.38
0.36 sec	2.815	12.14	-7.67	0.065	5.14E-01	-8.88E-02	2.37
0.364 sec	2.844	12.22	-7.87	0.065	5.25E-01	-8.84E-02	3.35
0.368 sec	2.873	12.27	-8.07	0.065	5.37E-01	-8.77E-02	4.33
0.372 sec	2.902	12.28	-8.27	0.064	5.48E-01	-8.68E-02	5.30
0.376 sec	2.931	12.24	-8.46	0.064	5.60E-01	-8.58E-02	6.25
0.38 sec	2.959	12.17	-8.64	0.064	5.71E-01	-8.45E-02	7.20
0.384 sec	2.988	12.05	-8.81	0.064	5.83E-01	-8.30E-02	8.12
0.388 sec	3.017	11.90	-8.96	0.064	5.95E-01	-8.13E-02	9.03
0.392 sec	3.045	11.70	-9.11	0.064	6.07E-01	-7.95E-02	9.92
0.396 sec	3.073	11.46	-9.23	0.064	6.19E-01	-7.74E-02	10.78
0.4 sec	3.101	11.19	-9.33	0.064	6.31E-01	-7.51E-02	11.62
0.404 sec	3.129	10.87	-9.41	0.064	6.43E-01	-7.26E-02	12.42
0.408 sec	3.157	10.52	-9.47	0.064	6.56E-01	-6.99E-02	13.20
0.412 sec	3.184	10.13	-9.50	0.064	6.68E-01	-6.70E-02	13.94
0.416 sec	3.212	9.71	-9.51	0.064	6.80E-01	-6.39E-02	14.65
0.42 sec	3.239	9.26	-9.49	0.063	6.93E-01	-6.06E-02	15.32
0.424 sec	3.266	8.77	-9.45	0.063	7.06E-01	-5.72E-02	15.95
0.428 sec	3.293	8.26	-9.38	0.063	7.18E-01	-5.36E-02	16.54
0.432 sec	3.319	7.72	-9.29	0.063	7.31E-01	-4.98E-02	17.09
0.436 sec	3.346	7.16	-9.17	0.063	7.44E-01	-4.59E-02	17.60
0.44 sec	3.372	6.58	-9.03	0.063	7.56E-01	-4.19E-02	18.06

0.444 sec	3.399	5.98	-8.87	0.063	7.69E-01	-3.77E-02	18.48
0.448 sec	3.425	5.36	-8.68	0.063	7.82E-01	-3.34E-02	18.85
0.452 sec	3.451	4.72	-8.48	0.063	7.95E-01	-2.89E-02	19.17
0.456 sec	3.477	4.06	-8.26	0.063	8.08E-01	-2.44E-02	19.44
0.46 sec	3.502	3.40	-8.02	0.063	8.21E-01	-1.97E-02	19.67
0.464 sec	3.528	2.72	-7.78	0.063	8.35E-01	-1.50E-02	19.85
0.468 sec	3.554	2.03	-7.52	0.063	8.48E-01	-1.02E-02	19.98
0.472 sec	3.579	1.33	-7.25	0.063	8.61E-01	-5.30E-03	20.06
0.476 sec	3.604	0.62	-6.97	0.062	8.75E-01	-3.32E-04	20.10
0.48 sec	3.630	-0.10	-6.69	0.062	8.88E-01	4.60E-03	20.08
0.484 sec	3.655	-0.82	-6.42	0.062	9.02E-01	9.70E-03	20.02
0.488 sec	3.680	-1.54	-6.14	0.062	9.16E-01	1.47E-02	19.91
0.492 sec	3.705	-2.27	-5.86	0.062	9.30E-01	1.97E-02	19.75
0.496 sec	3.730	-3.00	-5.59	0.062	9.44E-01	2.48E-02	19.55
0.5 sec	3.756	-3.74	-5.33	0.062	9.58E-01	2.98E-02	19.30
0.504 sec	3.781	-4.47	-5.08	0.062	9.72E-01	3.48E-02	19.01
0.508 sec	3.806	-5.20	-4.85	0.062	9.86E-01	3.98E-02	18.67
0.512 sec	3.831	-5.93	-4.62	0.062	1.00E+00	4.47E-02	18.29
0.516 sec	3.856	-6.66	-4.42	0.062	1.02E+00	4.96E-02	17.87
0.52 sec	3.881	-7.38	-4.23	0.062	1.03E+00	5.43E-02	17.41
0.524 sec	3.906	-8.10	-4.06	0.062	1.05E+00	5.90E-02	16.90
0.528 sec	3.931	-8.81	-3.92	0.061	1.06E+00	6.36E-02	16.36
0.532 sec	3.956	-9.51	-3.79	0.061	1.08E+00	6.81E-02	15.79
0.536 sec	3.982	-10.20	-3.69	0.061	1.09E+00	7.24E-02	15.17
0.54 sec	4.007	-10.88	-3.62	0.061	1.11E+00	7.67E-02	14.52
0.544 sec	4.032	-11.54	-3.57	0.061	1.12E+00	8.07E-02	13.84
0.548 sec	4.057	-12.20	-3.55	0.061	1.14E+00	8.46E-02	13.13
0.552 sec	4.083	-12.83	-3.55	0.061	1.15E+00	8.84E-02	12.39
0.556 sec	4.108	-13.45	-3.58	0.061	1.17E+00	9.20E-02	11.62

0.56 sec	4.133	-14.05	-3.64	0.061	1.19E+00	9.53E-02	10.82
0.564 sec	4.159	-14.62	-3.72	0.061	1.20E+00	9.85E-02	10.00
0.568 sec	4.184	-15.18	-3.83	0.061	1.22E+00	1.01E-01	9.16
0.572 sec	4.210	-15.70	-3.96	0.061	1.23E+00	1.04E-01	8.29
0.576 sec	4.235	-16.20	-4.12	0.061	1.25E+00	1.07E-01	7.41
0.58 sec	4.260	-16.67	-4.30	0.061	1.27E+00	1.09E-01	6.50
0.584 sec	4.286	-17.11	-4.50	0.060	1.28E+00	1.11E-01	5.58
0.588 sec	4.311	-17.52	-4.73	0.060	1.30E+00	1.13E-01	4.65
0.592 sec	4.336	-17.88	-4.97	0.060	1.32E+00	1.14E-01	3.70
0.596 sec	4.361	-18.21	-5.23	0.060	1.34E+00	1.15E-01	2.74
0.6 sec	4.387	-18.50	-5.50	0.060	1.35E+00	1.16E-01	1.77
0.604 sec	4.412	-18.74	-5.79	0.060	1.37E+00	1.17E-01	0.80
0.608 sec	4.437	-18.94	-6.09	0.060	1.39E+00	1.17E-01	-0.18
0.612 sec	4.462	-19.09	-6.39	0.060	1.41E+00	1.17E-01	-1.16
0.616 sec	4.487	-19.19	-6.70	0.060	1.43E+00	1.17E-01	-2.14
0.62 sec	4.511	-19.24	-7.00	0.060	1.44E+00	1.16E-01	-3.11
0.624 sec	4.536	-19.23	-7.31	0.060	1.46E+00	1.15E-01	-4.09
0.628 sec	4.561	-19.17	-7.61	0.060	1.48E+00	1.14E-01	-5.05
0.632 sec	4.585	-19.05	-7.90	0.060	1.50E+00	1.12E-01	-6.01
0.636 sec	4.609	-18.87	-8.17	0.059	1.52E+00	1.11E-01	-6.95
0.64 sec	4.634	-18.63	-8.43	0.059	1.53E+00	1.08E-01	-7.88
0.644 sec	4.657	-18.34	-8.67	0.059	1.55E+00	1.06E-01	-8.79
0.648 sec	4.681	-17.98	-8.88	0.059	1.57E+00	1.03E-01	-9.69
0.652 sec	4.705	-17.57	-9.07	0.059	1.59E+00	1.00E-01	-10.56
0.656 sec	4.728	-17.11	-9.22	0.059	1.61E+00	9.66E-02	-11.40
0.66 sec	4.752	-16.59	-9.35	0.059	1.63E+00	9.29E-02	-12.22
0.664 sec	4.775	-16.01	-9.44	0.059	1.65E+00	8.89E-02	-13.01
0.668 sec	4.798	-15.39	-9.49	0.059	1.66E+00	8.47E-02	-13.77
0.672 sec	4.821	-14.72	-9.51	0.059	1.68E+00	8.02E-02	-14.49

0.676 sec	4.843	-14.01	-9.50	0.059	1.70E+00	7.54E-02	-15.18
0.68 sec	4.866	-13.26	-9.44	0.059	1.72E+00	7.03E-02	-15.83
0.684 sec	4.888	-12.47	-9.35	0.059	1.74E+00	6.51E-02	-16.44
0.688 sec	4.910	-11.65	-9.22	0.059	1.76E+00	5.96E-02	-17.02
0.692 sec	4.932	-10.81	-9.06	0.059	1.78E+00	5.39E-02	-17.54
0.696 sec	4.954	-9.94	-8.87	0.058	1.80E+00	4.80E-02	-18.03
0.7 sec	4.976	-9.06	-8.64	0.058	1.81E+00	4.19E-02	-18.47
0.704 sec	4.997	-8.16	-8.40	0.058	1.83E+00	3.56E-02	-18.87
0.708 sec	5.019	-7.24	-8.12	0.058	1.85E+00	2.92E-02	-19.23
0.712 sec	5.040	-6.33	-7.83	0.058	1.87E+00	2.26E-02	-19.53
0.716 sec	5.061	-5.41	-7.52	0.058	1.89E+00	1.59E-02	-19.80
0.72 sec	5.082	-4.48	-7.20	0.058	1.91E+00	9.00E-03	-20.02
0.724 sec	5.103	-3.56	-6.87	0.058	1.93E+00	2.10E-03	-20.19
0.728 sec	5.124	-2.65	-6.53	0.058	1.95E+00	-4.90E-03	-20.32
0.732 sec	5.145	-1.74	-6.18	0.058	1.97E+00	-1.20E-02	-20.40
0.736 sec	5.166	-0.84	-5.84	0.058	1.99E+00	-1.91E-02	-20.44
0.74 sec	5.186	0.05	-5.50	0.058	2.01E+00	-2.63E-02	-20.44
0.744 sec	5.207	0.93	-5.16	0.058	2.03E+00	-3.36E-02	-20.40
0.748 sec	5.228	1.80	-4.83	0.058	2.04E+00	-4.08E-02	-20.32
0.752 sec	5.248	2.66	-4.51	0.058	2.06E+00	-4.80E-02	-20.19
0.756 sec	5.269	3.51	-4.20	0.058	2.08E+00	-5.53E-02	-20.03
0.76 sec	5.290	4.34	-3.90	0.058	2.10E+00	-6.25E-02	-19.83
0.764 sec	5.310	5.16	-3.62	0.057	2.12E+00	-6.96E-02	-19.59
0.768 sec	5.331	5.97	-3.36	0.057	2.14E+00	-7.68E-02	-19.32
0.772 sec	5.351	6.76	-3.11	0.057	2.16E+00	-8.38E-02	-19.02
0.776 sec	5.372	7.54	-2.88	0.057	2.18E+00	-9.08E-02	-18.68
0.78 sec	5.393	8.31	-2.67	0.057	2.20E+00	-9.77E-02	-18.30
0.784 sec	5.413	9.07	-2.48	0.057	2.23E+00	-1.04E-01	-17.90
0.788 sec	5.434	9.81	-2.31	0.057	2.25E+00	-1.11E-01	-17.46

0.792 sec	5.455	10.54	-2.16	0.057	2.27E+00	-1.18E-01	-17.00
0.796 sec	5.475	11.26	-2.04	0.057	2.29E+00	-1.24E-01	-16.51
0.8 sec	5.496	11.97	-1.94	0.057	2.31E+00	-1.30E-01	-15.99
0.804 sec	5.517	12.66	-1.86	0.057	2.33E+00	-1.36E-01	-15.44
0.808 sec	5.538	13.34	-1.80	0.057	2.35E+00	-1.42E-01	-14.87
0.812 sec	5.559	14.01	-1.77	0.057	2.37E+00	-1.48E-01	-14.27
0.816 sec	5.580	14.67	-1.76	0.057	2.39E+00	-1.53E-01	-13.65
0.82 sec	5.601	15.31	-1.78	0.057	2.42E+00	-1.59E-01	-13.00
0.824 sec	5.622	15.93	-1.82	0.057	2.44E+00	-1.64E-01	-12.34
0.828 sec	5.643	16.54	-1.88	0.056	2.46E+00	-1.69E-01	-11.65
0.832 sec	5.664	17.12	-1.97	0.056	2.48E+00	-1.73E-01	-10.95
0.836 sec	5.686	17.69	-2.08	0.056	2.50E+00	-1.78E-01	-10.22
0.84 sec	5.707	18.24	-2.21	0.056	2.53E+00	-1.82E-01	-9.48
0.844 sec	5.728	18.77	-2.37	0.056	2.55E+00	-1.86E-01	-8.72
0.848 sec	5.750	19.27	-2.55	0.056	2.57E+00	-1.89E-01	-7.94
0.852 sec	5.771	19.75	-2.75	0.056	2.59E+00	-1.92E-01	-7.15
0.856 sec	5.792	20.19	-2.97	0.056	2.62E+00	-1.95E-01	-6.35
0.86 sec	5.814	20.61	-3.21	0.056	2.64E+00	-1.98E-01	-5.53
0.864 sec	5.835	21.00	-3.47	0.056	2.66E+00	-2.00E-01	-4.71
0.868 sec	5.857	21.35	-3.74	0.056	2.69E+00	-2.02E-01	-3.87
0.872 sec	5.878	21.66	-4.03	0.056	2.71E+00	-2.04E-01	-3.03
0.876 sec	5.900	21.93	-4.34	0.056	2.73E+00	-2.05E-01	-2.17
0.88 sec	5.921	22.17	-4.65	0.056	2.76E+00	-2.06E-01	-1.32
0.884 sec	5.943	22.36	-4.97	0.056	2.78E+00	-2.06E-01	-0.45
0.888 sec	5.964	22.51	-5.30	0.056	2.81E+00	-2.07E-01	0.41
0.892 sec	5.986	22.61	-5.64	0.055	2.83E+00	-2.07E-01	1.28
0.896 sec	6.007	22.66	-5.97	0.055	2.85E+00	-2.06E-01	2.14
0.9 sec	6.028	22.67	-6.31	0.055	2.88E+00	-2.05E-01	3.00
0.904 sec	6.050	22.63	-6.64	0.055	2.90E+00	-2.04E-01	3.86

0.908 sec	6.071	22.53	-6.97	0.055	2.93E+00	-2.02E-01	4.71
0.912 sec	6.092	22.39	-7.28	0.055	2.95E+00	-2.00E-01	5.56
0.916 sec	6.113	22.19	-7.58	0.055	2.97E+00	-1.98E-01	6.40
0.92 sec	6.134	21.94	-7.87	0.055	3.00E+00	-1.95E-01	7.22
0.924 sec	6.155	21.65	-8.14	0.055	3.02E+00	-1.92E-01	8.04
0.928 sec	6.176	21.30	-8.39	0.055	3.05E+00	-1.89E-01	8.84
0.932 sec	6.197	20.91	-8.62	0.055	3.07E+00	-1.85E-01	9.63
0.936 sec	6.217	20.47	-8.83	0.055	3.10E+00	-1.81E-01	10.39
0.94 sec	6.238	19.98	-9.00	0.055	3.12E+00	-1.77E-01	11.14
0.944 sec	6.259	19.45	-9.15	0.055	3.15E+00	-1.72E-01	11.87
0.948 sec	6.279	18.87	-9.27	0.055	3.17E+00	-1.67E-01	12.58
0.952 sec	6.299	18.26	-9.36	0.055	3.19E+00	-1.61E-01	13.26
0.956 sec	6.319	17.60	-9.42	0.055	3.22E+00	-1.56E-01	13.92
0.96 sec	6.340	16.92	-9.44	0.054	3.24E+00	-1.49E-01	14.56
0.964 sec	6.359	16.19	-9.44	0.054	3.27E+00	-1.43E-01	15.17
0.968 sec	6.379	15.44	-9.40	0.054	3.29E+00	-1.36E-01	15.75
0.972 sec	6.399	14.66	-9.33	0.054	3.32E+00	-1.30E-01	16.30
0.976 sec	6.419	13.85	-9.22	0.054	3.34E+00	-1.22E-01	16.82
0.98 sec	6.438	13.01	-9.09	0.054	3.37E+00	-1.15E-01	17.31
0.984 sec	6.458	12.16	-8.92	0.054	3.39E+00	-1.07E-01	17.76
0.988 sec	6.477	11.28	-8.73	0.054	3.42E+00	-9.93E-02	18.19
0.992 sec	6.496	10.38	-8.51	0.054	3.44E+00	-9.12E-02	18.58
0.996 sec	6.515	9.47	-8.26	0.054	3.47E+00	-8.29E-02	18.93
1 sec	6.535	8.55	-7.99	0.054	3.49E+00	-7.44E-02	19.26

G.9 Exported data from Supersonic Simulation with no preload

Table 14: Data from supersonic simulation with no preload

Time	Body Velocity (m/s)	Ax (m/s^2)	Az (m/s^2)	Mach	Horizontal Displacement (m)	Vertical Displacement (m)	Attitude (degrees)
0 sec	0.00	21.92	-537.27	2.50	0.00E+00	0.00E+00	20.00
0.004 sec	1.99	2.91	-527.12	2.49	3.60E-03	1.30E-03	18.90
0.008 sec	3.99	-51.07	-509.01	2.48	1.48E-02	4.80E-03	15.74
0.012 sec	6.04	-131.19	-494.97	2.47	3.40E-02	9.40E-03	10.89
0.016 sec	8.12	-220.90	-496.99	2.46	6.18E-02	1.33E-02	4.85
0.02 sec	10.21	-296.38	-518.74	2.46	9.83E-02	1.43E-02	-1.72
0.024 sec	12.27	-332.18	-550.31	2.45	1.43E-01	1.04E-02	-8.15
0.028 sec	14.27	-310.83	-571.15	2.44	1.95E-01	3.29E-04	-13.70
0.032 sec	16.18	-230.06	-562.37	2.43	2.54E-01	-1.63E-02	-17.76
0.036 sec	18.02	-100.80	-520.06	2.42	3.19E-01	-3.85E-02	-19.88
0.04 sec	19.83	61.77	-458.09	2.41	3.90E-01	-6.45E-02	-19.90
0.044 sec	21.65	244.23	-400.04	2.41	4.68E-01	-9.16E-02	-17.90
0.048 sec	23.50	433.07	-369.17	2.40	5.55E-01	-1.17E-01	-14.14
0.052 sec	25.39	608.85	-381.22	2.39	6.50E-01	-1.37E-01	-9.02
0.056 sec	27.33	743.37	-437.96	2.38	7.55E-01	-1.48E-01	-3.01
0.06 sec	29.27	805.12	-522.21	2.37	8.68E-01	-1.48E-01	3.33
0.064 sec	31.20	772.11	-600.36	2.36	9.88E-01	-1.35E-01	9.36
0.068 sec	33.08	642.37	-636.20	2.36	1.11E+00	-1.08E-01	14.49
0.072 sec	34.89	432.26	-609.23	2.35	1.24E+00	-7.00E-02	18.19
0.076 sec	36.66	165.19	-524.64	2.34	1.38E+00	-2.28E-02	20.12
0.08 sec	38.39	-137.41	-410.83	2.33	1.52E+00	2.92E-02	20.09
0.084 sec	40.13	-455.90	-308.48	2.33	1.67E+00	8.12E-02	18.15
0.088 sec	41.89	-766.48	-256.36	2.32	1.83E+00	1.28E-01	14.48
0.092 sec	43.69	-1036.50	-277.68	2.31	1.99E+00	1.64E-01	9.45

0.096 sec	45.51	-1226.00	-370.11	2.30	2.17E+00	1.85E-01	3.51
0.1 sec	47.33	-1296.80	-503.13	2.30	2.35E+00	1.87E-01	-2.78
0.104 sec	49.12	-1224.90	-625.37	2.29	2.55E+00	1.68E-01	-8.84
0.108 sec	50.86	-1012.60	-683.85	2.28	2.74E+00	1.28E-01	-14.07
0.112 sec	52.53	-689.24	-649.32	2.27	2.94E+00	7.14E-02	-17.96
0.116 sec	54.14	-298.05	-531.94	2.27	3.14E+00	1.50E-03	-20.13
0.12 sec	55.72	121.87	-374.72	2.26	3.35E+00	-7.51E-02	-20.44
0.124 sec	57.30	542.86	-232.05	2.25	3.56E+00	-1.52E-01	-18.93
0.128 sec	58.90	942.74	-150.29	2.25	3.78E+00	-2.22E-01	-15.78
0.132 sec	60.54	1293.90	-157.05	2.24	4.01E+00	-2.79E-01	-11.28
0.136 sec	62.21	1557.90	-254.87	2.23	4.26E+00	-3.16E-01	-5.83
0.14 sec	63.91	1691.10	-416.85	2.22	4.51E+00	-3.30E-01	0.14
0.144 sec	65.60	1661.40	-589.75	2.22	4.77E+00	-3.16E-01	6.13
0.148 sec	67.27	1464.60	-710.91	2.21	5.03E+00	-2.76E-01	11.60
0.152 sec	68.89	1126.70	-733.83	2.20	5.29E+00	-2.11E-01	16.09
0.156 sec	70.46	689.51	-647.35	2.20	5.56E+00	-1.26E-01	19.19
0.16 sec	71.99	193.65	-478.35	2.19	5.83E+00	-2.83E-02	20.65
0.164 sec	73.50	-328.90	-280.49	2.18	6.10E+00	7.44E-02	20.36
0.168 sec	75.02	-850.22	-116.59	2.18	6.38E+00	1.74E-01	18.37
0.172 sec	76.56	-1337.20	-40.00	2.17	6.67E+00	2.62E-01	14.86
0.176 sec	78.12	-1746.60	-78.60	2.16	6.97E+00	3.30E-01	10.11
0.18 sec	79.71	-2028.40	-224.95	2.16	7.28E+00	3.72E-01	4.52
0.184 sec	81.30	-2136.50	-435.49	2.15	7.60E+00	3.82E-01	-1.47
0.188 sec	82.87	-2043.60	-640.85	2.14	7.93E+00	3.58E-01	-7.36
0.192 sec	84.40	-1753.80	-767.78	2.13	8.26E+00	3.01E-01	-12.66
0.196 sec	85.88	-1304.10	-767.99	2.13	8.59E+00	2.14E-01	-16.91
0.2 sec	87.30	-751.81	-639.65	2.12	8.92E+00	1.05E-01	-19.74
0.204 sec	88.69	-153.08	-426.83	2.12	9.25E+00	-1.75E-02	-20.95
0.208 sec	90.07	450.77	-197.96	2.11	9.58E+00	-1.45E-01	-20.49

0.212 sec	91.45	1031.70	-20.16	2.10	9.93E+00	-2.67E-01	-18.45
0.216 sec	92.85	1563.20	57.42	2.10	1.03E+01	-3.74E-01	-15.03
0.22 sec	94.29	2009.60	11.80	2.09	1.06E+01	-4.58E-01	-10.49
0.224 sec	95.76	2324.10	-148.63	2.09	1.10E+01	-5.12E-01	-5.16
0.228 sec	97.24	2458.80	-381.83	2.08	1.14E+01	-5.28E-01	0.57
0.232 sec	98.72	2384.00	-619.10	2.07	1.18E+01	-5.06E-01	6.28
0.236 sec	100.18	2102.70	-785.61	2.07	1.22E+01	-4.45E-01	11.54
0.24 sec	101.59	1650.60	-827.40	2.06	1.26E+01	-3.50E-01	15.93
0.244 sec	102.97	1079.80	-730.39	2.05	1.30E+01	-2.26E-01	19.12
0.248 sec	104.31	439.83	-522.80	2.05	1.34E+01	-8.40E-02	20.88
0.252 sec	105.63	-230.86	-263.79	2.04	1.38E+01	6.75E-02	21.08
0.256 sec	106.95	-901.69	-25.72	2.04	1.41E+01	2.17E-01	19.74
0.26 sec	108.28	-1539.90	124.73	2.03	1.46E+01	3.55E-01	16.95
0.264 sec	109.64	-2103.30	143.52	2.03	1.50E+01	4.69E-01	12.94
0.268 sec	111.02	-2540.00	21.51	2.02	1.54E+01	5.51E-01	7.98
0.272 sec	112.41	-2796.90	-211.24	2.01	1.59E+01	5.94E-01	2.44
0.276 sec	113.79	-2833.00	-490.58	2.01	1.63E+01	5.93E-01	-3.31
0.28 sec	115.16	-2632.80	-733.89	2.00	1.68E+01	5.46E-01	-8.84
0.284 sec	116.48	-2215.40	-864.99	2.00	1.72E+01	4.57E-01	-13.75
0.288 sec	117.77	-1631.00	-841.51	1.99	1.77E+01	3.31E-01	-17.65
0.292 sec	119.00	-944.67	-671.13	1.99	1.81E+01	1.77E-01	-20.27
0.296 sec	120.21	-215.88	-406.49	1.98	1.86E+01	6.50E-03	-21.42
0.3 sec	121.41	512.70	-122.86	1.97	1.90E+01	-1.70E-01	-21.09
0.304 sec	122.61	1212.40	106.49	1.97	1.95E+01	-3.39E-01	-19.32
0.308 sec	123.83	1857.20	226.34	1.96	1.99E+01	-4.91E-01	-16.28
0.312 sec	125.08	2412.90	207.40	1.96	2.04E+01	-6.15E-01	-12.18
0.316 sec	126.36	2833.50	51.04	1.95	2.09E+01	-7.02E-01	-7.29
0.32 sec	127.65	3068.50	-207.81	1.95	2.14E+01	-7.45E-01	-1.90
0.324 sec	128.94	3079.20	-504.17	1.94	2.19E+01	-7.39E-01	3.63

0.328 sec	130.23	2855.70	-758.03	1.94	2.25E+01	-6.84E-01	8.93
0.332 sec	131.49	2422.40	-898.59	1.93	2.30E+01	-5.82E-01	13.66
0.336 sec	132.71	1829.00	-886.97	1.93	2.35E+01	-4.40E-01	17.48
0.34 sec	133.90	1131.60	-726.62	1.92	2.40E+01	-2.68E-01	20.16
0.344 sec	135.07	378.06	-459.42	1.92	2.45E+01	-7.57E-02	21.51
0.348 sec	136.22	-396.09	-152.27	1.91	2.50E+01	1.25E-01	21.47
0.352 sec	137.37	-1161.70	119.62	1.91	2.55E+01	3.20E-01	20.04
0.356 sec	138.53	-1886.20	289.53	1.90	2.60E+01	5.00E-01	17.33
0.36 sec	139.71	-2527.50	314.12	1.90	2.66E+01	6.50E-01	13.52
0.364 sec	140.91	-3034.30	183.94	1.89	2.71E+01	7.62E-01	8.85
0.368 sec	142.13	-3353.40	-72.76	1.89	2.77E+01	8.27E-01	3.60
0.372 sec	143.34	-3442.20	-394.28	1.88	2.82E+01	8.38E-01	-1.89
0.376 sec	144.54	-3280.70	-698.42	1.87	2.88E+01	7.95E-01	-7.29
0.38 sec	145.71	-2880.60	-903.40	1.87	2.94E+01	6.98E-01	-12.24
0.384 sec	146.85	-2285.10	-952.48	1.86	2.99E+01	5.55E-01	-16.42
0.388 sec	147.95	-1556.70	-832.97	1.86	3.05E+01	3.74E-01	-19.55
0.392 sec	149.01	-759.31	-579.22	1.86	3.11E+01	1.66E-01	-21.44
0.396 sec	150.06	56.30	-258.33	1.85	3.16E+01	-5.53E-02	-21.99
0.4 sec	151.10	856.23	52.47	1.85	3.22E+01	-2.78E-01	-21.22
0.404 sec	152.15	1616.20	284.90	1.84	3.27E+01	-4.89E-01	-19.19
0.408 sec	153.22	2310.60	390.62	1.84	3.33E+01	-6.76E-01	-16.07
0.412 sec	154.32	2904.10	346.71	1.83	3.39E+01	-8.27E-01	-12.03
0.416 sec	155.43	3350.70	159.48	1.83	3.45E+01	-9.33E-01	-7.30
0.42 sec	156.56	3601.80	-133.55	1.82	3.52E+01	-9.87E-01	-2.14
0.424 sec	157.69	3620.90	-467.42	1.82	3.58E+01	-9.83E-01	3.16
0.428 sec	158.82	3398.00	-763.19	1.81	3.64E+01	-9.22E-01	8.29
0.432 sec	159.92	2955.00	-948.90	1.81	3.70E+01	-8.06E-01	12.95
0.436 sec	161.00	2338.90	-979.97	1.80	3.77E+01	-6.41E-01	16.87
0.44 sec	162.05	1605.10	-850.16	1.80	3.83E+01	-4.38E-01	19.81

0.444 sec	163.07	803.52	-590.46	1.79	3.89E+01	-2.07E-01	21.61
0.448 sec	164.08	-28.52	-259.10	1.79	3.95E+01	3.85E-02	22.17
0.452 sec	165.08	-862.97	72.13	1.79	4.01E+01	2.85E-01	21.48
0.456 sec	166.09	-1673.00	332.35	1.78	4.07E+01	5.20E-01	19.58
0.46 sec	167.11	-2425.10	465.14	1.78	4.14E+01	7.30E-01	16.58
0.464 sec	168.15	-3076.00	439.84	1.77	4.20E+01	9.03E-01	12.66
0.468 sec	169.20	-3575.50	258.58	1.77	4.27E+01	1.03E+00	8.03
0.472 sec	170.26	-3874.50	-42.56	1.76	4.33E+01	1.10E+00	2.95
0.476 sec	171.32	-3936.00	-399.13	1.76	4.40E+01	1.10E+00	-2.33
0.48 sec	172.37	-3745.20	-730.65	1.75	4.47E+01	1.05E+00	-7.49
0.484 sec	173.40	-3316.20	-959.07	1.75	4.54E+01	9.33E-01	-12.25
0.488 sec	174.39	-2690.90	-1029.50	1.75	4.61E+01	7.64E-01	-16.34
0.492 sec	175.35	-1928.80	-926.39	1.74	4.67E+01	5.50E-01	-19.52
0.496 sec	176.29	-1091.10	-676.80	1.74	4.74E+01	3.04E-01	-21.60
0.5 sec	177.20	-227.92	-340.23	1.73	4.80E+01	3.84E-02	-22.51
0.504 sec	178.11	626.20	10.14	1.73	4.87E+01	-2.32E-01	-22.21
0.508 sec	179.02	1448.10	304.87	1.73	4.94E+01	-4.95E-01	-20.75
0.512 sec	179.95	2216.80	489.54	1.72	5.00E+01	-7.36E-01	-18.25
0.516 sec	180.89	2904.80	530.62	1.72	5.07E+01	-9.44E-01	-14.83
0.52 sec	181.85	3474.00	418.89	1.71	5.14E+01	-1.11E+00	-10.67
0.524 sec	182.83	3879.30	172.28	1.71	5.22E+01	-1.21E+00	-5.97
0.528 sec	183.82	4077.30	-163.89	1.70	5.29E+01	-1.26E+00	-0.95
0.532 sec	184.82	4039.90	-522.61	1.70	5.36E+01	-1.24E+00	4.12
0.536 sec	185.80	3765.00	-828.68	1.70	5.44E+01	-1.16E+00	9.00
0.54 sec	186.76	3278.60	-1016.90	1.69	5.51E+01	-1.02E+00	13.43
0.544 sec	187.70	2626.90	-1048.20	1.69	5.58E+01	-8.20E-01	17.17
0.548 sec	188.62	1862.30	-917.80	1.68	5.65E+01	-5.80E-01	20.05
0.552 sec	189.51	1031.40	-653.63	1.68	5.72E+01	-3.08E-01	21.92
0.556 sec	190.39	169.23	-308.23	1.68	5.79E+01	-1.80E-02	22.69

0.56 sec	191.27	-698.71	52.40	1.67	5.86E+01	2.77E-01	22.33
0.564 sec	192.14	-1549.70	360.60	1.67	5.94E+01	5.62E-01	20.86
0.568 sec	193.03	-2356.40	558.23	1.66	6.01E+01	8.24E-01	18.37
0.572 sec	193.93	-3083.20	606.74	1.66	6.08E+01	1.05E+00	14.98
0.576 sec	194.84	-3685.90	494.34	1.66	6.16E+01	1.23E+00	10.86
0.58 sec	195.77	-4117.70	239.27	1.65	6.23E+01	1.35E+00	6.20
0.584 sec	196.70	-4337.00	-112.05	1.65	6.31E+01	1.40E+00	1.22
0.588 sec	197.63	-4316.90	-492.09	1.64	6.39E+01	1.39E+00	-3.84
0.592 sec	198.54	-4052.40	-824.52	1.64	6.47E+01	1.31E+00	-8.72
0.596 sec	199.43	-3564.30	-1040.30	1.64	6.55E+01	1.16E+00	-13.20
0.6 sec	200.30	-2896.10	-1094.50	1.63	6.63E+01	9.55E-01	-17.04
0.604 sec	201.13	-2103.60	-977.53	1.63	6.70E+01	7.02E-01	-20.04
0.608 sec	201.95	-1242.70	-716.75	1.63	6.78E+01	4.13E-01	-22.07
0.612 sec	202.75	-358.31	-367.09	1.62	6.85E+01	1.03E-01	-23.04
0.616 sec	203.54	518.59	4.16	1.62	6.93E+01	-2.14E-01	-22.92
0.62 sec	204.33	1367.40	331.70	1.62	7.00E+01	-5.25E-01	-21.76
0.624 sec	205.14	2170.60	562.03	1.61	7.08E+01	-8.16E-01	-19.62
0.628 sec	205.95	2905.90	658.68	1.61	7.16E+01	-1.07E+00	-16.62
0.632 sec	206.79	3542.40	605.32	1.61	7.24E+01	-1.29E+00	-12.90
0.636 sec	207.64	4040.60	408.24	1.60	7.32E+01	-1.44E+00	-8.60
0.64 sec	208.50	4358.80	97.79	1.60	7.40E+01	-1.54E+00	-3.92
0.644 sec	209.37	4462.60	-273.59	1.59	7.48E+01	-1.56E+00	0.94
0.648 sec	210.23	4335.60	-639.14	1.59	7.57E+01	-1.51E+00	5.78
0.652 sec	211.09	3986.10	-930.89	1.59	7.65E+01	-1.40E+00	10.36
0.656 sec	211.93	3444.90	-1094.60	1.58	7.73E+01	-1.22E+00	14.49
0.66 sec	212.75	2757.20	-1101.30	1.58	7.82E+01	-9.81E-01	17.98
0.664 sec	213.54	1970.60	-951.77	1.58	7.90E+01	-6.99E-01	20.67
0.668 sec	214.32	1126.20	-674.28	1.57	7.98E+01	-3.84E-01	22.44
0.672 sec	215.09	254.27	-317.33	1.57	8.05E+01	-4.87E-02	23.23

0.676 sec	215.85	-623.19	59.16	1.57	8.13E+01	2.92E-01	23.00
0.68 sec	216.62	-1487.30	393.25	1.56	8.21E+01	6.25E-01	21.78
0.684 sec	217.39	-2315.70	629.85	1.56	8.29E+01	9.36E-01	19.61
0.688 sec	218.17	-3078.90	728.96	1.56	8.38E+01	1.21E+00	16.60
0.692 sec	218.97	-3739.50	672.11	1.55	8.46E+01	1.44E+00	12.88
0.696 sec	219.77	-4255.20	466.04	1.55	8.55E+01	1.61E+00	8.60
0.7 sec	220.59	-4585.60	142.74	1.55	8.64E+01	1.71E+00	3.95
0.704 sec	221.40	-4698.90	-244.44	1.54	8.72E+01	1.74E+00	-0.89
0.708 sec	222.21	-4579.60	-628.71	1.54	8.81E+01	1.69E+00	-5.71
0.712 sec	223.00	-4232.80	-941.34	1.54	8.90E+01	1.57E+00	-10.31
0.716 sec	223.77	-3685.30	-1125.20	1.53	8.99E+01	1.39E+00	-14.47
0.72 sec	224.53	-2980.70	-1147.30	1.53	9.07E+01	1.14E+00	-18.02
0.724 sec	225.25	-2170.40	-1005.90	1.53	9.16E+01	8.42E-01	-20.79
0.728 sec	225.96	-1303.10	-729.78	1.52	9.24E+01	5.10E-01	-22.68
0.732 sec	226.66	-417.30	-370.02	1.52	9.33E+01	1.55E-01	-23.62
0.736 sec	227.35	460.81	12.62	1.52	9.41E+01	-2.08E-01	-23.58
0.74 sec	228.04	1313.90	358.85	1.51	9.49E+01	-5.66E-01	-22.59
0.744 sec	228.74	2127.40	618.77	1.51	9.58E+01	-9.04E-01	-20.72
0.748 sec	229.45	2883.70	756.32	1.51	9.66E+01	-1.21E+00	-18.05
0.752 sec	230.17	3557.30	751.83	1.50	9.75E+01	-1.47E+00	-14.68
0.756 sec	230.91	4115.30	604.13	1.50	9.84E+01	-1.68E+00	-10.75
0.76 sec	231.66	4520.00	332.23	1.50	9.93E+01	-1.82E+00	-6.40
0.764 sec	232.42	4736.30	-24.92	1.49	1.00E+02	-1.89E+00	-1.80
0.768 sec	233.18	4740.50	-412.38	1.49	1.01E+02	-1.88E+00	2.89
0.772 sec	233.93	4527.40	-767.71	1.49	1.02E+02	-1.80E+00	7.47
0.776 sec	234.68	4113.00	-1032.70	1.48	1.03E+02	-1.65E+00	11.77
0.78 sec	235.41	3530.40	-1164.50	1.48	1.04E+02	-1.42E+00	15.61
0.784 sec	236.12	2821.90	-1143.60	1.48	1.05E+02	-1.15E+00	18.84
0.788 sec	236.82	2029.40	-975.54	1.48	1.06E+02	-8.21E-01	21.34

0.792 sec	237.50	1187.90	-688.00	1.47	1.07E+02	-4.61E-01	23.01
0.796 sec	238.17	323.26	-325.15	1.47	1.07E+02	-8.16E-02	23.79
0.8 sec	238.83	-546.46	59.57	1.47	1.08E+02	3.05E-01	23.66
0.804 sec	239.50	-1405.80	410.64	1.46	1.09E+02	6.85E-01	22.63
0.808 sec	240.17	-2236.90	677.41	1.46	1.10E+02	1.04E+00	20.74
0.812 sec	240.85	-3015.90	820.62	1.46	1.11E+02	1.37E+00	18.07
0.816 sec	241.54	-3711.90	817.87	1.45	1.12E+02	1.65E+00	14.72
0.82 sec	242.24	-4288.30	667.24	1.45	1.13E+02	1.87E+00	10.81
0.824 sec	242.95	-4707.70	388.42	1.45	1.14E+02	2.02E+00	6.49
0.828 sec	243.66	-4937.60	20.92	1.45	1.15E+02	2.10E+00	1.91
0.832 sec	244.38	-4955.70	-380.72	1.44	1.16E+02	2.10E+00	-2.75
0.836 sec	245.08	-4755.90	-754.64	1.44	1.17E+02	2.02E+00	-7.33
0.84 sec	245.77	-4350.00	-1041.60	1.44	1.18E+02	1.86E+00	-11.65
0.844 sec	246.44	-3767.10	-1195.60	1.43	1.19E+02	1.63E+00	-15.54
0.848 sec	247.10	-3048.70	-1193.10	1.43	1.20E+02	1.35E+00	-18.85
0.852 sec	247.73	-2240.20	-1037.00	1.43	1.21E+02	1.01E+00	-21.45
0.856 sec	248.35	-1383.70	-755.27	1.43	1.22E+02	6.33E-01	-23.25
0.86 sec	248.96	-511.71	-393.60	1.42	1.22E+02	2.34E-01	-24.20
0.864 sec	249.56	353.37	-5.87	1.42	1.23E+02	-1.75E-01	-24.26
0.868 sec	250.16	1197.10	354.80	1.42	1.24E+02	-5.79E-01	-23.48
0.872 sec	250.76	2007.80	642.41	1.41	1.25E+02	-9.66E-01	-21.87
0.876 sec	251.38	2771.60	821.86	1.41	1.26E+02	-1.32E+00	-19.53
0.88 sec	252.01	3469.00	871.07	1.41	1.27E+02	-1.64E+00	-16.53
0.884 sec	252.65	4073.20	782.74	1.41	1.28E+02	-1.90E+00	-12.97
0.888 sec	253.30	4552.00	565.91	1.40	1.29E+02	-2.09E+00	-8.97
0.892 sec	253.96	4872.10	246.69	1.40	1.30E+02	-2.22E+00	-4.66
0.896 sec	254.63	5006.30	-133.24	1.40	1.31E+02	-2.26E+00	-0.19
0.9 sec	255.29	4939.40	-521.32	1.40	1.32E+02	-2.23E+00	4.30
0.904 sec	255.95	4673.30	-862.03	1.39	1.33E+02	-2.12E+00	8.65

0.908 sec	256.60	4226.90	-1106.40	1.39	1.34E+02	-1.93E+00	12.71
0.912 sec	257.24	3632.30	-1220.20	1.39	1.35E+02	-1.67E+00	16.33
0.916 sec	257.86	2927.40	-1189.10	1.38	1.36E+02	-1.36E+00	19.40
0.92 sec	258.47	2148.80	-1019.90	1.38	1.37E+02	-9.92E-01	21.80
0.924 sec	259.06	1326.70	-737.06	1.38	1.38E+02	-5.92E-01	23.46
0.928 sec	259.65	483.30	-379.02	1.38	1.39E+02	-1.70E-01	24.33
0.932 sec	260.23	-366.06	7.83	1.37	1.40E+02	2.62E-01	24.38
0.936 sec	260.81	-1209.00	374.46	1.37	1.41E+02	6.89E-01	23.61
0.94 sec	261.39	-2031.80	674.59	1.37	1.42E+02	1.10E+00	22.05
0.944 sec	261.98	-2816.60	869.79	1.37	1.43E+02	1.48E+00	19.76
0.948 sec	262.58	-3538.80	934.07	1.36	1.44E+02	1.81E+00	16.82
0.952 sec	263.19	-4168.60	857.36	1.36	1.45E+02	2.09E+00	13.32
0.956 sec	263.81	-4672.80	647.33	1.36	1.46E+02	2.31E+00	9.38
0.96 sec	264.43	-5019.70	329.20	1.36	1.47E+02	2.45E+00	5.12
0.964 sec	265.06	-5183.40	-56.60	1.35	1.48E+02	2.51E+00	0.68
0.968 sec	265.68	-5148.40	-459.09	1.35	1.49E+02	2.49E+00	-3.80
0.972 sec	266.29	-4913.40	-823.33	1.35	1.50E+02	2.38E+00	-8.17
0.976 sec	266.90	-4492.10	-1098.50	1.35	1.51E+02	2.20E+00	-12.28
0.98 sec	267.48	-3911.90	-1246.00	1.34	1.52E+02	1.95E+00	-16.00
0.984 sec	268.06	-3209.70	-1246.20	1.34	1.53E+02	1.63E+00	-19.19
0.988 sec	268.61	-2425.50	-1101.80	1.34	1.54E+02	1.26E+00	-21.75
0.992 sec	269.15	-1595.60	-835.70	1.34	1.55E+02	8.45E-01	-23.60
0.996 sec	269.68	-749.23	-486.52	1.33	1.56E+02	4.06E-01	-24.69
1 sec	270.21	93.78	-100.73	1.33	1.57E+02	-4.62E-02	-24.98

G.10 Data and graphs from supersonic simulation with -10% preload

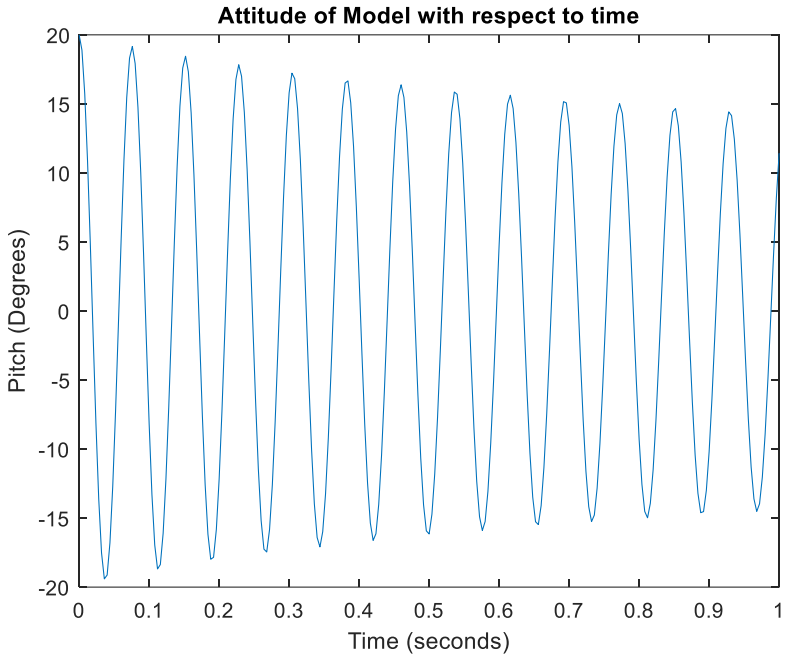

Figure 95: Attitude of model for -10% preload case

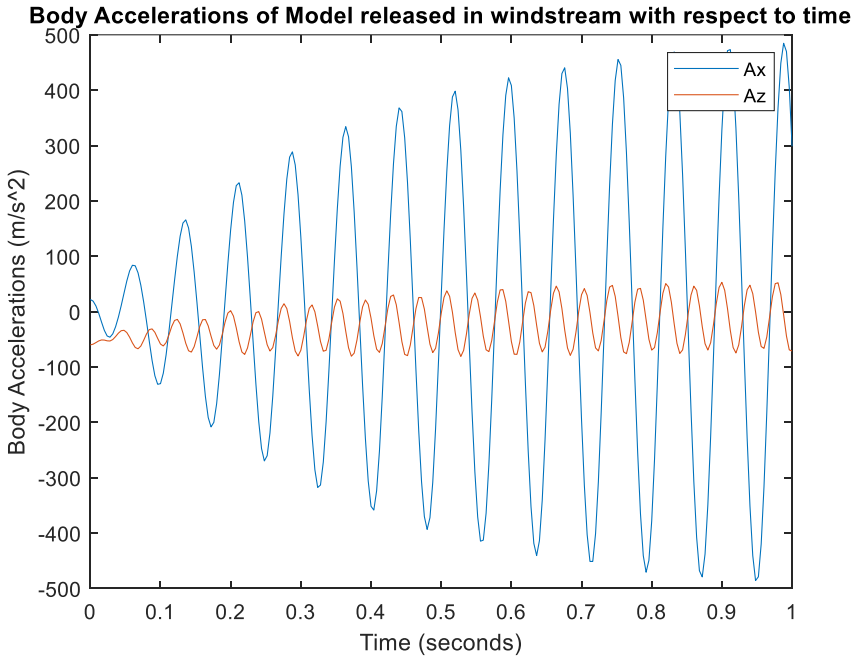

Figure 96: Accelerations of model for -10% preload case

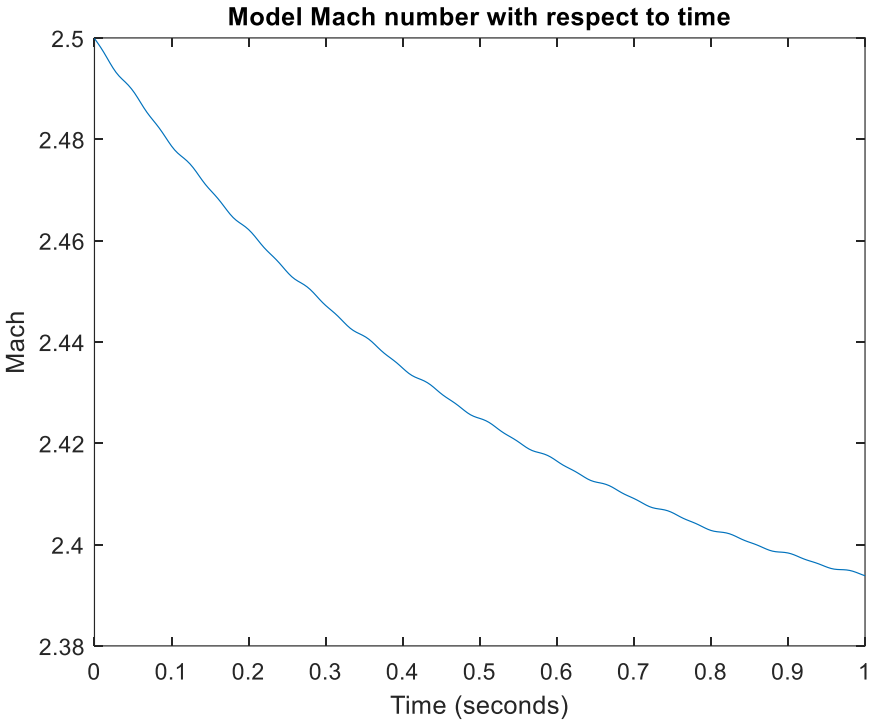

Figure 97: Mach for -10% preload case

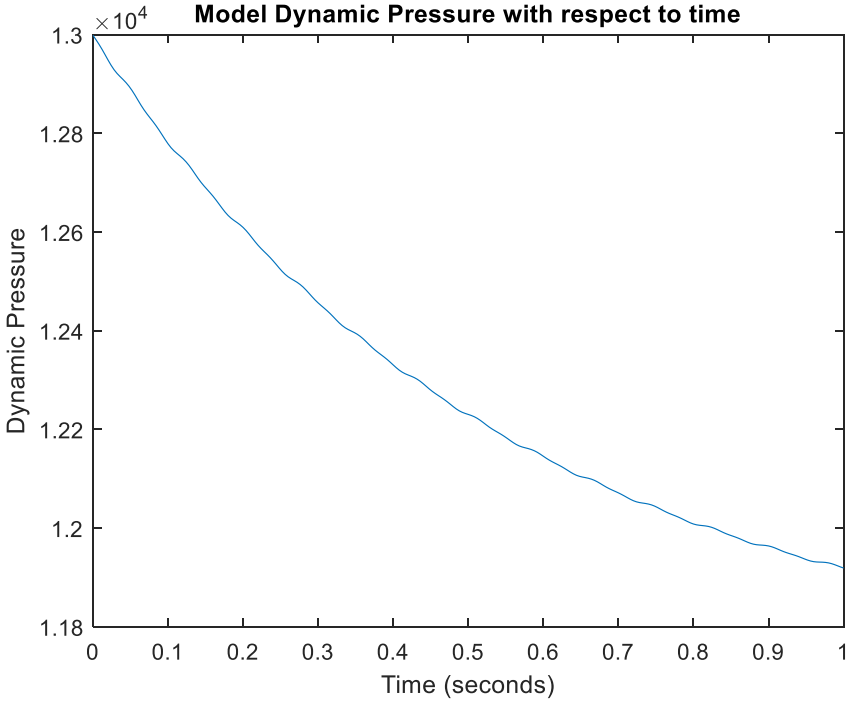

Figure 98: Dynamic pressure for -10% preload case

Table 15: Data from supersonic simulation with -10% preload

Time	Body Velocity (m/s)	Ax (m/s^2)	Az (m/s^2)	Mach	Horizontal Displacement (m)	Vertical Displacement (m)	Attitude (degrees)
0 sec	0.00	21.92	-10.96	2.50	0.00E+00	0.00E+00	20.00
0.004 sec	0.01	20.61	-10.51	2.50	-8.02E-05	-2.78E-05	18.89
0.008 sec	0.03	16.68	-9.23	2.50	-2.23E-04	-7.23E-05	15.73
0.012 sec	0.07	10.27	-7.29	2.50	-3.17E-04	-1.03E-04	10.86
0.016 sec	0.12	1.98	-5.10	2.50	-2.22E-04	-1.13E-04	4.81
0.02 sec	0.17	-6.87	-3.11	2.50	1.77E-04	-1.39E-04	-1.77
0.024 sec	0.22	-14.56	-1.43	2.50	9.06E-04	-2.40E-04	-8.16
0.028 sec	0.24	-19.68	0.19	2.50	1.90E-03	-4.54E-04	-13.62
0.032 sec	0.23	-21.90	1.83	2.50	2.90E-03	-7.52E-04	-17.50
0.036 sec	0.19	-21.81	3.08	2.50	3.80E-03	-1.00E-03	-19.36
0.04 sec	0.15	-20.01	3.41	2.50	4.40E-03	-1.30E-03	-19.05
0.044 sec	0.12	-16.62	2.73	2.50	4.70E-03	-1.40E-03	-16.68
0.048 sec	0.11	-11.51	1.27	2.50	4.90E-03	-1.40E-03	-12.57
0.052 sec	0.12	-4.66	-0.73	2.50	5.10E-03	-1.40E-03	-7.14
0.056 sec	0.16	3.43	-3.17	2.50	5.40E-03	-1.40E-03	-0.95
0.06 sec	0.21	11.52	-5.91	2.50	6.10E-03	-1.40E-03	5.35
0.064 sec	0.27	18.00	-8.46	2.50	7.10E-03	-1.20E-03	11.06
0.068 sec	0.30	21.72	-10.13	2.50	8.30E-03	-8.93E-04	15.55
0.072 sec	0.33	22.44	-10.55	2.50	9.60E-03	-4.88E-04	18.30
0.076 sec	0.34	20.41	-9.84	2.50	1.09E-02	-5.61E-05	19.03
0.08 sec	0.35	15.95	-8.41	2.50	1.20E-02	3.43E-04	17.68
0.084 sec	0.37	9.32	-6.64	2.50	1.32E-02	6.80E-04	14.40
0.088 sec	0.40	0.99	-4.93	2.50	1.45E-02	9.37E-04	9.55
0.092 sec	0.45	-8.09	-3.58	2.50	1.59E-02	1.10E-03	3.67
0.096 sec	0.50	-16.41	-2.68	2.50	1.77E-02	1.10E-03	-2.62
0.1 sec	0.53	-22.34	-1.83	2.50	1.97E-02	8.37E-04	-8.63

0.104 sec	0.54	-24.91	-0.50	2.50	2.19E-02	3.78E-04	-13.66
0.108 sec	0.53	-24.26	1.40	2.50	2.41E-02	-2.37E-04	-17.11
0.112 sec	0.49	-21.29	3.25	2.50	2.61E-02	-8.88E-04	-18.60
0.116 sec	0.46	-16.75	4.27	2.50	2.78E-02	-1.50E-03	-18.03
0.12 sec	0.43	-10.90	4.06	2.50	2.93E-02	-1.90E-03	-15.52
0.124 sec	0.42	-3.83	2.63	2.50	3.07E-02	-2.30E-03	-11.38
0.128 sec	0.43	4.20	0.19	2.50	3.22E-02	-2.50E-03	-6.04
0.132 sec	0.47	12.40	-2.99	2.50	3.38E-02	-2.50E-03	-0.07
0.136 sec	0.52	19.43	-6.37	2.50	3.57E-02	-2.40E-03	5.93
0.14 sec	0.56	23.89	-9.14	2.50	3.79E-02	-2.00E-03	11.27
0.144 sec	0.59	25.07	-10.49	2.50	4.02E-02	-1.50E-03	15.37
0.148 sec	0.61	23.09	-10.20	2.50	4.26E-02	-7.49E-04	17.75
0.152 sec	0.62	18.42	-8.68	2.50	4.50E-02	1.95E-05	18.18
0.156 sec	0.64	11.54	-6.60	2.50	4.72E-02	7.42E-04	16.61
0.16 sec	0.66	2.94	-4.64	2.50	4.95E-02	1.40E-03	13.24
0.164 sec	0.69	-6.67	-3.24	2.50	5.19E-02	1.80E-03	8.43
0.168 sec	0.73	-16.07	-2.60	2.50	5.45E-02	2.00E-03	2.70
0.172 sec	0.77	-23.66	-2.47	2.50	5.74E-02	2.00E-03	-3.33
0.176 sec	0.80	-27.97	-2.13	2.50	6.05E-02	1.60E-03	-9.01
0.18 sec	0.81	-28.39	-0.88	2.50	6.38E-02	9.63E-04	-13.66
0.184 sec	0.79	-25.42	1.30	2.50	6.69E-02	8.68E-05	-16.74
0.188 sec	0.75	-20.18	3.60	2.50	6.99E-02	-8.49E-04	-17.92
0.192 sec	0.71	-13.52	5.05	2.50	7.26E-02	-1.70E-03	-17.13
0.196 sec	0.69	-5.82	5.07	2.50	7.52E-02	-2.40E-03	-14.50
0.2 sec	0.68	2.65	3.56	2.50	7.76E-02	-3.00E-03	-10.35
0.204 sec	0.70	11.40	0.71	2.50	8.01E-02	-3.30E-03	-5.11
0.208 sec	0.73	19.42	-3.01	2.50	8.28E-02	-3.40E-03	0.69
0.212 sec	0.77	25.36	-6.79	2.50	8.58E-02	-3.20E-03	6.41
0.216 sec	0.81	28.05	-9.57	2.50	8.89E-02	-2.60E-03	11.43

0.22 sec	0.84	27.12	-10.56	2.50	9.23E-02	-1.80E-03	15.18
0.224 sec	0.86	22.96	-9.67	2.50	9.56E-02	-8.61E-04	17.25
0.228 sec	0.87	16.20	-7.55	2.50	9.89E-02	1.72E-04	17.41
0.232 sec	0.88	7.46	-5.09	2.50	1.02E-01	1.10E-03	15.68
0.236 sec	0.90	-2.59	-3.09	2.50	1.05E-01	2.00E-03	12.24
0.24 sec	0.93	-13.00	-2.03	2.50	1.09E-01	2.50E-03	7.47
0.244 sec	0.97	-22.40	-1.97	2.50	1.12E-01	2.80E-03	1.88
0.248 sec	1.00	-29.16	-2.37	2.50	1.16E-01	2.70E-03	-3.93
0.252 sec	1.03	-32.01	-2.31	2.50	1.20E-01	2.20E-03	-9.31
0.256 sec	1.03	-30.62	-1.03	2.50	1.24E-01	1.40E-03	-13.63
0.26 sec	1.01	-25.78	1.39	2.50	1.28E-01	2.77E-04	-16.39
0.264 sec	0.97	-18.75	4.02	2.50	1.32E-01	-8.85E-04	-17.31
0.268 sec	0.94	-10.43	5.73	2.50	1.36E-01	-2.00E-03	-16.33
0.272 sec	0.91	-1.33	5.83	2.50	1.39E-01	-2.90E-03	-13.60
0.276 sec	0.91	8.13	4.16	2.50	1.42E-01	-3.60E-03	-9.44
0.28 sec	0.92	17.26	0.95	2.50	1.46E-01	-4.00E-03	-4.29
0.284 sec	0.95	24.92	-3.16	2.50	1.50E-01	-4.00E-03	1.33
0.288 sec	0.99	29.80	-7.14	2.50	1.53E-01	-3.70E-03	6.81
0.292 sec	1.03	30.94	-9.82	2.50	1.57E-01	-3.10E-03	11.54
0.296 sec	1.05	28.25	-10.43	2.50	1.62E-01	-2.10E-03	14.99
0.3 sec	1.07	22.32	-9.05	2.50	1.66E-01	-8.71E-04	16.78
0.304 sec	1.07	13.90	-6.50	2.50	1.70E-01	3.68E-04	16.72
0.308 sec	1.09	3.74	-3.82	2.50	1.74E-01	1.50E-03	14.84
0.312 sec	1.11	-7.34	-1.89	2.50	1.78E-01	2.50E-03	11.35
0.316 sec	1.14	-18.23	-1.17	2.50	1.82E-01	3.10E-03	6.62
0.32 sec	1.17	-27.43	-1.56	2.49	1.86E-01	3.40E-03	1.16
0.324 sec	1.20	-33.34	-2.33	2.49	1.91E-01	3.30E-03	-4.44
0.328 sec	1.22	-34.86	-2.41	2.49	1.96E-01	2.70E-03	-9.55
0.332 sec	1.22	-31.95	-1.03	2.49	2.01E-01	1.60E-03	-13.58

0.336 sec	1.19	-25.60	1.61	2.49	2.06E-01	3.74E-04	-16.07
0.34 sec	1.16	-17.13	4.46	2.49	2.10E-01	-9.67E-04	-16.75
0.344 sec	1.12	-7.52	6.30	2.50	2.14E-01	-2.20E-03	-15.61
0.348 sec	1.10	2.62	6.39	2.50	2.19E-01	-3.30E-03	-12.80
0.352 sec	1.10	12.76	4.52	2.50	2.23E-01	-4.10E-03	-8.64
0.356 sec	1.11	22.03	1.01	2.50	2.27E-01	-4.50E-03	-3.57
0.36 sec	1.14	29.23	-3.37	2.50	2.31E-01	-4.50E-03	1.89
0.364 sec	1.18	33.10	-7.42	2.49	2.36E-01	-4.10E-03	7.14
0.368 sec	1.21	32.89	-9.92	2.49	2.41E-01	-3.30E-03	11.61
0.372 sec	1.23	28.73	-10.17	2.49	2.45E-01	-2.20E-03	14.80
0.376 sec	1.24	21.35	-8.40	2.49	2.50E-01	-8.15E-04	16.35
0.38 sec	1.25	11.62	-5.54	2.49	2.55E-01	5.85E-04	16.10
0.384 sec	1.26	0.38	-2.76	2.49	2.60E-01	1.90E-03	14.09
0.388 sec	1.28	-11.43	-0.96	2.49	2.65E-01	2.90E-03	10.55
0.392 sec	1.31	-22.55	-0.56	2.49	2.69E-01	3.60E-03	5.86
0.396 sec	1.34	-31.41	-1.31	2.49	2.75E-01	3.90E-03	0.53
0.4 sec	1.37	-36.48	-2.31	2.49	2.80E-01	3.70E-03	-4.88
0.404 sec	1.38	-36.83	-2.43	2.49	2.85E-01	3.00E-03	-9.75
0.408 sec	1.38	-32.63	-0.92	2.49	2.91E-01	1.80E-03	-13.52
0.412 sec	1.35	-25.04	1.90	2.49	2.96E-01	4.06E-04	-15.76
0.416 sec	1.32	-15.43	4.88	2.49	3.01E-01	-1.10E-03	-16.24
0.42 sec	1.28	-4.83	6.77	2.49	3.06E-01	-2.50E-03	-14.96
0.424 sec	1.26	6.09	6.78	2.49	3.11E-01	-3.60E-03	-12.08
0.428 sec	1.26	16.66	4.71	2.49	3.16E-01	-4.50E-03	-7.93
0.432 sec	1.27	25.92	0.95	2.49	3.21E-01	-4.90E-03	-2.93
0.436 sec	1.30	32.60	-3.60	2.49	3.26E-01	-4.90E-03	2.38
0.44 sec	1.34	35.52	-7.64	2.49	3.31E-01	-4.40E-03	7.43
0.444 sec	1.37	34.13	-9.92	2.49	3.36E-01	-3.50E-03	11.67
0.448 sec	1.38	28.74	-9.84	2.49	3.42E-01	-2.20E-03	14.61

0.452 sec	1.40	20.18	-7.74	2.49	3.47E-01	-7.14E-04	15.94
0.456 sec	1.40	9.41	-4.69	2.49	3.53E-01	8.10E-04	15.52
0.46 sec	1.41	-2.65	-1.88	2.49	3.58E-01	2.20E-03	13.41
0.464 sec	1.43	-14.95	-0.25	2.49	3.63E-01	3.30E-03	9.84
0.468 sec	1.46	-26.12	-0.13	2.49	3.69E-01	4.10E-03	5.19
0.472 sec	1.49	-34.57	-1.15	2.49	3.75E-01	4.30E-03	-0.03
0.476 sec	1.51	-38.82	-2.30	2.49	3.81E-01	4.00E-03	-5.27
0.48 sec	1.52	-38.12	-2.39	2.49	3.87E-01	3.20E-03	-9.92
0.484 sec	1.51	-32.84	-0.75	2.49	3.93E-01	1.90E-03	-13.45
0.488 sec	1.49	-24.23	2.21	2.49	3.99E-01	3.91E-04	-15.47
0.492 sec	1.45	-13.72	5.27	2.49	4.04E-01	-1.20E-03	-15.77
0.496 sec	1.42	-2.35	7.14	2.49	4.10E-01	-2.70E-03	-14.36
0.5 sec	1.40	9.14	7.03	2.49	4.15E-01	-3.90E-03	-11.43
0.504 sec	1.40	19.96	4.77	2.49	4.20E-01	-4.80E-03	-7.28
0.508 sec	1.41	29.08	0.81	2.49	4.26E-01	-5.20E-03	-2.36
0.512 sec	1.44	35.21	-3.84	2.49	4.31E-01	-5.20E-03	2.81
0.516 sec	1.47	37.26	-7.81	2.49	4.37E-01	-4.60E-03	7.68
0.52 sec	1.50	34.85	-9.85	2.49	4.43E-01	-3.60E-03	11.70
0.524 sec	1.52	28.42	-9.46	2.49	4.49E-01	-2.20E-03	14.43
0.528 sec	1.52	18.90	-7.11	2.49	4.55E-01	-5.84E-04	15.57
0.532 sec	1.53	7.31	-3.93	2.49	4.61E-01	1.00E-03	14.99
0.536 sec	1.54	-5.37	-1.16	2.49	4.67E-01	2.50E-03	12.79
0.54 sec	1.56	-17.97	0.29	2.49	4.73E-01	3.70E-03	9.19
0.544 sec	1.59	-29.07	0.16	2.49	4.79E-01	4.40E-03	4.58
0.548 sec	1.61	-37.05	-1.06	2.49	4.85E-01	4.60E-03	-0.54
0.552 sec	1.64	-40.53	-2.29	2.49	4.91E-01	4.20E-03	-5.60
0.556 sec	1.64	-38.90	-2.30	2.49	4.98E-01	3.30E-03	-10.06
0.56 sec	1.63	-32.70	-0.52	2.49	5.04E-01	2.00E-03	-13.38
0.564 sec	1.60	-23.27	2.54	2.49	5.11E-01	3.45E-04	-15.20

0.568 sec	1.57	-12.03	5.63	2.49	5.17E-01	-1.30E-03	-15.34
0.572 sec	1.54	-0.08	7.43	2.49	5.23E-01	-2.90E-03	-13.82
0.576 sec	1.52	11.80	7.18	2.49	5.29E-01	-4.20E-03	-10.83
0.58 sec	1.52	22.75	4.74	2.49	5.34E-01	-5.10E-03	-6.70
0.584 sec	1.53	31.65	0.62	2.49	5.40E-01	-5.50E-03	-1.85
0.588 sec	1.56	37.22	-4.07	2.49	5.46E-01	-5.40E-03	3.20
0.592 sec	1.59	38.47	-7.92	2.49	5.53E-01	-4.70E-03	7.89
0.596 sec	1.61	35.16	-9.72	2.49	5.59E-01	-3.60E-03	11.72
0.6 sec	1.63	27.86	-9.06	2.49	5.65E-01	-2.10E-03	14.25
0.604 sec	1.64	17.56	-6.51	2.49	5.72E-01	-4.36E-04	15.21
0.608 sec	1.64	5.32	-3.26	2.49	5.78E-01	1.30E-03	14.51
0.612 sec	1.65	-7.80	-0.57	2.49	5.84E-01	2.80E-03	12.21
0.616 sec	1.67	-20.57	0.70	2.49	5.91E-01	3.90E-03	8.59
0.62 sec	1.70	-31.50	0.36	2.49	5.97E-01	4.70E-03	4.03
0.624 sec	1.72	-38.99	-1.02	2.49	6.04E-01	4.80E-03	-0.99
0.628 sec	1.74	-41.74	-2.27	2.49	6.11E-01	4.40E-03	-5.91
0.632 sec	1.74	-39.29	-2.18	2.49	6.18E-01	3.40E-03	-10.18
0.636 sec	1.73	-32.31	-0.28	2.49	6.25E-01	2.00E-03	-13.31
0.64 sec	1.70	-22.20	2.87	2.49	6.31E-01	2.77E-04	-14.95
0.644 sec	1.67	-10.40	5.94	2.49	6.38E-01	-1.50E-03	-14.94
0.648 sec	1.64	2.00	7.65	2.49	6.44E-01	-3.10E-03	-13.32
0.652 sec	1.62	14.14	7.25	2.49	6.50E-01	-4.40E-03	-10.28
0.656 sec	1.62	25.11	4.63	2.49	6.57E-01	-5.30E-03	-6.16
0.66 sec	1.63	33.73	0.40	2.49	6.63E-01	-5.70E-03	-1.38
0.664 sec	1.66	38.74	-4.29	2.49	6.69E-01	-5.50E-03	3.55
0.668 sec	1.69	39.26	-8.00	2.49	6.76E-01	-4.80E-03	8.09
0.672 sec	1.71	35.17	-9.56	2.49	6.83E-01	-3.60E-03	11.73
0.676 sec	1.72	27.13	-8.66	2.49	6.90E-01	-2.00E-03	14.09
0.68 sec	1.73	16.19	-5.95	2.49	6.96E-01	-2.78E-04	14.88

0.684 sec	1.74	3.45	-2.67	2.49	7.03E-01	1.50E-03	14.05
0.688 sec	1.75	-9.97	-0.08	2.49	7.10E-01	3.00E-03	11.68
0.692 sec	1.77	-22.80	1.01	2.49	7.16E-01	4.20E-03	8.04
0.696 sec	1.79	-33.50	0.48	2.49	7.23E-01	4.90E-03	3.52
0.7 sec	1.81	-40.49	-1.00	2.49	7.30E-01	5.00E-03	-1.40
0.704 sec	1.83	-42.56	-2.23	2.49	7.38E-01	4.50E-03	-6.18
0.708 sec	1.83	-39.38	-2.04	2.49	7.45E-01	3.50E-03	-10.28
0.712 sec	1.81	-31.74	-0.01	2.49	7.52E-01	2.00E-03	-13.23
0.716 sec	1.78	-21.07	3.18	2.49	7.59E-01	1.94E-04	-14.70
0.72 sec	1.75	-8.83	6.22	2.49	7.66E-01	-1.60E-03	-14.56
0.724 sec	1.72	3.89	7.81	2.49	7.73E-01	-3.20E-03	-12.85
0.728 sec	1.71	16.20	7.24	2.49	7.79E-01	-4.50E-03	-9.77
0.732 sec	1.71	27.10	4.48	2.49	7.86E-01	-5.40E-03	-5.66
0.736 sec	1.72	35.40	0.16	2.49	7.93E-01	-5.80E-03	-0.95
0.74 sec	1.74	39.88	-4.50	2.49	7.99E-01	-5.60E-03	3.86
0.744 sec	1.77	39.73	-8.04	2.49	8.06E-01	-4.80E-03	8.26
0.748 sec	1.79	34.96	-9.36	2.49	8.13E-01	-3.60E-03	11.74
0.752 sec	1.80	26.29	-8.25	2.49	8.21E-01	-1.90E-03	13.92
0.756 sec	1.81	14.83	-5.42	2.49	8.28E-01	-1.14E-04	14.57
0.76 sec	1.82	1.71	-2.15	2.49	8.34E-01	1.70E-03	13.63
0.764 sec	1.83	-11.92	0.32	2.49	8.41E-01	3.20E-03	11.19
0.768 sec	1.85	-24.73	1.23	2.49	8.49E-01	4.40E-03	7.54
0.772 sec	1.87	-35.15	0.55	2.49	8.56E-01	5.10E-03	3.05
0.776 sec	1.89	-41.63	-1.01	2.49	8.63E-01	5.20E-03	-1.78
0.78 sec	1.90	-43.06	-2.19	2.49	8.71E-01	4.60E-03	-6.43
0.784 sec	1.90	-39.24	-1.88	2.49	8.78E-01	3.50E-03	-10.37
0.788 sec	1.89	-31.03	0.26	2.49	8.86E-01	1.90E-03	-13.15
0.792 sec	1.86	-19.91	3.48	2.49	8.93E-01	1.02E-04	-14.47
0.796 sec	1.82	-7.33	6.45	2.49	9.00E-01	-1.70E-03	-14.21

0.8 sec	1.80	5.62	7.92	2.49	9.07E-01	-3.40E-03	-12.41
0.804 sec	1.78	18.00	7.19	2.49	9.14E-01	-4.70E-03	-9.30
0.808 sec	1.78	28.79	4.29	2.49	9.21E-01	-5.60E-03	-5.20
0.812 sec	1.79	36.75	-0.09	2.49	9.28E-01	-5.90E-03	-0.55
0.816 sec	1.82	40.70	-4.69	2.49	9.35E-01	-5.60E-03	4.15
0.82 sec	1.84	39.94	-8.06	2.49	9.42E-01	-4.80E-03	8.41
0.824 sec	1.86	34.57	-9.16	2.49	9.50E-01	-3.50E-03	11.73
0.828 sec	1.87	25.38	-7.85	2.49	9.57E-01	-1.80E-03	13.76
0.832 sec	1.88	13.49	-4.94	2.49	9.64E-01	5.12E-05	14.28
0.836 sec	1.89	0.08	-1.70	2.49	9.72E-01	1.90E-03	13.23
0.84 sec	1.90	-13.67	0.65	2.49	9.79E-01	3.40E-03	10.73
0.844 sec	1.91	-26.39	1.39	2.49	9.86E-01	4.60E-03	7.06
0.848 sec	1.94	-36.50	0.57	2.49	9.94E-01	5.20E-03	2.62
0.852 sec	1.96	-42.49	-1.02	2.49	1.00E+00	5.30E-03	-2.13
0.856 sec	1.97	-43.32	-2.14	2.49	1.01E+00	4.60E-03	-6.65
0.86 sec	1.96	-38.92	-1.71	2.49	1.02E+00	3.50E-03	-10.45
0.864 sec	1.95	-30.23	0.53	2.49	1.02E+00	1.80E-03	-13.07
0.868 sec	1.92	-18.75	3.76	2.49	1.03E+00	3.15E-06	-14.25
0.872 sec	1.88	-5.90	6.65	2.49	1.04E+00	-1.80E-03	-13.87
0.876 sec	1.86	7.20	7.98	2.49	1.05E+00	-3.50E-03	-12.00
0.88 sec	1.84	19.59	7.09	2.49	1.05E+00	-4.80E-03	-8.86
0.884 sec	1.84	30.21	4.07	2.49	1.06E+00	-5.70E-03	-4.78
0.888 sec	1.86	37.82	-0.35	2.49	1.07E+00	-6.00E-03	-0.19
0.892 sec	1.88	41.27	-4.87	2.49	1.08E+00	-5.70E-03	4.42
0.896 sec	1.90	39.95	-8.05	2.49	1.08E+00	-4.80E-03	8.55
0.9 sec	1.92	34.04	-8.94	2.49	1.09E+00	-3.40E-03	11.73
0.904 sec	1.93	24.41	-7.47	2.49	1.10E+00	-1.70E-03	13.61
0.908 sec	1.94	12.19	-4.49	2.49	1.11E+00	2.16E-04	14.00
0.912 sec	1.94	-1.44	-1.30	2.49	1.11E+00	2.00E-03	12.85

0.916 sec	1.95	-15.25	0.91	2.49	1.12E+00	3.60E-03	10.30
0.92 sec	1.97	-27.82	1.50	2.49	1.13E+00	4.70E-03	6.62
0.924 sec	1.99	-37.60	0.57	2.49	1.14E+00	5.30E-03	2.21
0.928 sec	2.01	-43.10	-1.05	2.49	1.14E+00	5.30E-03	-2.45
0.932 sec	2.02	-43.38	-2.08	2.49	1.15E+00	4.70E-03	-6.86
0.936 sec	2.02	-38.46	-1.52	2.49	1.16E+00	3.40E-03	-10.51
0.94 sec	2.00	-29.36	0.79	2.49	1.17E+00	1.80E-03	-13.00
0.944 sec	1.97	-17.58	4.03	2.49	1.18E+00	-9.87E-05	-14.04
0.948 sec	1.94	-4.54	6.82	2.49	1.18E+00	-2.00E-03	-13.56
0.952 sec	1.91	8.65	8.00	2.49	1.19E+00	-3.60E-03	-11.61
0.956 sec	1.90	21.00	6.96	2.49	1.20E+00	-4.90E-03	-8.44
0.96 sec	1.90	31.42	3.83	2.49	1.21E+00	-5.70E-03	-4.37
0.964 sec	1.91	38.66	-0.61	2.49	1.21E+00	-6.00E-03	0.16
0.968 sec	1.93	41.64	-5.03	2.49	1.22E+00	-5.60E-03	4.67
0.972 sec	1.96	39.80	-8.03	2.49	1.23E+00	-4.70E-03	8.67
0.976 sec	1.97	33.43	-8.71	2.49	1.24E+00	-3.30E-03	11.72
0.98 sec	1.98	23.41	-7.10	2.49	1.24E+00	-1.50E-03	13.46
0.984 sec	1.99	10.91	-4.08	2.49	1.25E+00	3.79E-04	13.73
0.988 sec	1.99	-2.86	-0.96	2.49	1.26E+00	2.20E-03	12.49
0.992 sec	2.00	-16.67	1.13	2.49	1.27E+00	3.70E-03	9.89
0.996 sec	2.02	-29.07	1.57	2.49	1.28E+00	4.90E-03	6.20
1 sec	2.04	-38.50	0.54	2.49	1.28E+00	5.40E-03	1.83

G.11 Data and graphs from supersonic simulation with +10% preload

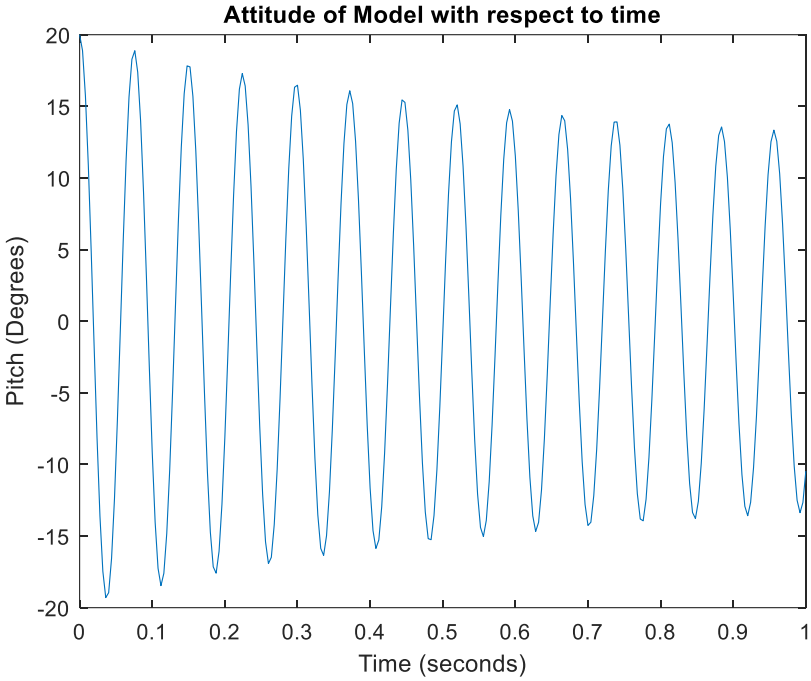

Figure 99: Attitude of model for +10 preload case

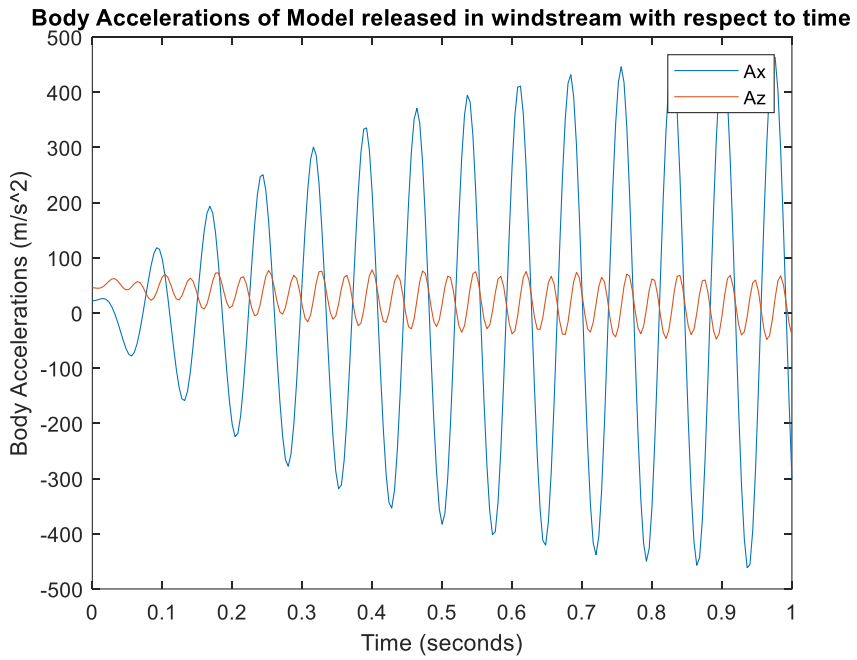

Figure 100: Accelerations of model for +10 preload case

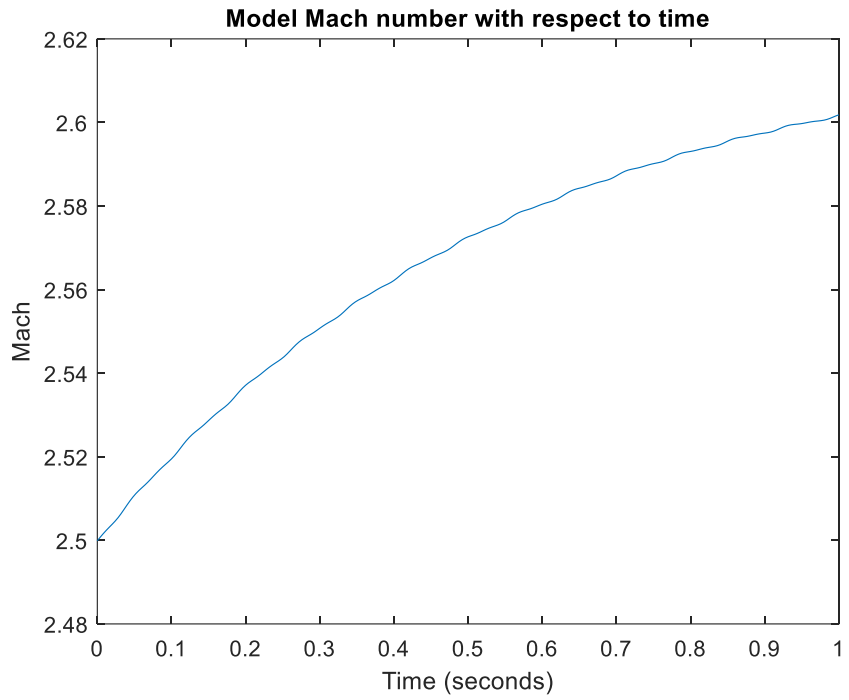

Figure 101: Mach for +10% preload case

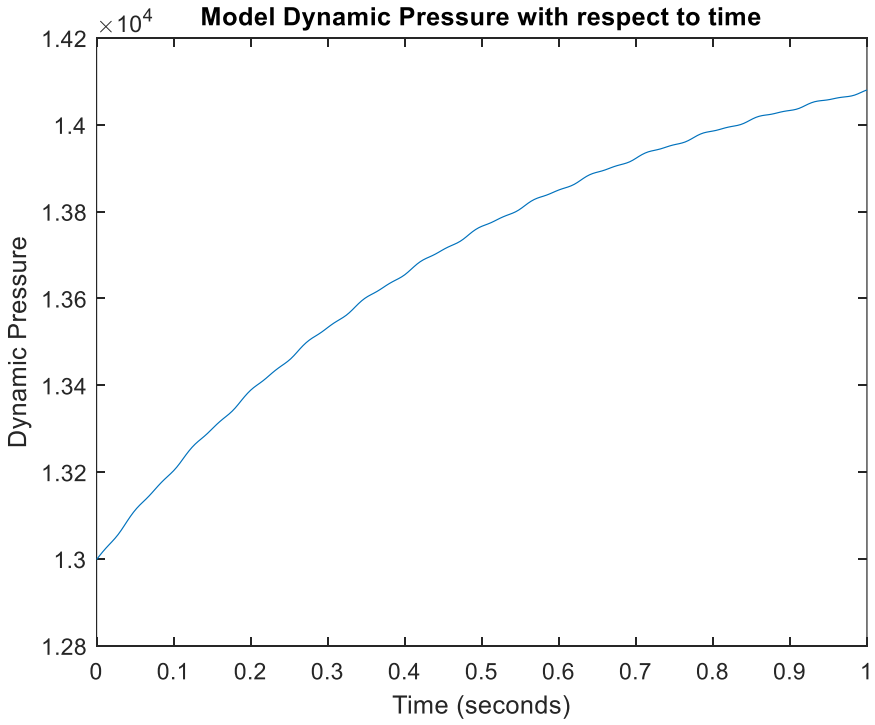

Figure 102: Dynamic pressure for +10% preload case

Table 16: Data from supersonic simulation with +10% preload

Time	Body Velocity (m/s)	Ax (m/s^2)	Az (m/s^2)	Mach	Horizontal Displacement (m)	Vertical Displacement (m)	Attitude (degrees)
0 sec	0.00	21.92	45.92	2.50	0.00E+00	0.00E+00	20.00
0.004 sec	-0.20	22.52	45.32	2.50	-4.83E-04	-1.70E-04	18.89
0.008 sec	-0.39	24.03	44.79	2.50	-1.90E-03	-5.96E-04	15.73
0.012 sec	-0.58	25.63	45.45	2.50	-4.00E-03	-1.10E-03	10.86
0.016 sec	-0.75	26.15	48.16	2.50	-6.90E-03	-1.50E-03	4.81
0.02 sec	-0.91	24.37	52.75	2.50	-1.04E-02	-1.70E-03	-1.77
0.024 sec	-1.09	19.39	57.95	2.50	-1.45E-02	-1.30E-03	-8.16
0.028 sec	-1.28	10.83	61.72	2.51	-1.90E-02	-4.57E-04	-13.61
0.032 sec	-1.50	-1.14	62.14	2.51	-2.42E-02	1.00E-03	-17.47
0.036 sec	-1.73	-15.88	58.55	2.51	-3.03E-02	3.00E-03	-19.30
0.04 sec	-1.98	-32.32	52.18	2.51	-3.73E-02	5.50E-03	-18.95
0.044 sec	-2.21	-49.03	45.69	2.51	-4.55E-02	8.10E-03	-16.55
0.048 sec	-2.42	-64.05	41.89	2.51	-5.47E-02	1.05E-02	-12.40
0.052 sec	-2.61	-74.69	42.50	2.51	-6.49E-02	1.23E-02	-6.94
0.056 sec	-2.78	-77.88	47.15	2.51	-7.59E-02	1.31E-02	-0.74
0.06 sec	-2.93	-71.44	53.16	2.51	-8.73E-02	1.26E-02	5.55
0.064 sec	-3.08	-55.38	56.77	2.51	-9.92E-02	1.08E-02	11.23
0.068 sec	-3.24	-31.71	55.17	2.51	-1.11E-01	7.90E-03	15.64
0.072 sec	-3.41	-3.19	47.93	2.51	-1.24E-01	4.00E-03	18.28
0.076 sec	-3.59	27.64	37.34	2.52	-1.37E-01	-4.87E-04	18.88
0.08 sec	-3.76	58.40	27.59	2.52	-1.51E-01	-5.10E-03	17.38
0.084 sec	-3.93	86.26	23.14	2.52	-1.66E-01	-9.40E-03	13.97
0.088 sec	-4.08	107.56	26.73	2.52	-1.82E-01	-1.27E-02	9.02
0.092 sec	-4.23	118.29	37.91	2.52	-1.99E-01	-1.45E-02	3.07
0.096 sec	-4.37	115.25	52.76	2.52	-2.16E-01	-1.45E-02	-3.23
0.1 sec	-4.53	97.44	65.27	2.52	-2.34E-01	-1.26E-02	-9.17

0.104 sec	-4.71	66.69	69.91	2.52	-2.52E-01	-8.80E-03	-14.03
0.108 sec	-4.90	27.05	64.50	2.52	-2.70E-01	-3.60E-03	-17.25
0.112 sec	-5.12	-16.83	51.45	2.52	-2.89E-01	2.60E-03	-18.47
0.116 sec	-5.33	-60.85	36.42	2.52	-3.09E-01	9.10E-03	-17.60
0.12 sec	-5.54	-101.47	25.67	2.52	-3.30E-01	1.53E-02	-14.81
0.124 sec	-5.72	-134.65	23.55	2.52	-3.53E-01	2.03E-02	-10.44
0.128 sec	-5.88	-155.37	30.96	2.53	-3.76E-01	2.35E-02	-4.95
0.132 sec	-6.02	-158.67	44.53	2.53	-4.00E-01	2.43E-02	1.08
0.136 sec	-6.15	-142.19	57.56	2.53	-4.24E-01	2.26E-02	7.00
0.14 sec	-6.28	-107.80	63.13	2.53	-4.49E-01	1.84E-02	12.13
0.144 sec	-6.42	-60.56	57.71	2.53	-4.73E-01	1.22E-02	15.88
0.148 sec	-6.57	-6.25	42.86	2.53	-4.98E-01	4.60E-03	17.82
0.152 sec	-6.73	50.07	24.48	2.53	-5.23E-01	-3.60E-03	17.75
0.156 sec	-6.88	103.78	10.37	2.53	-5.49E-01	-1.16E-02	15.69
0.16 sec	-7.02	149.61	6.98	2.53	-5.77E-01	-1.83E-02	11.89
0.164 sec	-7.15	181.42	16.67	2.53	-6.05E-01	-2.30E-02	6.75
0.168 sec	-7.28	193.27	36.27	2.53	-6.34E-01	-2.50E-02	0.86
0.172 sec	-7.40	181.49	57.93	2.53	-6.63E-01	-2.39E-02	-5.14
0.176 sec	-7.54	146.51	72.29	2.53	-6.93E-01	-1.98E-02	-10.55
0.18 sec	-7.71	93.20	72.86	2.53	-7.22E-01	-1.31E-02	-14.72
0.184 sec	-7.89	29.08	59.53	2.53	-7.52E-01	-4.40E-03	-17.15
0.188 sec	-8.09	-38.37	38.55	2.53	-7.83E-01	5.20E-03	-17.59
0.192 sec	-8.28	-103.14	19.07	2.54	-8.14E-01	1.48E-02	-16.06
0.196 sec	-8.45	-159.86	9.07	2.54	-8.47E-01	2.32E-02	-12.77
0.2 sec	-8.60	-202.43	12.55	2.54	-8.81E-01	2.95E-02	-8.10
0.204 sec	-8.74	-223.86	27.98	2.54	-9.15E-01	3.27E-02	-2.54
0.208 sec	-8.85	-218.71	48.28	2.54	-9.51E-01	3.25E-02	3.30
0.212 sec	-8.96	-186.19	63.52	2.54	-9.86E-01	2.87E-02	8.77
0.216 sec	-9.08	-131.14	65.79	2.54	-1.02E+00	2.18E-02	13.24

0.22 sec	-9.21	-61.49	53.26	2.54	-1.06E+00	1.24E-02	16.19
0.224 sec	-9.34	14.80	30.88	2.54	-1.09E+00	1.60E-03	17.29
0.228 sec	-9.47	90.88	8.12	2.54	-1.13E+00	-9.50E-03	16.42
0.232 sec	-9.60	160.09	-5.11	2.54	-1.16E+00	-1.95E-02	13.70
0.236 sec	-9.72	214.86	-2.50	2.54	-1.20E+00	-2.74E-02	9.44
0.24 sec	-9.83	247.16	15.73	2.54	-1.24E+00	-3.21E-02	4.11
0.244 sec	-9.94	250.43	42.54	2.54	-1.28E+00	-3.30E-02	-1.70
0.248 sec	-10.05	222.25	66.50	2.54	-1.32E+00	-2.98E-02	-7.31
0.252 sec	-10.19	166.04	76.88	2.54	-1.36E+00	-2.30E-02	-12.07
0.256 sec	-10.34	90.23	69.09	2.54	-1.40E+00	-1.32E-02	-15.40
0.26 sec	-10.51	5.06	47.08	2.55	-1.44E+00	-1.50E-03	-16.92
0.264 sec	-10.68	-80.40	21.01	2.55	-1.48E+00	1.08E-02	-16.48
0.268 sec	-10.85	-158.87	2.02	2.55	-1.52E+00	2.24E-02	-14.21
0.272 sec	-11.00	-223.27	-2.20	2.55	-1.57E+00	3.18E-02	-10.37
0.276 sec	-11.12	-265.52	9.96	2.55	-1.61E+00	3.79E-02	-5.39
0.28 sec	-11.23	-277.71	33.10	2.55	-1.66E+00	3.99E-02	0.19
0.284 sec	-11.32	-255.74	56.36	2.55	-1.70E+00	3.75E-02	5.75
0.288 sec	-11.42	-202.16	68.27	2.55	-1.75E+00	3.10E-02	10.65
0.292 sec	-11.52	-125.22	62.55	2.55	-1.79E+00	2.10E-02	14.32
0.296 sec	-11.64	-35.13	41.19	2.55	-1.83E+00	8.60E-03	16.34
0.3 sec	-11.76	58.79	13.28	2.55	-1.88E+00	-4.80E-03	16.47
0.304 sec	-11.87	148.25	-9.08	2.55	-1.92E+00	-1.77E-02	14.73
0.308 sec	-11.98	224.61	-15.87	2.55	-1.97E+00	-2.86E-02	11.31
0.312 sec	-12.08	278.37	-3.40	2.55	-2.02E+00	-3.62E-02	6.61
0.316 sec	-12.17	300.63	23.81	2.55	-2.07E+00	-3.95E-02	1.14
0.32 sec	-12.26	285.98	54.38	2.55	-2.12E+00	-3.81E-02	-4.46
0.324 sec	-12.37	235.13	74.77	2.55	-2.17E+00	-3.21E-02	-9.55
0.328 sec	-12.50	155.57	75.73	2.55	-2.21E+00	-2.21E-02	-13.51
0.332 sec	-12.64	59.01	57.23	2.55	-2.26E+00	-9.30E-03	-15.86

0.336 sec	-12.80	-42.74	28.22	2.56	-2.31E+00	5.00E-03	-16.35
0.34 sec	-12.95	-139.96	1.68	2.56	-2.36E+00	1.90E-02	-14.97
0.344 sec	-13.09	-224.32	-11.32	2.56	-2.41E+00	3.12E-02	-11.93
0.348 sec	-13.21	-286.96	-5.58	2.56	-2.46E+00	4.02E-02	-7.56
0.352 sec	-13.31	-318.44	16.29	2.56	-2.52E+00	4.48E-02	-2.35
0.356 sec	-13.40	-311.75	44.29	2.56	-2.57E+00	4.45E-02	3.12
0.36 sec	-13.48	-266.27	64.98	2.56	-2.62E+00	3.90E-02	8.24
0.364 sec	-13.56	-188.91	68.00	2.56	-2.68E+00	2.92E-02	12.41
0.368 sec	-13.66	-90.93	51.36	2.56	-2.73E+00	1.61E-02	15.13
0.372 sec	-13.76	16.16	22.14	2.56	-2.78E+00	1.20E-03	16.09
0.376 sec	-13.86	122.18	-6.91	2.56	-2.84E+00	-1.39E-02	15.19
0.38 sec	-13.96	217.38	-22.96	2.56	-2.89E+00	-2.74E-02	12.55
0.384 sec	-14.05	291.27	-18.46	2.56	-2.95E+00	-3.78E-02	8.48
0.388 sec	-14.13	333.25	5.46	2.56	-3.00E+00	-4.38E-02	3.43
0.392 sec	-14.20	335.27	39.01	2.56	-3.06E+00	-4.45E-02	-2.03
0.396 sec	-14.29	295.08	67.50	2.56	-3.11E+00	-3.99E-02	-7.26
0.4 sec	-14.40	218.09	77.99	2.56	-3.17E+00	-3.04E-02	-11.63
0.404 sec	-14.52	115.98	65.94	2.56	-3.23E+00	-1.72E-02	-14.62
0.408 sec	-14.66	2.57	37.52	2.56	-3.28E+00	-1.80E-03	-15.87
0.412 sec	-14.80	-109.98	5.97	2.56	-3.34E+00	1.42E-02	-15.27
0.416 sec	-14.93	-211.66	-15.10	2.56	-3.40E+00	2.88E-02	-12.95
0.42 sec	-15.05	-292.89	-17.06	2.57	-3.46E+00	4.04E-02	-9.18
0.424 sec	-15.14	-343.27	0.69	2.57	-3.52E+00	4.76E-02	-4.38
0.428 sec	-15.22	-353.62	30.14	2.57	-3.58E+00	4.94E-02	0.91
0.432 sec	-15.29	-320.20	57.41	2.57	-3.64E+00	4.56E-02	6.10
0.436 sec	-15.36	-247.54	69.15	2.57	-3.70E+00	3.66E-02	10.58
0.44 sec	-15.43	-146.73	59.26	2.57	-3.76E+00	2.34E-02	13.82
0.444 sec	-15.52	-30.85	31.86	2.57	-3.82E+00	7.60E-03	15.45
0.448 sec	-15.61	88.07	-1.03	2.57	-3.88E+00	-9.10E-03	15.27

0.452 sec	-15.70	199.03	-24.87	2.57	-3.94E+00	-2.48E-02	13.33
0.456 sec	-15.77	290.72	-28.82	2.57	-4.00E+00	-3.77E-02	9.85
0.46 sec	-15.84	351.36	-10.43	2.57	-4.07E+00	-4.61E-02	5.24
0.464 sec	-15.91	370.82	22.99	2.57	-4.13E+00	-4.91E-02	0.00
0.468 sec	-15.98	344.07	56.96	2.57	-4.19E+00	-4.62E-02	-5.24
0.472 sec	-16.07	273.96	76.14	2.57	-4.26E+00	-3.77E-02	-9.87
0.476 sec	-16.17	171.13	71.85	2.57	-4.32E+00	-2.47E-02	-13.32
0.48 sec	-16.29	50.34	46.68	2.57	-4.38E+00	-8.60E-03	-15.18
0.484 sec	-16.42	-74.08	12.76	2.57	-4.44E+00	8.70E-03	-15.25
0.488 sec	-16.54	-190.31	-14.79	2.57	-4.51E+00	2.53E-02	-13.57
0.492 sec	-16.65	-287.80	-24.41	2.57	-4.57E+00	3.91E-02	-10.36
0.496 sec	-16.74	-355.53	-12.31	2.57	-4.64E+00	4.87E-02	-5.99
0.5 sec	-16.81	-382.83	16.02	2.57	-4.71E+00	5.27E-02	-0.93
0.504 sec	-16.87	-363.28	47.42	2.57	-4.77E+00	5.07E-02	4.23
0.508 sec	-16.93	-298.69	66.71	2.57	-4.84E+00	4.29E-02	8.90
0.512 sec	-16.99	-199.00	64.23	2.57	-4.91E+00	3.01E-02	12.52
0.516 sec	-17.07	-78.09	40.69	2.57	-4.97E+00	1.39E-02	14.67
0.52 sec	-17.14	50.38	6.51	2.57	-5.04E+00	-3.90E-03	15.10
0.524 sec	-17.22	174.11	-23.15	2.57	-5.11E+00	-2.13E-02	13.77
0.528 sec	-17.29	281.00	-34.95	2.57	-5.17E+00	-3.63E-02	10.84
0.532 sec	-17.35	358.39	-23.09	2.58	-5.24E+00	-4.70E-02	6.65
0.536 sec	-17.41	394.63	7.98	2.58	-5.31E+00	-5.22E-02	1.68
0.54 sec	-17.47	382.30	44.96	2.58	-5.38E+00	-5.11E-02	-3.50
0.544 sec	-17.54	321.66	71.22	2.58	-5.45E+00	-4.39E-02	-8.27
0.548 sec	-17.62	221.65	74.76	2.58	-5.52E+00	-3.14E-02	-12.06
0.552 sec	-17.73	97.13	54.46	2.58	-5.59E+00	-1.51E-02	-14.40
0.556 sec	-17.84	-35.98	20.40	2.58	-5.66E+00	3.10E-03	-15.03
0.56 sec	-17.96	-164.05	-11.78	2.58	-5.73E+00	2.11E-02	-13.91
0.564 sec	-18.06	-275.42	-28.27	2.58	-5.80E+00	3.69E-02	-11.21

0.568 sec	-18.14	-358.51	-22.34	2.58	-5.87E+00	4.85E-02	-7.24
0.572 sec	-18.21	-401.64	3.17	2.58	-5.94E+00	5.47E-02	-2.45
0.576 sec	-18.26	-396.30	36.53	2.58	-6.02E+00	5.45E-02	2.63
0.58 sec	-18.31	-341.65	61.76	2.58	-6.09E+00	4.80E-02	7.39
0.584 sec	-18.36	-245.90	66.42	2.58	-6.16E+00	3.59E-02	11.29
0.588 sec	-18.42	-123.00	47.85	2.58	-6.23E+00	1.97E-02	13.85
0.592 sec	-18.49	12.14	14.30	2.58	-6.30E+00	1.20E-03	14.78
0.596 sec	-18.56	145.95	-19.25	2.58	-6.38E+00	-1.75E-02	13.97
0.6 sec	-18.62	265.49	-37.75	2.58	-6.45E+00	-3.41E-02	11.53
0.604 sec	-18.67	357.48	-32.52	2.58	-6.52E+00	-4.68E-02	7.74
0.608 sec	-18.72	409.09	-5.14	2.58	-6.60E+00	-5.40E-02	3.05
0.612 sec	-18.77	411.01	32.81	2.58	-6.67E+00	-5.48E-02	-2.02
0.616 sec	-18.82	361.06	64.37	2.58	-6.75E+00	-4.90E-02	-6.85
0.62 sec	-18.90	266.24	75.09	2.58	-6.82E+00	-3.73E-02	-10.88
0.624 sec	-18.99	140.85	60.38	2.58	-6.90E+00	-2.11E-02	-13.59
0.628 sec	-19.09	1.81	27.83	2.58	-6.97E+00	-2.40E-03	-14.68
0.632 sec	-19.20	-135.62	-7.26	2.58	-7.04E+00	1.67E-02	-14.04
0.636 sec	-19.29	-258.61	-29.49	2.58	-7.12E+00	3.40E-02	-11.79
0.64 sec	-19.37	-354.97	-29.60	2.58	-7.19E+00	4.75E-02	-8.20
0.644 sec	-19.43	-412.36	-7.84	2.58	-7.27E+00	5.56E-02	-3.68
0.648 sec	-19.48	-420.68	25.80	2.58	-7.35E+00	5.72E-02	1.27
0.652 sec	-19.52	-376.71	55.35	2.58	-7.43E+00	5.21E-02	6.07
0.656 sec	-19.56	-286.71	66.34	2.58	-7.50E+00	4.08E-02	10.15
0.66 sec	-19.61	-164.13	53.13	2.58	-7.58E+00	2.49E-02	13.03
0.664 sec	-19.67	-24.71	21.52	2.59	-7.66E+00	6.00E-03	14.36
0.668 sec	-19.72	116.83	-14.27	2.59	-7.73E+00	-1.36E-02	14.00
0.672 sec	-19.78	246.75	-38.16	2.59	-7.81E+00	-3.16E-02	11.99
0.676 sec	-19.83	351.19	-39.14	2.59	-7.89E+00	-4.60E-02	8.58
0.68 sec	-19.87	416.47	-16.09	2.59	-7.97E+00	-5.50E-02	4.15

0.684 sec	-19.91	431.76	21.36	2.59	-8.05E+00	-5.74E-02	-0.77
0.688 sec	-19.95	392.80	56.59	2.59	-8.13E+00	-5.30E-02	-5.61
0.692 sec	-20.01	304.56	73.46	2.59	-8.21E+00	-4.23E-02	-9.79
0.696 sec	-20.09	180.40	64.42	2.59	-8.29E+00	-2.65E-02	-12.79
0.7 sec	-20.18	37.72	34.43	2.59	-8.36E+00	-7.50E-03	-14.26
0.704 sec	-20.28	-106.92	-2.12	2.59	-8.44E+00	1.24E-02	-14.04
0.708 sec	-20.37	-239.47	-28.88	2.59	-8.52E+00	3.09E-02	-12.18
0.712 sec	-20.45	-347.15	-34.51	2.59	-8.60E+00	4.60E-02	-8.94
0.716 sec	-20.50	-417.08	-16.89	2.59	-8.68E+00	5.57E-02	-4.68
0.72 sec	-20.55	-438.00	15.86	2.59	-8.77E+00	5.89E-02	0.13
0.724 sec	-20.58	-404.69	48.30	2.59	-8.85E+00	5.52E-02	4.91
0.728 sec	-20.61	-321.44	64.63	2.59	-8.93E+00	4.49E-02	9.12
0.732 sec	-20.65	-200.84	56.66	2.59	-9.01E+00	2.94E-02	12.24
0.736 sec	-20.70	-59.02	27.78	2.59	-9.09E+00	1.04E-02	13.90
0.74 sec	-20.75	88.29	-8.96	2.59	-9.17E+00	-9.80E-03	13.91
0.744 sec	-20.80	226.58	-36.99	2.59	-9.25E+00	-2.89E-02	12.28
0.748 sec	-20.84	341.48	-43.48	2.59	-9.33E+00	-4.47E-02	9.21
0.752 sec	-20.88	418.68	-24.93	2.59	-9.42E+00	-5.53E-02	5.05
0.756 sec	-20.91	446.14	11.05	2.59	-9.50E+00	-5.93E-02	0.28
0.76 sec	-20.94	417.83	48.57	2.59	-9.58E+00	-5.62E-02	-4.54
0.764 sec	-20.99	336.85	70.49	2.59	-9.67E+00	-4.65E-02	-8.82
0.768 sec	-21.06	215.36	66.83	2.59	-9.75E+00	-3.12E-02	-12.04
0.772 sec	-21.14	70.82	39.98	2.59	-9.83E+00	-1.22E-02	-13.81
0.776 sec	-21.23	-79.17	3.06	2.59	-9.91E+00	8.30E-03	-13.94
0.78 sec	-21.31	-219.49	-27.11	2.59	-1.00E+01	2.78E-02	-12.43
0.784 sec	-21.39	-336.69	-37.57	2.59	-1.01E+01	4.41E-02	-9.50
0.788 sec	-21.44	-417.48	-24.10	2.59	-1.02E+01	5.53E-02	-5.48
0.792 sec	-21.48	-449.73	7.02	2.59	-1.03E+01	6.00E-02	-0.83
0.796 sec	-21.51	-426.60	41.18	2.59	-1.03E+01	5.76E-02	3.92

0.8 sec	-21.53	-350.51	61.84	2.59	-1.04E+01	4.83E-02	8.20
0.804 sec	-21.56	-232.97	58.71	2.59	-1.05E+01	3.33E-02	11.50
0.808 sec	-21.60	-90.22	32.93	2.59	-1.06E+01	1.44E-02	13.43
0.812 sec	-21.65	61.26	-3.81	2.59	-1.07E+01	-6.30E-03	13.76
0.816 sec	-21.69	206.22	-34.87	2.59	-1.08E+01	-2.62E-02	12.46
0.82 sec	-21.73	329.83	-46.09	2.59	-1.08E+01	-4.32E-02	9.68
0.824 sec	-21.76	417.25	-31.89	2.59	-1.09E+01	-5.51E-02	5.76
0.828 sec	-21.78	455.55	2.05	2.59	-1.10E+01	-6.05E-02	1.15
0.832 sec	-21.81	437.23	40.81	2.59	-1.11E+01	-5.87E-02	-3.61
0.836 sec	-21.85	363.66	66.73	2.59	-1.12E+01	-4.99E-02	-7.96
0.84 sec	-21.91	245.74	67.91	2.59	-1.13E+01	-3.52E-02	-11.34
0.844 sec	-21.98	100.70	44.43	2.60	-1.14E+01	-1.63E-02	-13.36
0.848 sec	-22.06	-53.14	7.93	2.60	-1.15E+01	4.40E-03	-13.78
0.852 sec	-22.14	-199.68	-24.70	2.60	-1.15E+01	2.47E-02	-12.58
0.856 sec	-22.21	-324.83	-39.25	2.60	-1.16E+01	4.21E-02	-9.92
0.86 sec	-22.26	-414.91	-29.72	2.60	-1.17E+01	5.46E-02	-6.13
0.864 sec	-22.30	-457.17	-0.63	2.60	-1.18E+01	6.05E-02	-1.63
0.868 sec	-22.32	-443.45	34.38	2.60	-1.19E+01	5.93E-02	3.06
0.872 sec	-22.34	-374.51	58.43	2.60	-1.20E+01	5.10E-02	7.38
0.876 sec	-22.36	-260.68	59.61	2.60	-1.21E+01	3.66E-02	10.83
0.88 sec	-22.40	-118.07	37.02	2.60	-1.22E+01	1.78E-02	12.97
0.884 sec	-22.43	36.29	0.93	2.60	-1.22E+01	-3.00E-03	13.56
0.888 sec	-22.47	186.49	-32.27	2.60	-1.23E+01	-2.37E-02	12.54
0.892 sec	-22.50	317.26	-47.42	2.60	-1.24E+01	-4.16E-02	10.03
0.896 sec	-22.53	413.39	-37.24	2.60	-1.25E+01	-5.47E-02	6.33
0.9 sec	-22.55	461.20	-5.64	2.60	-1.26E+01	-6.13E-02	1.87
0.904 sec	-22.57	452.00	33.58	2.60	-1.27E+01	-6.06E-02	-2.82
0.908 sec	-22.60	385.64	62.57	2.60	-1.28E+01	-5.28E-02	-7.19
0.912 sec	-22.65	271.78	67.99	2.60	-1.29E+01	-3.87E-02	-10.70

0.916 sec	-22.72	127.23	47.85	2.60	-1.30E+01	-2.00E-02	-12.92
0.92 sec	-22.79	-29.24	12.31	2.60	-1.30E+01	9.59E-04	-13.58
0.924 sec	-22.87	-180.69	-21.99	2.60	-1.31E+01	2.18E-02	-12.64
0.928 sec	-22.93	-312.41	-39.93	2.60	-1.32E+01	4.00E-02	-10.23
0.932 sec	-22.98	-410.39	-33.99	2.60	-1.33E+01	5.36E-02	-6.65
0.936 sec	-23.01	-461.38	-7.13	2.60	-1.34E+01	6.07E-02	-2.29
0.94 sec	-23.03	-456.18	28.09	2.60	-1.35E+01	6.05E-02	2.33
0.944 sec	-23.04	-394.10	54.73	2.60	-1.36E+01	5.31E-02	6.67
0.948 sec	-23.06	-284.32	59.65	2.60	-1.37E+01	3.93E-02	10.21
0.952 sec	-23.09	-142.60	40.15	2.60	-1.38E+01	2.08E-02	12.53
0.956 sec	-23.12	13.62	5.12	2.60	-1.39E+01	-1.91E-04	13.34
0.96 sec	-23.15	167.88	-29.48	2.60	-1.40E+01	-2.13E-02	12.56
0.964 sec	-23.18	304.52	-47.85	2.60	-1.40E+01	-4.00E-02	10.29
0.968 sec	-23.20	407.98	-41.28	2.60	-1.41E+01	-5.40E-02	6.79
0.972 sec	-23.22	464.04	-12.09	2.60	-1.42E+01	-6.17E-02	2.47
0.976 sec	-23.24	463.02	27.02	2.60	-1.43E+01	-6.21E-02	-2.15
0.98 sec	-23.26	403.48	58.32	2.60	-1.44E+01	-5.51E-02	-6.53
0.984 sec	-23.31	293.88	67.36	2.60	-1.45E+01	-4.16E-02	-10.13
0.988 sec	-23.36	150.49	50.39	2.60	-1.46E+01	-2.32E-02	-12.50
0.992 sec	-23.43	-7.65	16.12	2.60	-1.47E+01	-2.20E-03	-13.37
0.996 sec	-23.50	-162.92	-19.23	2.60	-1.48E+01	1.91E-02	-12.65
1 sec	-23.56	-300.03	-39.92	2.60	-1.49E+01	3.80E-02	-10.46

APPENDIX H: MARK 2 GRABBER SCHEMATICS

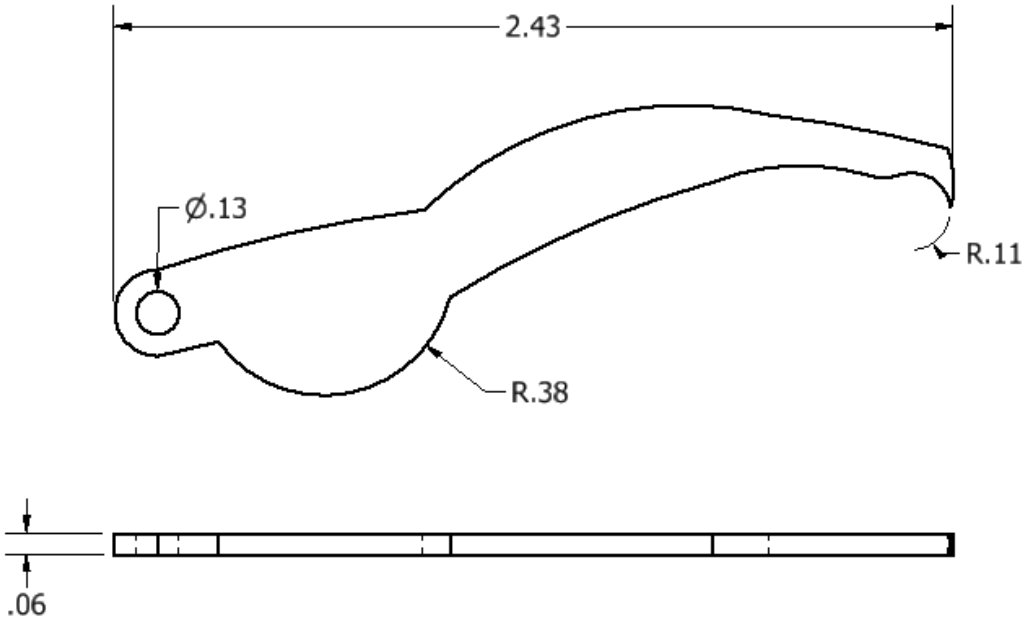

Figure 103: Long gripper for Mark 2 grabber. Dimensions in inches.

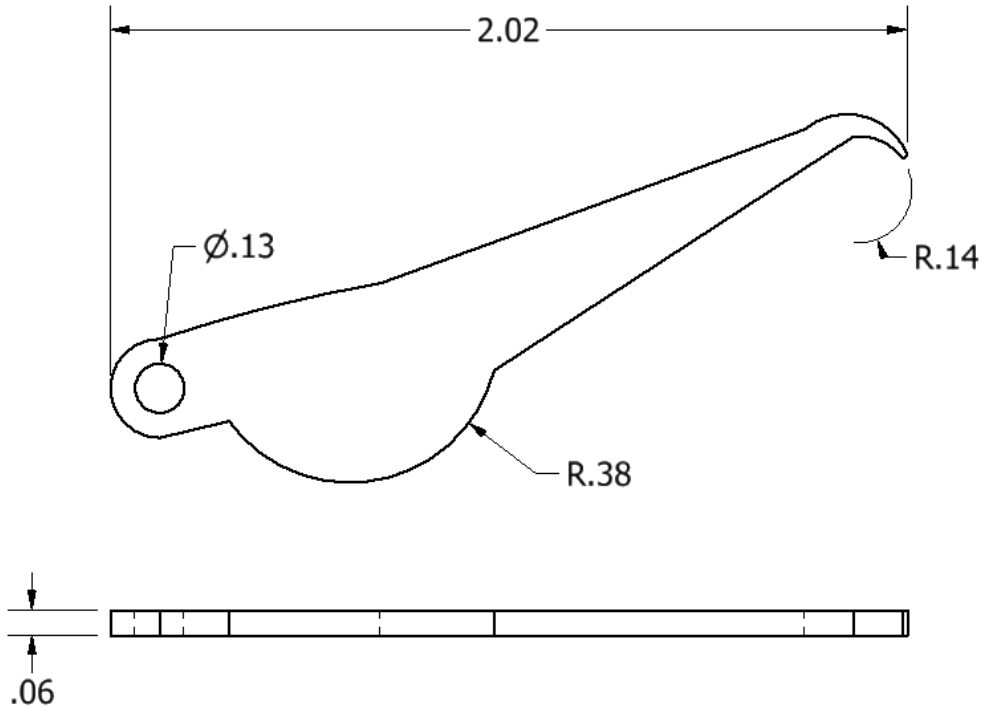

Figure 104: Short gripper for Mark 2 grabber. Dimensions in inches.

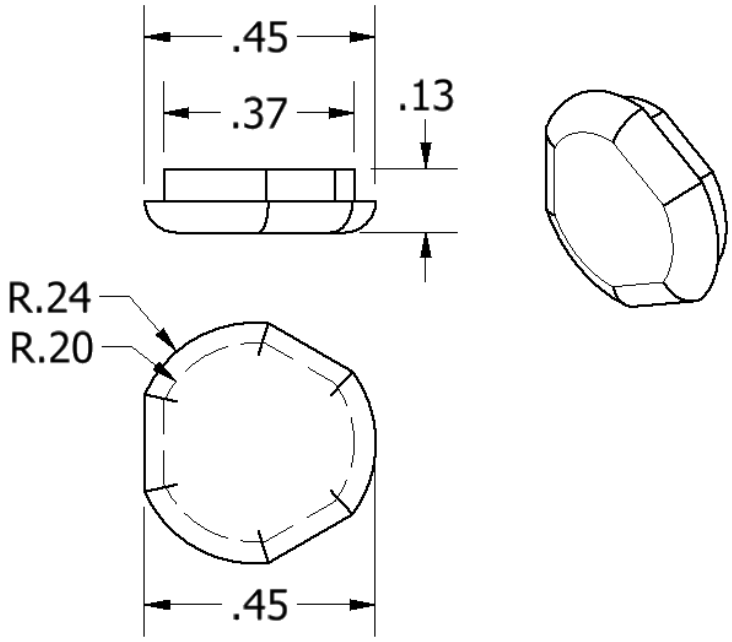

Figure 105: Aero fairing cap for Mark 2 grabber. Dimensions in inches.

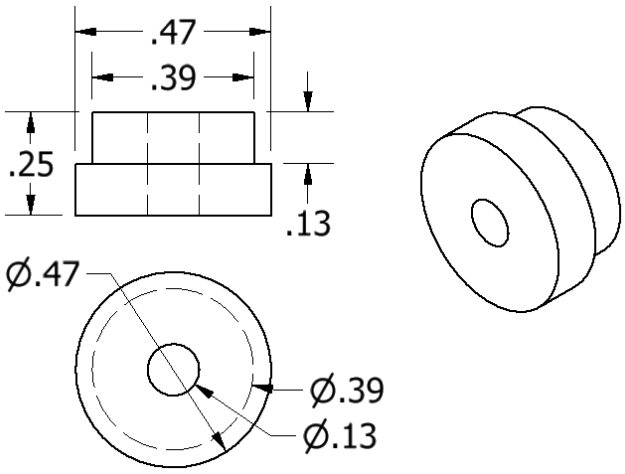

Figure 106: End cap for Mark 2 grabber. Dimensions in inches.

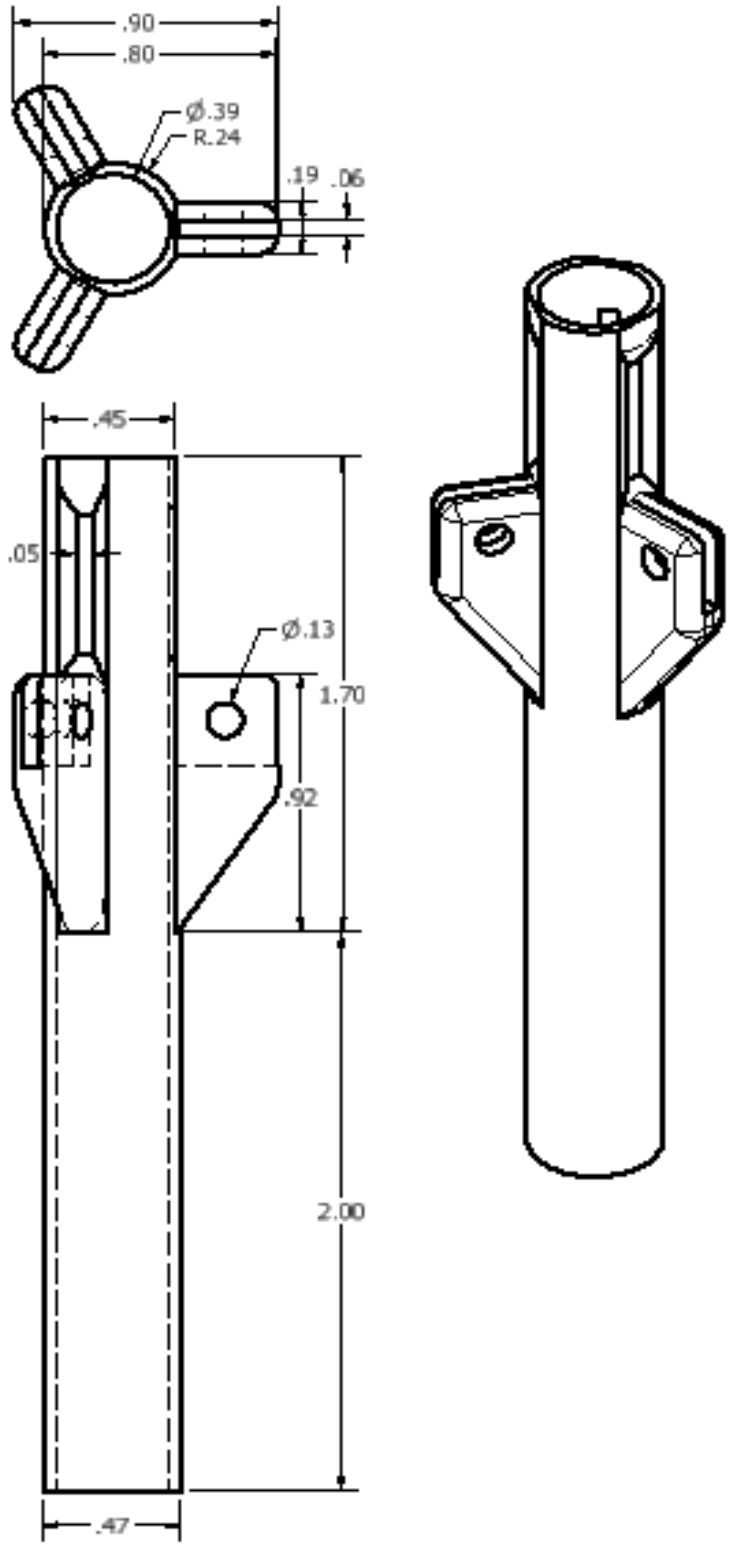

Figure 107: Outer rod for Mark 2 grabber. Dimensions in inches.

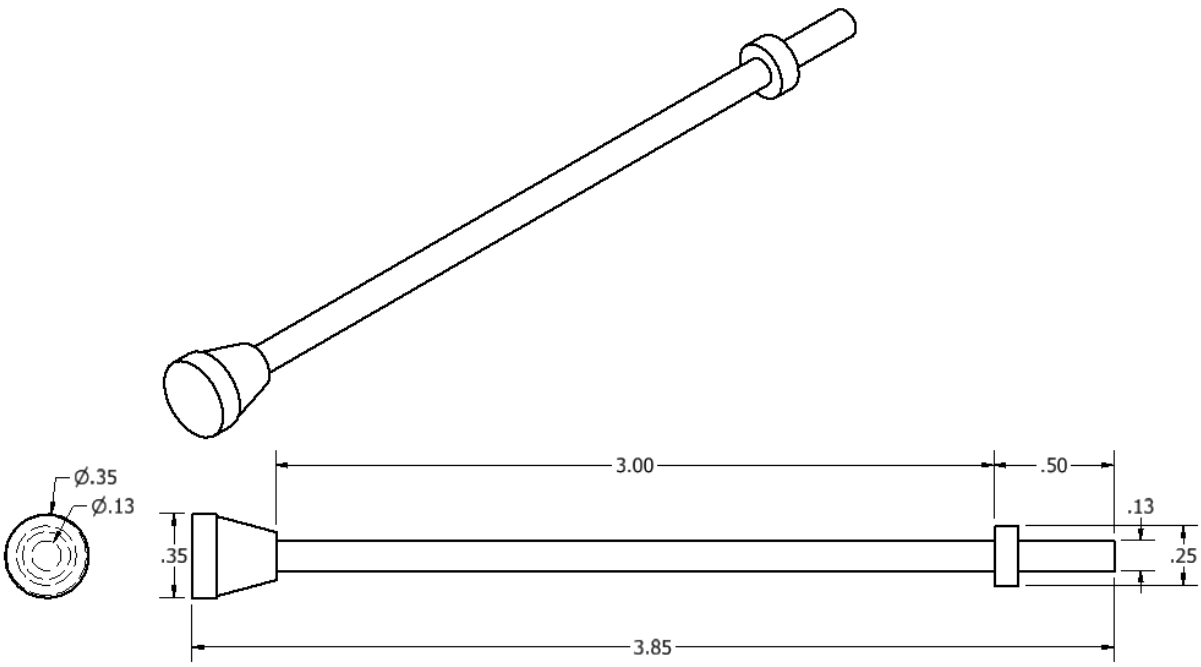

Figure 108: Inner rod for Mark 2 grabber. Dimensions in inches.

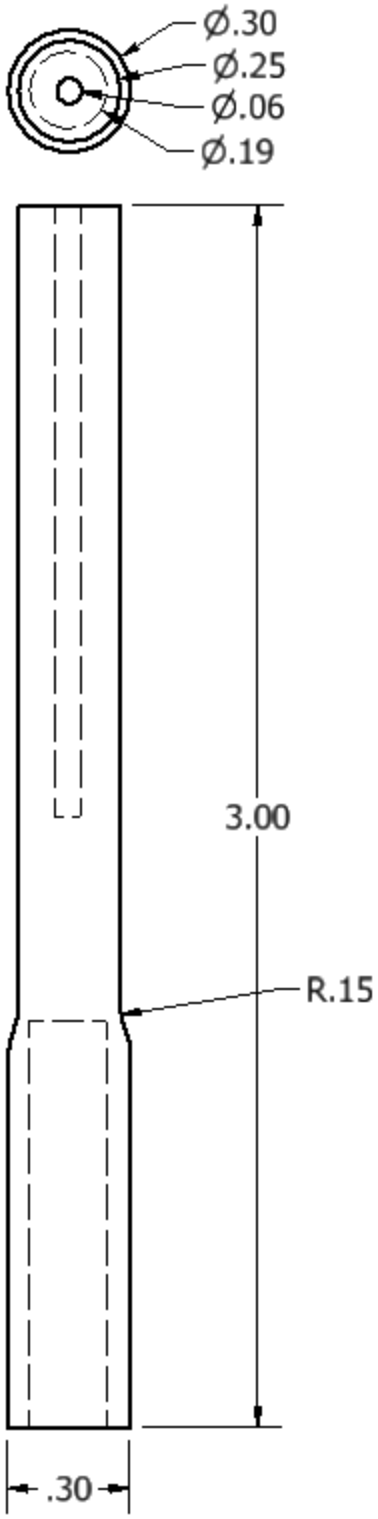

Figure 109: Connector rod for Mark 2 grabber. Dimensions in inches.

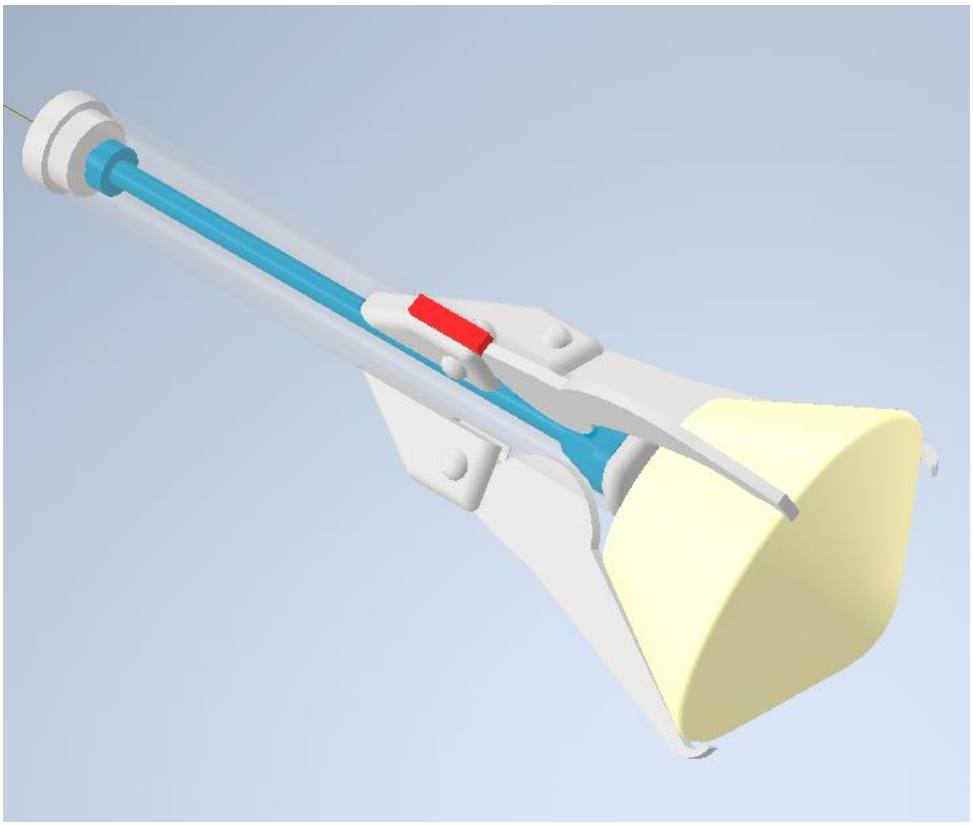

Figure 110: 3D rendering of Mark 2 grabber.

VITA

Kristen M. Carey

Mechanical & Aerospace Engineering
Old Dominion University
214A Kaufman Hall, Norfolk, VA 23529

Email:

Kmcarey99@gmail.com

Education:

M.S. Aerospace Engineering, Old Dominion University, May 2023.
B.S. Mechanical Engineering, Old Dominion University, December 2020.

Academic Employment:

Graduate Research Assistant to Dr. Colin Britcher, Department of Mechanical & Aerospace Engineering, Old Dominion University, January 2020 – May 2022.

Professional Employment:

Wind Tunnel Test Engineer with Analytical Services and Materials, at the Transonic Dynamics Tunnel at NASA Langley Research Center, May 2022 – Present.